nagra National Cooperative for the Disposal of Radioactive Waste

TECHNICAL REPORT 91-01E

GRIMSEL TEST SITE

FRACTURE SYSTEM FLOW TEST

A. PAHL
L. LIEDTKE
A. NAUJOKS
V. BRÄUER

JUNE 1992

Federal Institute for Geoscience and Natural Resources, Hannover, Federal Republic of Germany

GRIMSEL TEST SITE/SWITZERLAND
A JOINT RESEARCH PROGRAM BY

- NAGRA - National Cooperative for the Disposal of Radioactive Waste, Wettingen, Switzerland
- BGR - Federal Institute for Geoscience and Natural Resources, Hannover, Federal Republic of Germany
- GSF - Research Centre for Environmental Sciences, Munich, Federal Republic of Germany

Hardstrasse 73, CH-5430 Wettingen/Switzerland, Telephone +41-56-37 11 11

nagra National Cooperative for the Disposal of Radioactive Waste

TECHNICAL REPORT 91-01E

GRIMSEL TEST SITE

FRACTURE SYSTEM FLOW TEST

A. PAHL
L. LIEDTKE
A. NAUJOKS
V. BRÄUER

JUNE 1992

Federal Institute for Geoscience and Natural Resources, Hannover, Federal Republic of Germany

GRIMSEL TEST SITE/SWITZERLAND
A JOINT RESEARCH PROGRAM BY

- NAGRA - National Cooperative for the Disposal of Radioactive Waste, Wettingen, Switzerland
- BGR - Federal Institute for Geoscience and Natural Resources, Hannover, Federal Republic of Germany
- GSF - Research Centre for Environmental Sciences, Munich, Federal Republic of Germany

Hardstrasse 73, CH-5430 Wettingen/Switzerland, Telephone +41-56-37 11 11

FOREWORD

Concepts for the disposal of radioactive waste in geological formations place a significant emphasis on acquiring extensive knowledge of the proposed host rock and the surrounding strata. For this reason, Nagra has, since May 1984, been operating the **Grimsel Test Site (GTS)** which is located at a depth of 450 m in the crystalline rock of the Aar Massif of the Central Swiss Alps. The general objectives of the research being carried out in this underground laboratory include

- the build-up of know-how in planning, performing and interpreting field experiments in various scientific and technical disciplines and

- the acquisition of practical experience in the development of investigation methodologies, measuring techniques and test equipment which will be of use during actual repository site explorations.

The GTS is operated by Nagra and, on the basis of a German-Swiss cooperative agreement, various experiments are carried out by Nagra, the "Bundesanstalt für Geowissenschaften und Rohstoffe, Hannover" (BGR) and the "Forschungszentrum für Umwelt und Gesundheit, München" (GSF). The Grimsel projects of both GSF and BGR are supported by the German Federal Ministry for Research and Technology (BMFT). NTB 85-46 (German version NTB 85-47) provides an overview of the German-Swiss investigation programme. In a special issue of the Nagra Bulletin 1988 (German version "Nagra Informiert 1+2/1988"), the status of the programme up to 1988 is described.

VORWORT

Bei Konzepten, welche die Endlagerung radioaktiver Abfälle in geologischen Formationen vorsehen, ist die Kenntnis des Wirtgesteins und der angrenzenden Gesteinsschichten von grundlegender Bedeutung. Die Nagra betreibt deshalb seit Mai 1984 das **Felslabor Grimsel (FLG)** in 450 m Tiefe im Kristallin des Aarmassivs. Die generelle Zielsetzung für die Arbeiten in diesem System von Versuchsstollen umfasst

- den Aufbau von Know-how in der Planung, Ausführung und Interpretation von Untergrundversuchen in verschiedenen wissenschaftlichen und technischen Fachgebieten, und

- den Erwerb praktischer Erfahrung in der Entwicklung und der Anwendung von Untersuchungsmethoden, Messverfahren und Messgeräten, die für die Erkundung von potentiellen Endlagerstandorten in Frage kommen.

Im Felslabor der Nagra werden, auf der Basis eines deutsch-schweizerischen Zusammenarbeitsvertrages, verschiedene Versuche von den beiden deutschen Partnern Bundesanstalt für Geowissenschaften und Rohstoffe, Hannover (BGR) und Forschungszentrum für Umwelt und Gesundheit GmbH, München (GSF) durchgeführt. Das Deutsche Bundesministerium für Forschung und Technologie (BMFT) fördert die Arbeiten der BGR und der GSF im FLG. Der NTB 85-47 (englische Version NTB 85-46) enhält eine Uebersicht des FLG und die Zusammenfassung der Untersuchungsprogramme mit Status August 1985. In der Ausgabe 1+2/1988 des Heftes "Nagra informiert" bzw. der englischen Spezialausgabe "Nagra Bulletin 1988" ist der Stand der Arbeiten anfangs 1988 beschrieben.

Der vorliegende Bericht wurde im Rahmen der erwähnten Zusammenarbeitsverträge erstellt. Die Autoren haben ihre eigenen Ansichten und Schlussfolgerungen dargelegt. Diese müssen nicht unbedingt mit denjenigen der Nagra oder des beteiligten Partner übereinstimmen.

AVANT - PROPOS

Lors d'études de concepts de stockage de déchets radioactifs dans des formations géologiques, on attache une grande importance à l'acquisition d'informations étendues sur la roche d'accueil et les formations rocheuses environnantes. C'est pour cette raison que la Cédra exploite depuis mai 1984 son **laboratoire souterrain du Grimsel (LSG)** situé à 450 m de profondeur dans le cristallin du massif de l'Aar, situé au milieu des Alpes centrales. Les principaux objectifs des recherches effectuées dans ce réseau de galeries comprennent:

- l'acquisition de savoir-faire dans diverses disciplines techniques et scientifiques en ce qui concerne la conception, la réalisation et l'interprétation d'expériences in situ, ainsi que

- l'accumulation d'expériences pratiques dans la mise au point et l'application de méthodes d'investigation, de techniques et d'appareillages de mesure, qui pourraient être utilisés lors de l'exploration de sites potentiels de dépôts finals.

Le LSG est exploité par la Cédra et diverses expériences y sont réalisées par celle-ci et deux institutions allemandes: la "Bundesanstalt für Geowissenschaften und Rohstoffe, Hannover" (BGR) et le "Forschungszentrum für Umwelt und Gesundheit GmbH, München" (GSF) dans le cadre d'un traité de collaboration germano-suisse. Les projets poursuivis au Grimsel par la BGR et le GSF sont financés par le Ministère fédéral allemand de la recherche et de la technologie (BMFT). Les rapports NTB 85-46 (version anglaise) et NTB 85-47 (version allemande) présentent un aperçu du laboratoire souterrain et un résumé des programmes de recherches avec état au mois d'août 1985. L'état d'avancement de ce programme en 1988 est présenté dans la publication "Cédra informe 1+2/1988" (version française) et "Nagra informiert 1+2/1988" (version allemande), ainsi que dans une édition spéciale en anglais (Nagra Bulletin 1988).

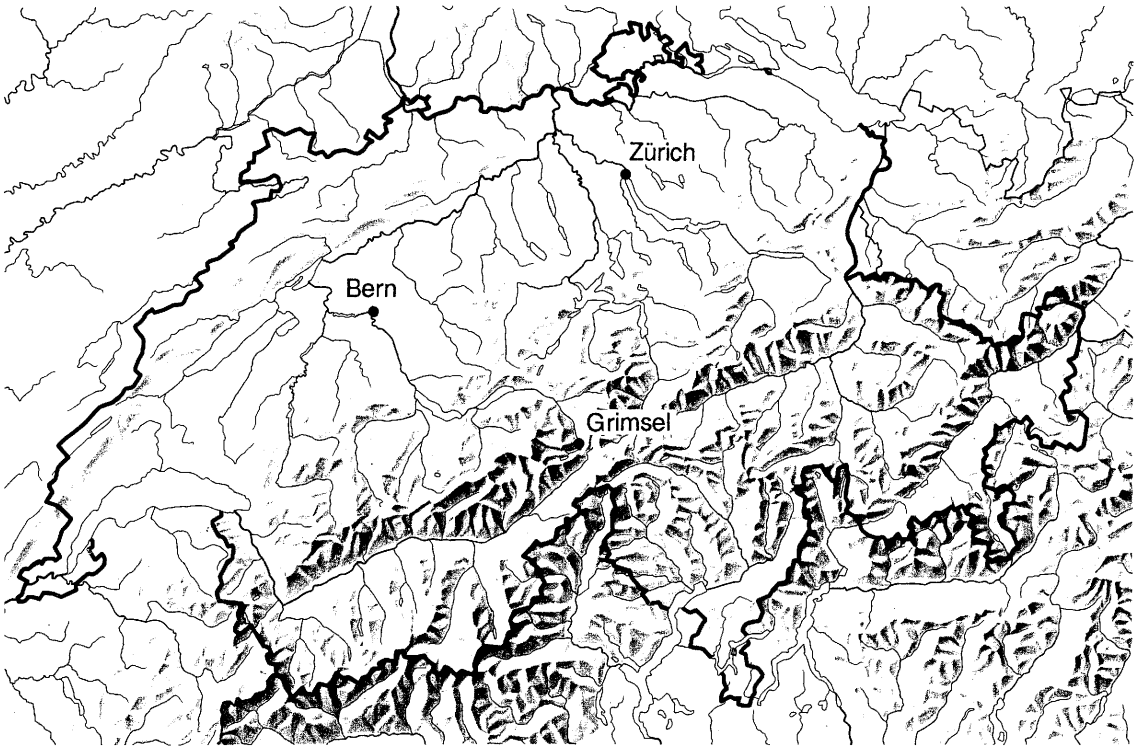

Location of Nagra's underground test facility at the Grimsel Pass in the Central Alps (Bernese Alps) of Switzerland (approximate scale 1 cm = 25 km).

Geographische Lage des Nagra Felslabors am Grimselpass (Berner Oberland) in den schweizerischen Zentralalpen (Massstab: 1 cm = ca. 25 km)

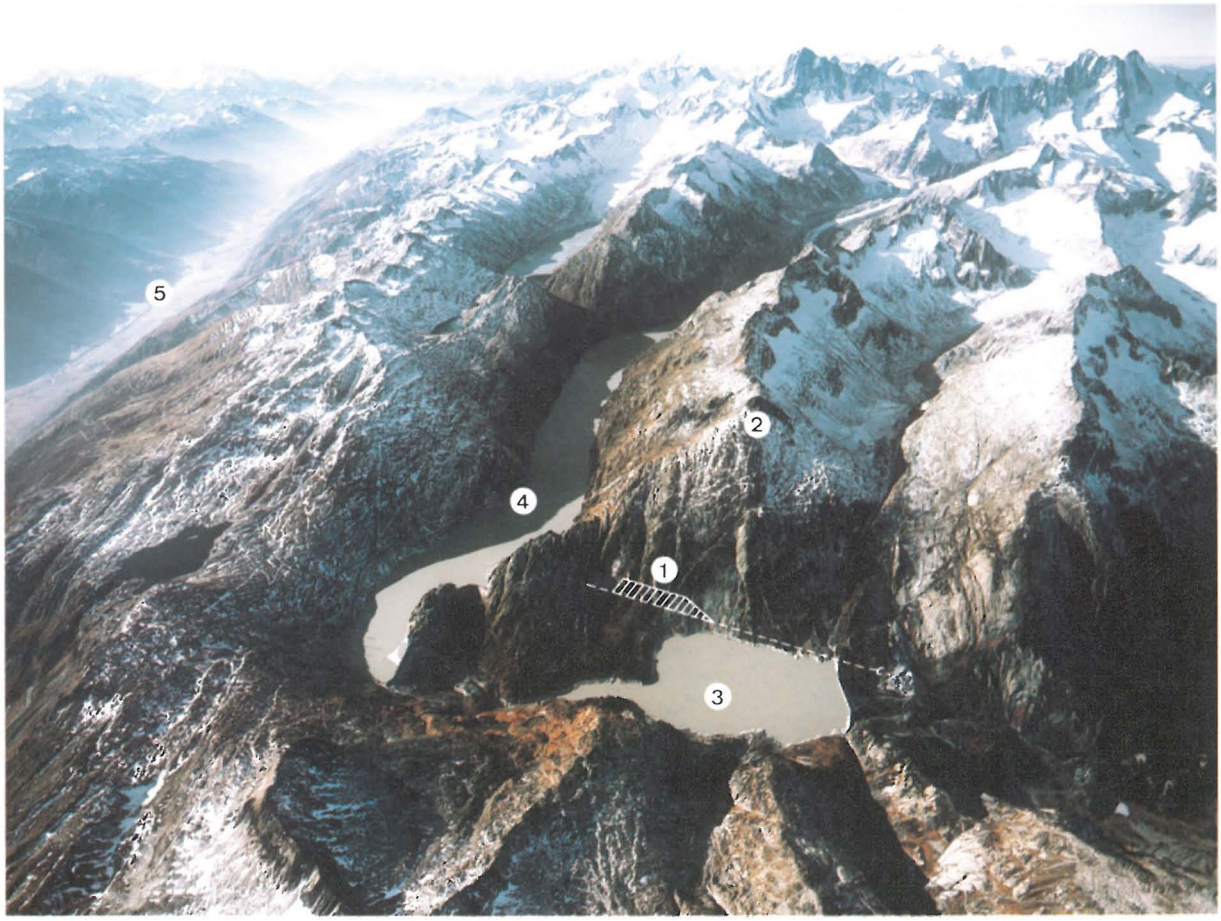

GRIMSEL-GEBIET

Blick nach Westen

1 Felslabor
2 Juchlistock
3 Räterichsbodensee
4 Grimselsee
5 Rhonetal

GRIMSEL AREA

View looking West

1 Test Site
2 Juchlistock
3 Lake Raeterichsboden
4 Lake Grimsel
5 Rhone Valley

FLG FELSLABOR GRIMSEL
GTS *GRIMSEL TEST SITE*

Situation

0 100 m

- Zugangsstollen/*Access tunnel*
- Fräsvortrieb/*by tunnel boring machine*
- Sprengvortrieb/*excavated by blasting*
- Zentraler Aaregranit ZAGR / *Central Aaregranite CAGR*
- Biotitreicher ZAGR / *CAGR with high content of biotite*
- Grimsel-Granodiorit / *Grimsel-Granodiorite*
- Scherzone/*Shear zone*
- Lamprophyr/*Lamprophyre*
- Wasserzutritt/*Water inflow*
- SB Sondierbohrung/*Exploratory borehole*
- US US Bohrung/*US borehole*
- ZB Zentraler Bereich/*Central facilities*
- AU Auflockerung/*Excavation effects*
- BK Bohrlochkranz/*Fracture system flow*
- EM El.magn. HF-Messungen/*-measurements*
- FRI Kluftzone/*Fracture zone investigation*
- GS Gebirgsspannungen/*Rock stresses*
- HPA Hydr. Parameter/*Hydr. parameters*
- MI Migration/*Migration*
- MOD Hydrodyn. Modellierung/*H. modeling*
- NM Neigungsmesser/*Tiltmeters*
- UR Untertageradar/*Underground radar*
- US Seismik/*Underground seismic testing*
- VE Ventilationstest/*Ventilation test*
- WT Wärmeversuch/*Heat test*

A — A Schnitt/*Section*

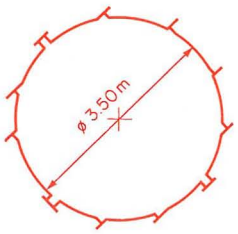

6/88

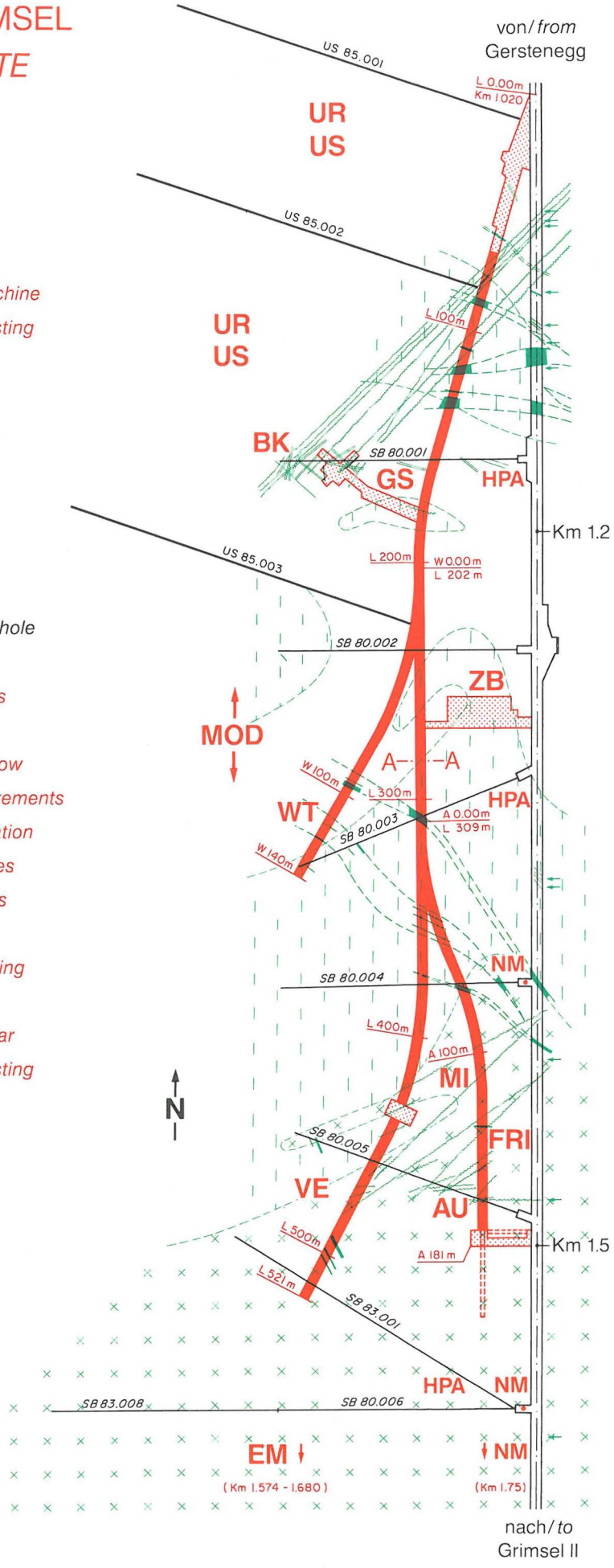

ABSTRACT:

Within the scope of a German-Swiss joint cooperation project between the Nationale Genossenschaft für die Lagerung radioaktiver Abfälle (NAGRA; Swiss National Cooperative for the Disposal of Radioactive Waste), the Bundesanstalt für Geowissenschaften und Rohstoffe (BGR; Federal Institute for Geoscience and Natural Resources) and the Forschungszentrum für Umwelt und Gesundheit (GSF; Research Centre for Environmental Sciences), studies are being conducted in the Grimsel rock laboratory on the hydrogeological, rock-mechanical, geophysical and geochemical properties of crystalline rocks. In-situ tests and numerical model calculations are carried out by the BGR within the "Fracture System Flow Test" project (BK) to investigate the significance of flow and transport processes in fissured rock.

After drilling cored boreholes, project phase BK I (up to 1987) focused on the geological investigation and hydrogeological assessment of the fracture systems encountered in the granite. When the flow testing equipment had been set up, tests with a duration of a few hours or days were conducted. Based on improvements in the test equipment, the tests in phase BK II (up to 1990) were extended to several weeks and months. This report deals primarily with the results of project phase II, during which 100 in-situ tests were carried out.

The principle of the Fracture System Flow Test is primarily to determine the hydraulic conditions at several observation points distributed spatially in the section of rock mass selected for the test. Specially developed probes are installed in the boreholes to monitor pressure, temperature and electrical resistivity. This data is digitized by the electronic processor within the probe before being sent to

the main computer outside the borehole. The original binary data is converted into ASCII and is stored in an archive.

A detailed knowledge of the main hydraulic connecting paths is used for three-dimensional model calculations in which the rock is represented as a discontinuum of joint systems and not as a homogeneous continuum. Simplified analytical and numerical calculations are made to determine the mass transport and hydraulic parameters. It was found, however, that homogeneous modelling of the rock mass yields only an approximation, because the flow processes are obviously influenced by channels and because, in long-term tests, two zones of lamprophyre become evident as hydraulic barriers.

For the preliminary three-dimensional model calculations, the DURST finite-element program system, developed within the scope of the project, has proved itself for simulating flow and mass transport processes. Versions for PCs and mainframe computers are available; the program is being extended to simulate multiphase flow. It is used internationally under the name ROCKFLOW.

This report was prepared within the scope of the research project "Bohrlochkranzversuch (Fracture System Flow Test)" which is financed by the Federal Ministry of Research and Technology (Project no. KWA 53045).

ZUSAMMENFASSUNG

Im Rahmen einer deutsch-schweizerischen Zusammenarbeit zwischen der Nationalen Genossenschaft für die Lagerung radioaktiver Abfälle (NAGRA), der Bundesanstalt für Geowissenschaften und Rohstoffe (BGR) und dem Forschungszentrum für Umwelt und Gesundheit (GSF) werden im Felslabor Grimsel Forschungsarbeiten zur Erkundung der hydrogeologischen, felsmechanischen, geophysikalischen und geochemischen Eigenschaften kristalliner Gebirgsformationen durchgeführt. Innerhalb des Projekts Bohrlochkranzversuch (BK) untersucht die BGR anhand von In-situ-Versuchen und numerischen Modellrechnungen die Bedeutung von Strömungs- und Transportvorgängen im geklüfteten Fels.

Im Mittelpunkt der Projektphase BK I (bis 1987) stand nach dem Abteufen von Kernbohrungen zunächst die geologische Erkundung und hydrogeologische Bewertung der in der ausgewählten Granit - Formation angetroffenen Kluftsysteme und nach dem Aufbau der Durchströmungsanlage die Durchführung kürzerer Versuche mit einer Dauer von einigen Stunden bzw. Tagen. Die Phase BK II (bis 1990) war, basierend auf Weiterentwicklungen der Versuchsgeräte, durch längere Versuchsperioden mit einer Dauer von mehreren Wochen bzw. Monaten gekennzeichnet. Im vorliegenden Bericht werden im wesentlichen die Ergebnisse der Projektphase II dargestellt, in der insgesamt 100 In-situ-Versuche durchgeführt wurden.

Das Prinzip des Bohrlochkranzversuchs besteht zunächst darin, in dem betrachteten Gebirgsausschnitt während eines Versuchs die Reaktion in möglichst vielen Beobachtungspunkten zu ermitteln. Zur Ermittlung der erforderlichen Meßdaten sind in den Bohrungen speziell entwickelte Sonden installiert, mit denen Druck, Temperatur und elektrischer Widerstand in den einzelnen Beobachtungsintervallen konti-

nuierlich registriert werden. Diese Meßwerte werden in situ digitalisiert und von einer zentralen Computer-Anlage aufgezeichnet. Die ursprünglich in binärer Form anfallenden Daten werden zur weiteren Auswertung in ASCII-Daten konvertiert und archiviert.

Die genaue Kenntnis der wesentlichen hydraulischen Verbindungswege soll als Grundlage für dreidimensionale Modellrechnungen dienen, in denen das Gebirge nicht als homogenes Kontinuum, sondern als aus Kluftscharen bestehendes Diskontinuum angenommen wird. Die Auswertung der In-situ-Versuche zur Bestimmung von hydraulischen und den Stofftransport beschreibenden Kennwerten erfolgt zunächst durch vereinfachende analytische und numerische Berechnungen. Dabei zeigt sich jedoch, daß eine homogene Modellierung der betrachteten Gebirgsbereiche nur mit Einschränkungen möglich ist, da die Strömungsvorgänge offenbar durch Fließkanäle beeinflußt werden und bei Langzeitversuchen außerdem hydraulische Begrenzungen in Form von zwei Schieferungszonen wirksam werden.

Bei ersten dreidimensionalen Modellrechnungen hat sich das im Rahmen des Projekts entwickelte Finite-Elemente-Programmsystem DURST zur Simulation von Durchströmungs- und Stofftransport-Prozessen bewährt. Es liegt mittlerweile in Versionen für PCs und Großrechner vor und wird gegenwärtig für die Simulation von Mehrphasen-Strömungen erweitert. Das Programm hat unter dem Namen ROCKFLOW eine internationale Verbreitung gefunden.

Der vorliegende Bericht entstand im Rahmen des vom Bundesministerium für Forschung und Technologie finanzierten Forschungsprojekts "Bohrlochkranzversuch" (Förderkennzeichen KWA 53045).

RESUME

Une collaboration allemande-suisse entre la Société coopérative nationale pour l'entreposage des déchets radioactifs (CEDRA), la "Bundesanstalt für Geowissenschaften und Rohstoffe, Hannover" (BGR) et le "Forschungszentrum für Umwelt und Gesundheit, München" (GSF) a été mise sur pied pour effectuer au laboratoire souterrain du Grimsel des travaux de recherche sur le comportement hydrogéologique, mécanique et géophysique des roches cristallines. En particulier, dans le cadre du projet "Bohrlochkranzversuch" (BK), la BGR étudie les phénomènes d'écoulement et de transport en roche fissurée.

Dans la première phase du projet BK (BK I, jusqu'en 1987), on s'est attaché à la réalisation des forages carottés disposés en éventail à partir de galeries, à leur lever géologique et à l'interprétation hydrogéologique des systèmes fissurés d'un ensemble granitique choisi. Après l'installation d'un dispositif de mesure ad hoc, on a effectué une série d'essais hydrauliques de quelques heures à un jour de durée chacun. Au cours de la deuxième phase du projet (BK II, jusqu'en 1990), on a effectué, après avoir développé le dispositif de mesure, des essais hydrauliques d'une durée de quelques semaines à plusieurs mois. Le présent rapport décrit pour la plupart des résultats de cette dernière phase, au cours de laquelle on a effectué plus de 100 essais in situ.

Le principe des essais en éventail ("Bohrlochkranzversuch") consistè à recueillir la réaction d'une portion de roche donnée à une impulsion, en un nombre aussi grand que possible de points. Pour cela, on a installé dans les forages

des sondes développées à cet effet, capables d'enregistrer en continu la pression, la température et la conductibilité électrique de l'eau dans les intervalles d'observation. Les données sont digitalisées et enregistrées sur place par un ordinateur central, qui traduit le code binaire initial en code ASCII pour l'archivage et le traitement des informations.

La connaissance précise des principales voies d'ecoulement hydraulique sert de base á l'élaboration d'un modèle de calcul tridimensionnel, traitant le massif non pas comme un continuum, mais comme un milieu discontinu qui est constitué d'un réseau de diaclases. L'analyse des essais consiste á définir les paramètres qui décrivent le transport hydraulique et le transport de matière. Elle s'est d'abord effectuée par des calculs analytiques et numériques simplifiés. Toutefois, il s'est avéré que le traitement du massif comme un milieu homogène ne peut se faire qu'au prix des restrictions importantes, car le compartement hydraulique est visiblement influencé par des chenaux d'écoulement, et des limites hydrauliques, correspondant à deux zones de schistosité, se font sentir lors des essais de longue durée.

Pour le traitement tridimensionnel du massif, on a développé dans le cadre de ce projet le code á éléments finis DURST, qui s'est avéré tout à fait capable de simuler les processus de transport déau et de matière. Il en existe une version pour gros ordinateur et une version pour PC. Ce code a fait l'objet d'une extension pour la simulation des écoulements polyphasiques, et a été diffusé sur le plan international sous le label ROCKFLOW.

Le présent rapport fait partie du projet de recherche "Bohrlochkranzversuch" (référence KWA 53045), financé par le Ministère allemand pour la recherche et la technologie ("Bundesministerium für Forschung und Technologie").

Table of Contents Page

List of Appendixes

List of Enclosures

List of Figures Page

Page

Page

Page

Page

Page

Page

Page

List of Tables Page

1. Introduction and Objectives

To guarantee the long-term safety of subsurface waste disposal sites, multiple, independent man-made and natural barriers are used to impede the escape of hazardous substances (LANGER et al., 1989). For a comprehensive safety analysis it is necessary to assess the individual barrier systems, to analyze the physical and geochemical processes within the near and far fields of a final repository, and to assess "worst-case" scenarios.

A probability risk analysis is made to assess man-made barriers (waste matrix and containment). Geotechnical barriers (borehole fill, borehole seal, backfill, bulkheads) are assessed on the basis of a demonstration of the geotechnical safety. The assessment of geological barriers (e.g. host rock) takes potential geochemical, hydrogeological and tectonic processes into consideration. Not only hydraulic factors, but also those that may affect the transport of hazardous substances must be taken into consideration when hydrogeological barriers are assessed.

Mechanisms affecting the flow of fluids include gravity, convergence of cavities, degassing, depressurizing of gases, and tectonic movements. The most important factors affecting the spread of hazardous substances are convective transport, dispersive and diffusive transport, reactions with the rock (e.g. adsorption, desorption, retention, retardation), and the rates at which substances dissolve.

Different kinds of rock formations in all parts of the world are being studied to determine their suitability for use as host rocks for final repositories for radioactive wastes. In Germany, interest is focused on the numerous salt domes in the northern part of the country. Granite formations are

regarded as a possible alternative; in Sweden and Switzerland, for example, they are given a higher priority than in Germany.

The quantitative determination of the spread of hazardous substances along fractures is becoming increasingly the focal point of research, since fractures are generally assumed to be present in crystalline rocks. Studies have indicated that the permeability of fractured rock may show extreme differences. Thus, the barrier efficiency for a specific location cannot be determined on the basis of theoretical considerations. Because homogeneous zones with a virtually impermeable rock matrix containing no fractures are generally of limited extent, the question as to the size of the rock mass to be investigated is inevitable.

The following classification, for example, can be regarded as suitable; the problem that is to be investigated determines the size of the volume of rock that must be taken into consideration:

A Several hundred meters to several kilometers in extent; fractures cannot be individually assessed.
B Several meters to about 100 meters in extent; locations of the major fractures are known.
C A few to several tens of meters in extent; location and size of only one or several fractures are rather precisely known.
D A few decimeters to several meters in extent; location and size of a fracture are precisely known.

The Fracture System Flow Test (called BK in the remainder of this report) of the Federal Institute for Geoscience and Natural Resources corresponds to case B. In some cases,

the instruments installed in the underground laboratory are used to investigate even larger zones several hundred meters in extent. Within the scope of a Swiss–German cooperation project (BREWITZ & PAHL, 1986), the BGR is studying the effect of fractured rock formations as barriers to flow and mass transport. For this purpose, a comprehensive test program has been conducted since 1985 in the Grimsel Test Site (Fig. 1), operated by the National Cooperative for the Disposal of Radioactive Waste (NAGRA). These studies are focused on a specific rock zone in which water percolation is not determined mainly by the porosity of the rock matrix but by the fractures in the rock.

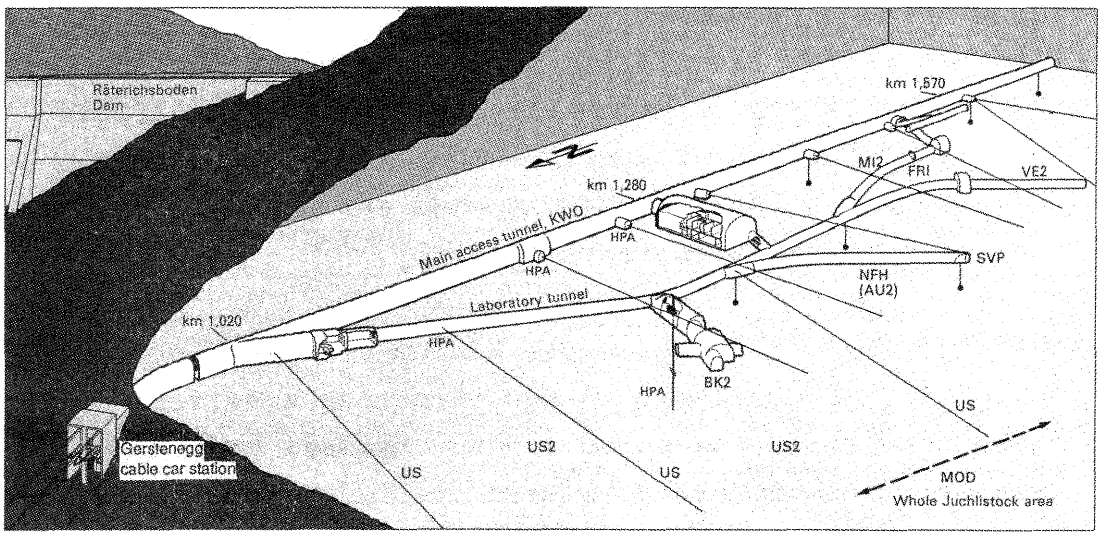

US Exploration borehole
US-borehole
AU2 Excavation effects
BK2 Fracture system flow test
FRI Fracture zone investigation
HPA Hydraulic parameters
MI2 Migration test
MOD Hydrodynamic modelling
NFH Near-field hydraulics
SVP Predict. ahead of tunnel face
US2 Underground seismics
VE2 Ventilation test

Fig. 1: Location of test sites in the underground laboratory

The methods developed within the scope of the Fracture System Flow Test Project for investigating fracture systems utilize a combination of geology, in-situ experiments and model calculations. Geological mapping and target-oriented arrangement of boreholes furnish information for an initial

estimate of the structure of the fracture system and provide a basis for in-situ hydraulic tests. Flow and mass transport detected during the experiment can be simulated by numeric model calculations. Model calculations can be validated and the refined geological interpretation can be checked by additional drilling. The objective is a description of the fracture zone using three-dimensional models with specific dimensions, boundary conditions, hydraulic and mass transport properties.

The location of the Fracture System Flow Test gallery was determined on the basis of boreholes drilled in the 1980s, discharge rates measured for these boreholes, hydraulic tests, and the dip and strike of the fractures in the rock.

The granite or granodiorite in the central part of the Fracture System Flow Test area is bounded by two lamprophyre shear zones forming effective hydraulic barriers. This means that three separate rock zones with great differences in their hydraulic head and permeability are available for in-situ tests (Fig. 2).

The objective of the Fracture System Flow Test project is to obtain information on a specific rock zone from a systematic network of boreholes. In the Grimsel Test Site, four parallel fans of boreholes were drilled according to geological criteria; the boreholes were drilled downwards at angles between 10° and 90° and are, therefore, water-filled.

For an improved understanding of the transport of substances dissolved in water in fracture systems, the flow of water and the spread of brine (as a tracer) was studied. The flow rate of the water in the rock was determined as a function of distance and hydraulic gradient; the possibili-

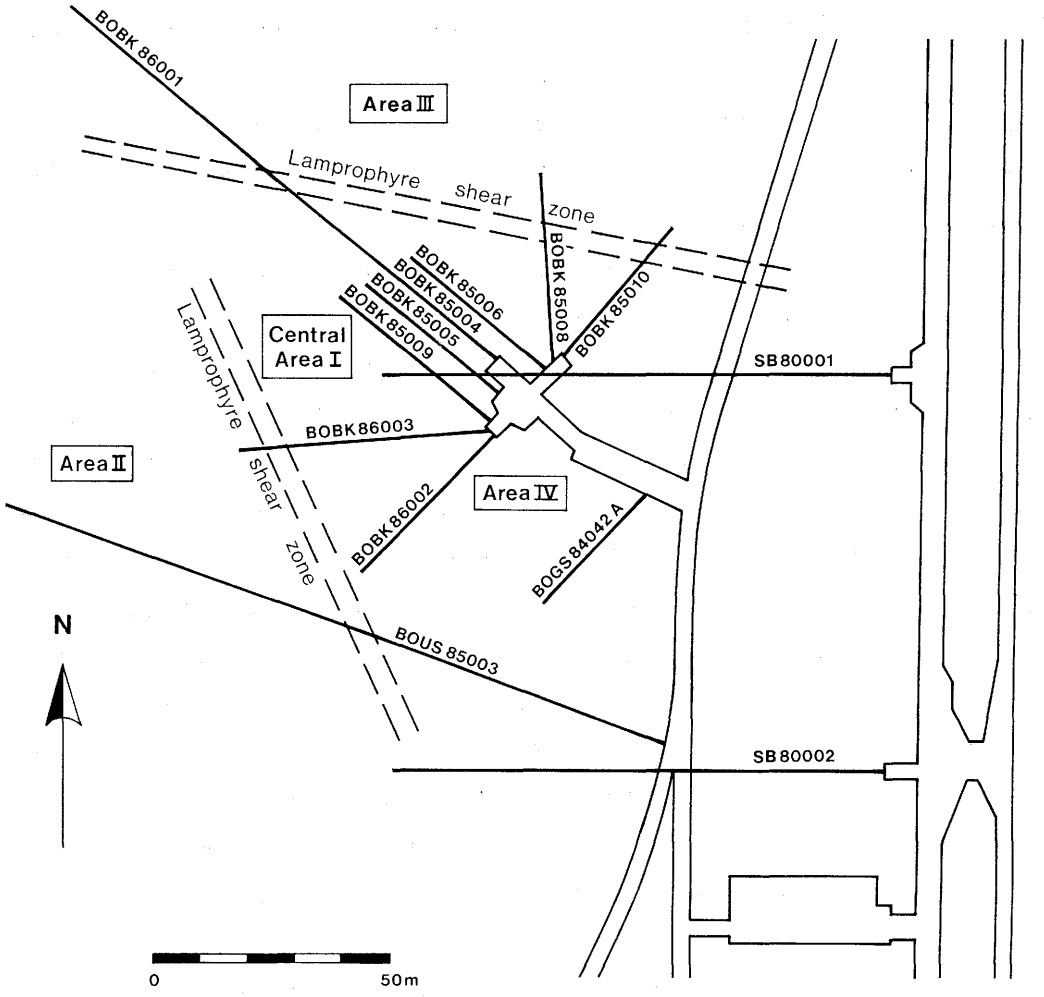

Fig. 2: Plan of the Fracture System Flow Test Site

ty of inclusions of air in the rock were also taken into consideration.

This report deals with the following research and development:

- further development of in-situ methods to test hydraulic conditions in rock (Chapter 2),
- further development of computer programs for model calculations (Chapter 3),
- geological investigations (Chapter 4),
- in-situ tests and model calculations (Chapter 5).

2. The Flow Test Equipment at the Grimsel Test Site

The main equipment for the BGR flow tests at the Grimsel Test Site are packers, probes, computers, pumps, and flow gauges (LIEDTKE & PAHL, 1984). Before in-situ tests are carried out, packers are installed in the boreholes. The function of the packers is to hydraulically isolate specific sections of the borehole. This makes it possible to inject fluids into defined borehole intervals (usually fixed interval lenghts of 1 m) or to determine the discharge from a selected interval of the borehole (e.g. from an interval containing a single fracture). Packers are particularly suited to eliminate the hydraulic short circuits between specific fractures or fracture zones created when a borehole was drilled. In general, pneumatic packers (pressures of 20 – 40 bar) are used for the flow tests. Occasionally, mechanical packers are also used; because the walls of the borehole are smooth, they produce a reliable seal even if high injection pressures are used.

The hydraulic reaction of the fracture system to a test is monitored continuously (Fig. 3). The probes are connected with each other and with the packers by water-tight connections. Up to ten test sections with one probe each can be installed in one borehole (multipacker-probe system). The values registered in-situ by the sensors are sent by the computer in the probe to the data acquisition system. The pressure data provide information on the hydraulic reaction within the fracture system. Temperature and electrical resistivity provide data on transport mechanisms (tracer tests, Section 5.2.2). For example, the injected fluid can contain a tracer that changes the electrical conductivity of the water or it can be heated and the elevated water temperatures (60 – 70°C) can be traced. In addition to the digital values from the probes shown in Figures 4 and 5, analog data is recorded; such data can include pressures

between and in packers, injection and discharge rates, electrical conductivity, humidity, and air pressure and temperature in the drift (at present 24 parameters). Thus, about 100 parameters (digital and analog) are acquired and stored in a central computer.

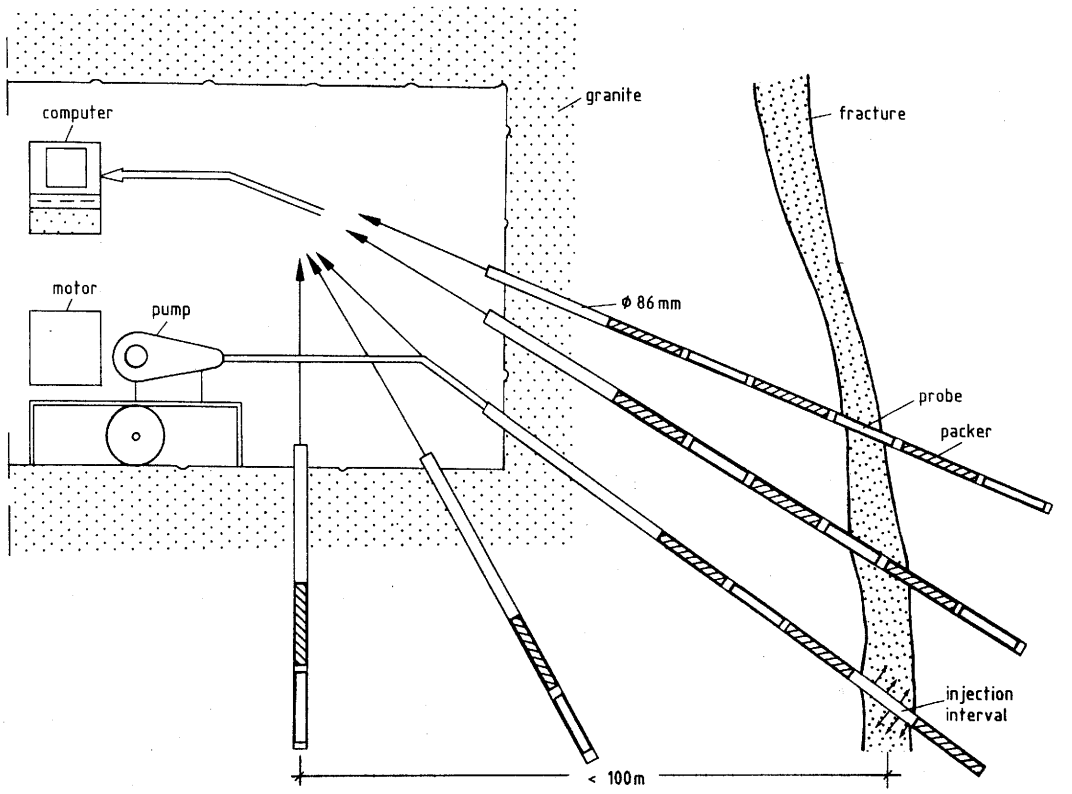

Fig. 3: Schematic diagram of the experimental layout

The main computer is an HP 9836 with a BASIC operating system with hard disk and diskette station, printer and plotter. The minimum interval between readings of one data set is 20 – 30 s (100 parameters). If the interrogation cycle is restricted to the analog data and, for example, the digital data for few boreholes, this time decreases to a minimum of 10 seconds. In addition, PCs connected to analog-digital (AD) converters can be used for decentralized data acquisition of analog data from individual observation points.

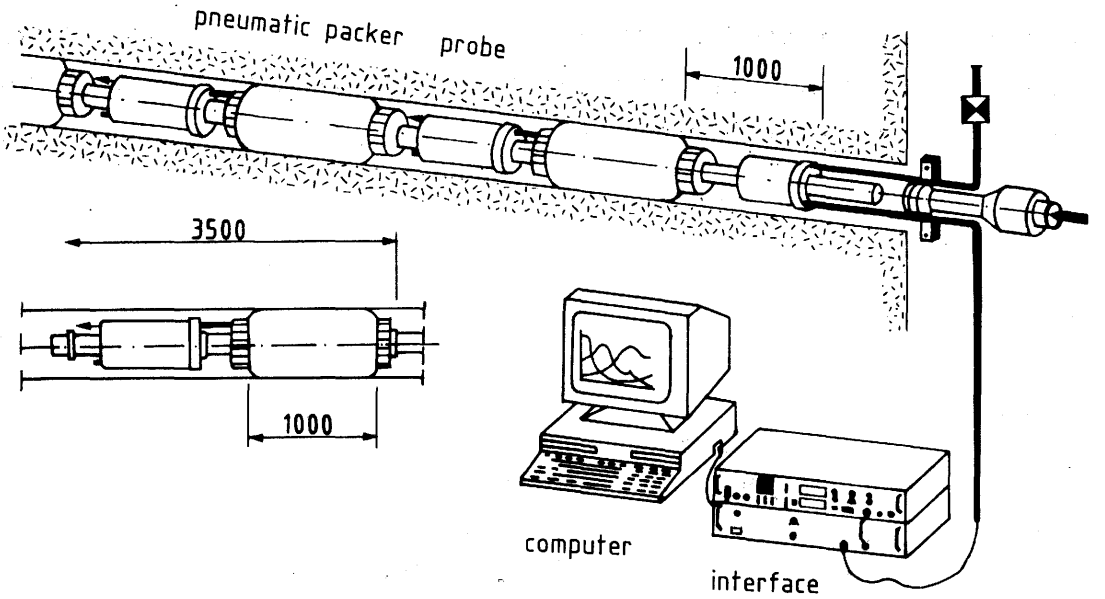

Fig. 4: Injection system

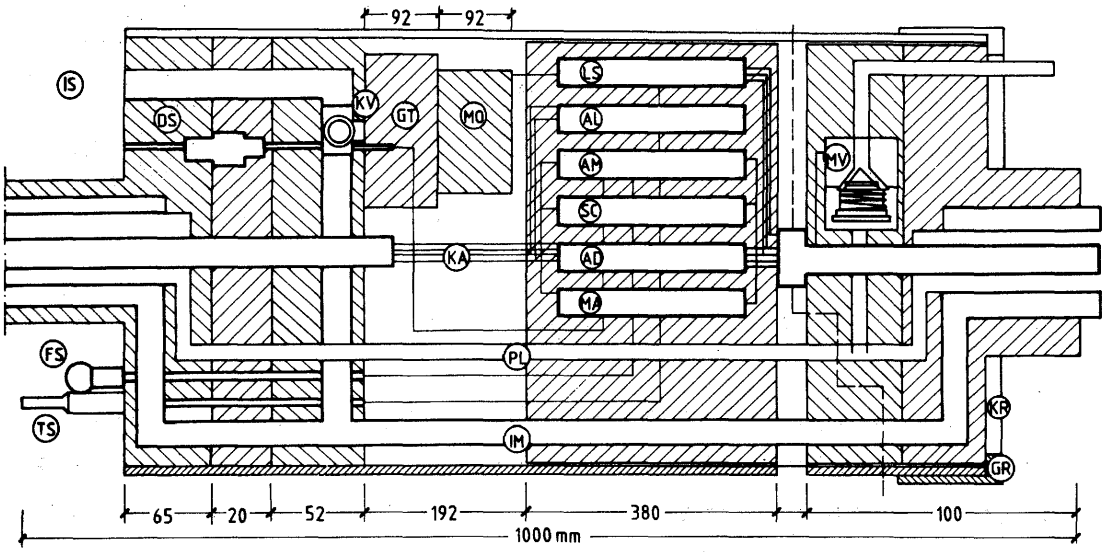

AD = AD converter and multiplexer
AL = address decoder for power switches
AM = address decoder for interrogation of sensors
DS = pressure sensor
FS = humidity sensor
GR = ring nut
GT = gearing
IM = injection line
IS = injection interval
KA = 4-conductor cable
KR = lock nut
KV = ball valve
LS = power switch
MA = amplifier
MO = motor
MV = magnetic valve
PL = compressed air for packer
SC = computer
TS = temperature sensor

Fig. 5: Schematic diagram of the probe

The precision of the equipment is sufficient to adequately measure permeability differences in the rock. The precision of the piezoelectric transducer is 0.01 – 0.1 bar, that of the temperature sensors 0.01 – 0.1°C. Flow rates are more difficult to measure. The flow rate provided by a pump varies considerably; by averaging values, however, the required precision of 0.1 l/min can be obtained. In the case of long-term tests, which cannot be continuously supervised, any susceptibility to failure of the system is very important. The data acquisition system, including the computer system, multiprogrammer, AD converter (ADC), level decoder and the amplifier, has been operating for six years without significant interruption.

An important aspect is the long-term tightness of the packer–probe systems, which have been considerably improved during the project. Many of the probes have been operating perfectly for more than a year. The long-term life of the packers has been considerably improved. The known problems of pneumatic packers can be avoided by testing them before and after installation. Only if the watertightness of the installed system has been demonstrated over a period of 24 hours can a long-term test be started. Adjustments made during a test, especially in the injection borehole, are usually associated with systematic error (bias). Normally, however, loss of pressure in the packers is <0.1 bar/day. As the permeability of the studied fractures is relatively high, compliance effects due to deformation of the packer are negligible. The advantage of pneumatic packers is that inflating and deflating takes little time.

The system is, in general, not sensitive to leaks. The problem is that the installation of a multipacker-probe system in several boreholes requires considerable time and personnel if it is to be carried out with the necessary care. Therefore, a simplified configuration adapted to the individual test might be preferable. Failure of the probes has been reduced considerably by modifications in the TORBEN data acquisition and process control program. The complicated system is justified by the fundamental advantage of in-situ digitizing of the data. Not only can delays be avoided, but also errors in measuring the pressure due to losses caused by changes in the flow direction or energy losses caused by changes in the flow cross section (LANGER et al., 1989).

Control of the test by computer as envisaged in the TORBEN program is based on the flow rate, which is kept constant within set limiting values. Moreover, the valve can be adjusted by a motor controlled interactively. A recently developed probe system allows regulation of the flow rate in any injection section by computers in the probes. This system has been successfully tested and is to be used during phase III of the Fracture System Flow Test at the Grimsel Test Site.

A schematic summary of the systems used for the Fracture System Flow Test is shown in Figure 6.

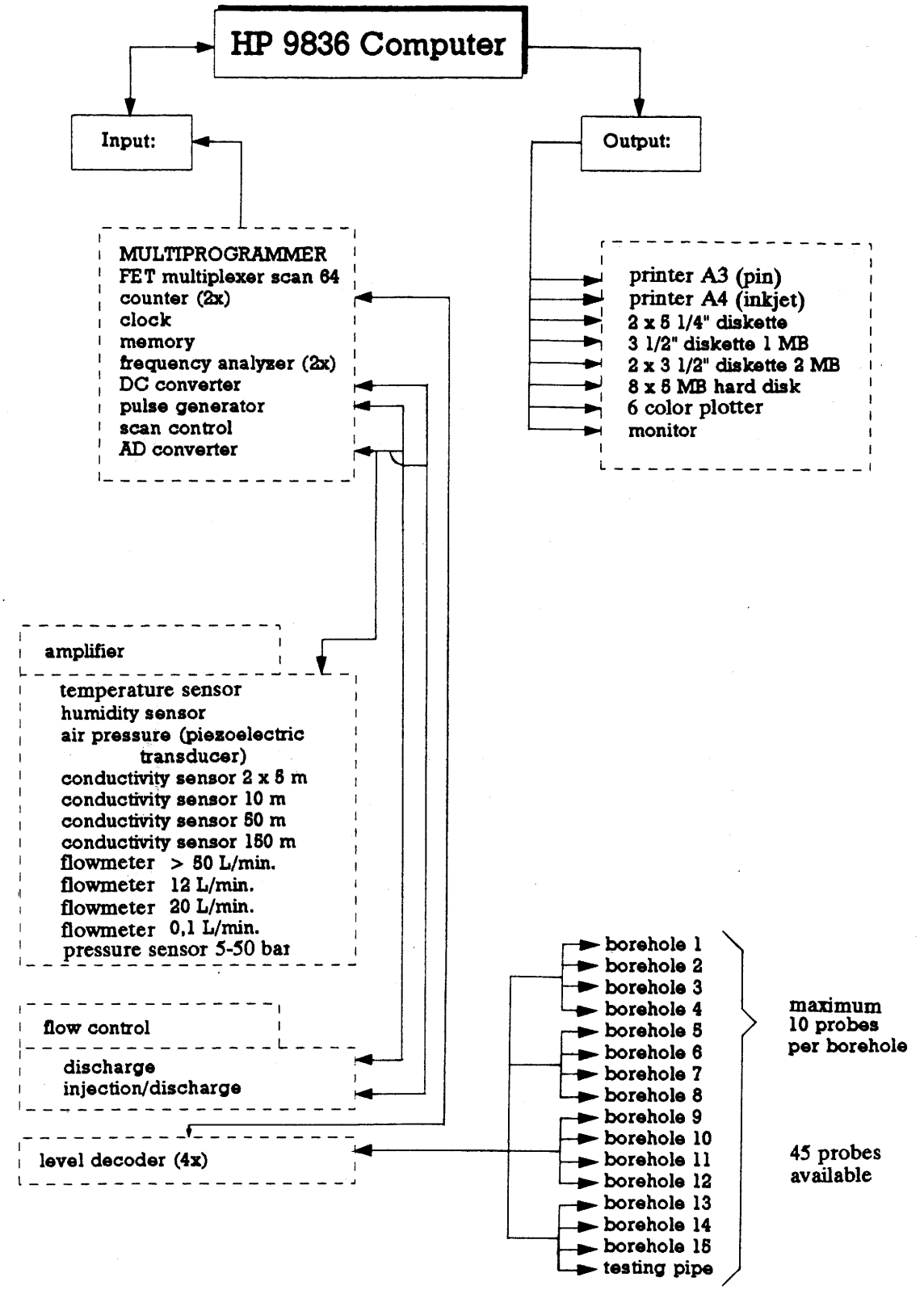

Fig. 6: Data acquisition for the Fracture System Flow Test

3. Development of Computer Programs

A large number of computer programs have been developed for process control, storage, printing and plotting of the test data, as well as for the interpretation of the data. The linking of the computer programs can be seen in Figure 7. The TORBEN program controls acquisition and storage of the test data, as well as the test conditions if necessary. The SIMONE program retrieves data from storage media and produces graphics and converts the data from BDAT format to ASCII for PCs. The test data are used as input data for graphic and statistical programs. The THEIS program calculates transmissivities and storage coefficients. The programs KLUFTMOD and 3D produce spatial representations of the fractures (Fig. 8). The DURST finite-element program is used for three-dimensional model calculations.

The computer programs may be briefly described as follows:

TORBEN is installed on an HP 9836 computer. This program controls the interrogation interval and the motor that regulates the injection rate. During the test, some of the test data is plotted either on the screen or plotter or is printed. The data are stored in binary form (BDAT) on diskettes and/or hard disk. The programming language is HP-BASIC.

SIMONE is also installed on the HP 9836 computer. This program can be used to print or plot selected data. The programming language is HP-BASIC. SIMONE can also be run on IBM-compatible computers via an HT-BASIC interpreter. The PC version of the program converts the selected binary data into ASCII format. The data from individual recording cycles can be converted into a single file.

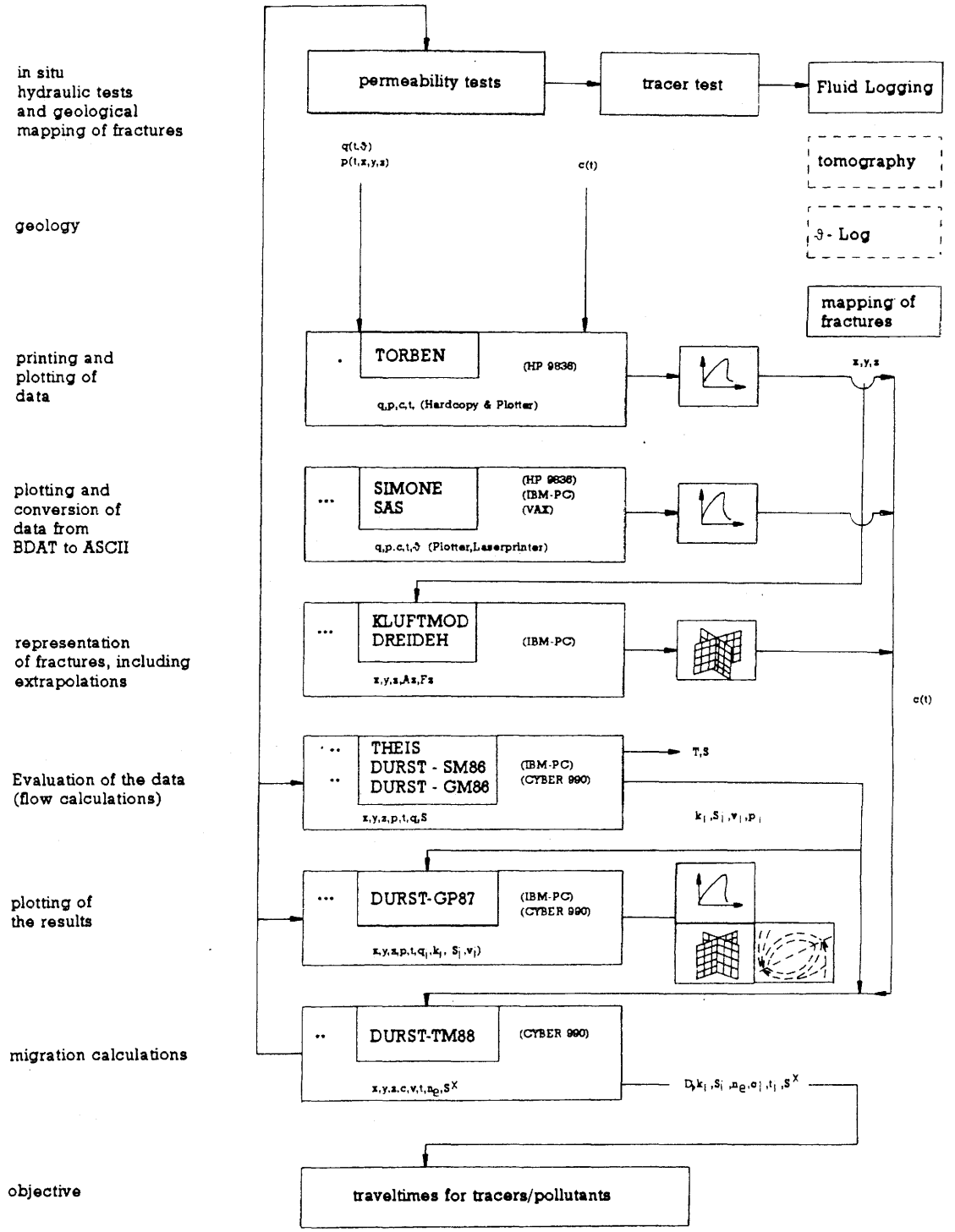

Fig. 7: Linking of the most important computer programs for the Fracture System Flow Test project

KLUFTMOD is used to extrapolate data on fractures and plot them on a polar net or a Schmidt net. Depth, azimuth, dip, weighting factor, and other information (e.g. on minerals in fractures) are included. The graphic output on the polar or Schmidt net can be done on the screen or plotter and can be restricted to individual borehole intervals. The programming language is BASIC.

3D plots perspective views of linear (e.g. boreholes) or planar features (e.g. fractures) in the coordinate system of the Grimsel Test Site. Each fracture plane is defined by the x,y,z coordinates of the center of the fracture, together with its azimuth, dip, and dimensions. The perspective view can be visualized on the screen or a plotter. Parts of fracture planes concealed by other fractures are suppressed. The programming language is BASIC.

DURST (Durchströmung und Stofftransport; English name: ROCKFLOW) is used to calculate three-dimensional fluid flow and mass transfer problems using the finite-element method. It consists of six single programs in various versions (except for the graphics package) for PCs, workstations and mainframe computers. The programming language is FORTRAN.

The following types of finite elements are used by the program: isoparametric hexagonal elements to represent a "homogeneous" rock mass, plane isoparametric quadrilateral elements to represent fractures, and straight line elements to represent

linear channels. Triangular, prismatic and tetrahedral elements can be generated by letting nodes coincide. All of these element types can be arbitrarily combined.

This program package was developed by the Institut für Strömungsmechanik und Elektronisches Rechnen im Bauwesen (Institute for Fluid Mechanics and Computation Applications in Civil Engineering) of the University of Hannover (KRÖHN & ZIELKE, 1990; WOLLRATH & ZIELKE, 1990).

DURST-SM86: Both steady-state and non-steady-state flow in porous and fractured rock can be calculated with this program (flow model: SM). A generalized Darcy's law is used to describe flow, taking into account anisotropic permeabilities and nonlinear flow for parallel plate and pipe flow. Hydraulic heads and flow rates as a function of time can be specified as boundary conditions at the nodes of the model. Hydraulic heads and the input at the nodes are calculated by the SM program. Darcy velocities at specific points can be calculated for each finite element.

DURST-TM86: The spread of an ideal dissolved substance in the groundwater in both porous and fractured rock can be simulated with this program (transport model: TM) (GÄRTNER, 1987; KRÖHN & ZIELKE, 1990). Input for TM is restricted to transport-specific data: discretization intervals, velocity data, time functions and hydraulic parameter values are obtained from the SM program. Since only Darcy velocities are calculated by SM, the velocities are corrected by taking into account a different porosity for each finite element.

In the physically simplest case, the TM calculation can be restricted to purely advective transport. Additionally, diffusive effects can be modeled according to the First FICK Law. Depending on the model, isotropic molecular diffusion or velocity-dependent dispersion can be taken into account using SCHEIDEGGER's equations (Section 5.2). Moreover, if the half-life is given, the decay of radioactive substances can be simulated.

Sources and sinks can be assigned to specific nodes in the model. The concentrations at all nodes must be given at the beginning of the calculations (initial conditions) and the concentrations along the boundaries at which the groundwater enters the area of calculation must be known throughout the simulation (boundary conditions).
The concentrations at each node and transport across the model boundaries are calculated by the TM program.

DURST-GM88: Steady-state and non-steady-state flow of gasses in porous and fractured rock can be calculated with this program (gas model: GM). The porosity coefficient must be set to zero for steady-state calculations. Hydraulic heads and flow rates as a function of time can be given as boundary conditions at any nodal point. Pressure, density, inflow at selected nodes and Darcy velocities within selected elements are calculated.

DURST-TD88: The spread of an ideal dissolved substance in a flowing, compressible fluid in porous and fractured rock can be simulated with this program (gas-transport model: TD). Input for TD is restricted to transport-specific data: discretization intervals, velocities, densities, inflow and

and other parameter values are obtained from the GM program.

In the physically simplest case, the TD calculation can be restricted to purely advective transport. Additionally, diffusive effects can be modeled according to the First FICK Law. Depending on the model, isotropic molecular diffusion or velocity-dependent dispersion can be taken into account using SCHEIDEGGER's equations (Section 5.2). Moreover, if the half-life is given, the decay of radioactive substances can be simulated.

The concentrations at all nodes must be given at the beginning of the calculations (initial conditions) and the concentrations along the boundaries at which the groundwater enters the area of calculation must be known throughout the simulation (boundary conditions). The concentrations at each node and transport across the model boundaries are calculated by the TD program.

DURST-GP87: This program is the graphics post-processor for the SM and TM programs within the DURST program system. Hydraulic heads, velocities and concentrations at selected times can be plotted along the boundaries (linear or planar) of the finite elements. These parameters can also be plotted as a function of time at selected nodes. For plots along planar boundaries, hydraulic heads and concentrations are represented as isolines and velocities as vector fields.

DURST-KG: Planar fracture networks consisting of line elements are generated with this program fracture generator, developed by the Institute for Fluid Mechanics of the University of Hannover; WOLLRATH

& ZIELKE, 1990). Orientation, length and aperture of the fractures in these networks are calculated using random distribution functions; it is also possible to take individual, known fractures into consideration. The simulation models generated by this program are then used for flow and transport calculations using the SM and TM programs, respectively.

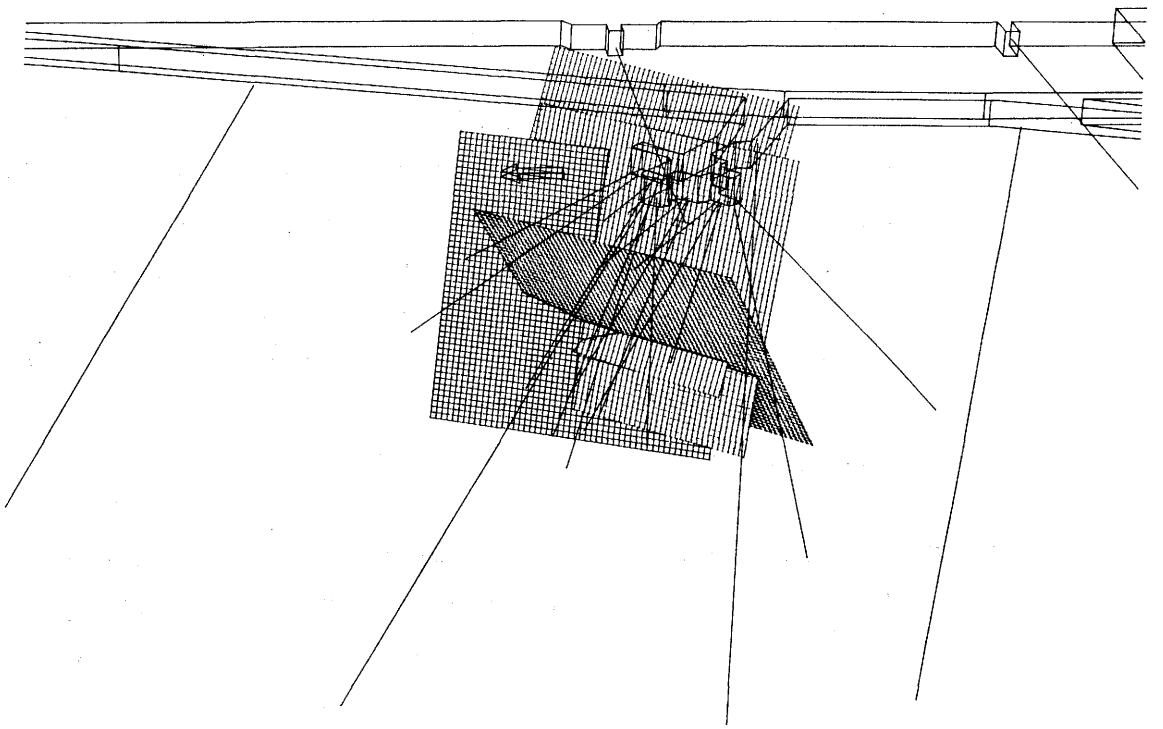

Fig. 8: Grimsel Test Site: four fractures in the central part of the Fracture System Flow Test area; looking down at a 20° angle to the east

4. Geological Studies

4.1 Geological Description of the Test Site

The Grimsel Test Site is located at a depth of 400 – 450 m below the peak of the Juchlistock in the southern part of the Central Aare Massif. The granitic rocks, Central Aare Granite (ZAGr) and Grimsel Granodiorite (GrGr) represent more than 90 % of the rock exposed in the drifts and galleries of the laboratory. Locally, it is difficult to distinguish them macroscopically from one other (STALDER, 1984). Both the Central Aare Granite and the Grimsel Granodiorite are cut in the laboratory by several decimeter- to meter-thick lamprophyre dikes.

Tension joints of Alpine origin, characterized mostly by a hydrothermally altered, sometimes porous rock selvedge, are typical of the Grimsel Test Site. The permeability of the rock in these zones is greater than that of the intact rock and, in addition to the fractured rock zones, these zones are the most important for the flow of groundwater in the rock. The regional geology of the Grimsel area and the laboratory is described by KEUSEN et al. (1989) and a detailed geological description of the Fracture System Flow Test area is given by BRÄUER et al. (1989).

4.2 Geological Studies in the Fracture System Flow Test Area

4.2.1 Layout and Objective of the Boreholes

Originally, it was planned to drill a circle of boreholes around a central injection borehole for the hydraulic tests.

On the basis of the mapping of the fractures, this configuration was modified so that the boreholes would pass through hydraulically significant fractures at known depths at predetermined angles. Thus, the geological evaluation of the first few boreholes determined the orientation of the subsequent boreholes. The gently dipping to perpendicular fan-like configuration of the boreholes (Fig. 9) allowed positioning of the packers for fluid injection and observation of the hydraulic response within numerous intervals with representative hydraulic conditions in the rock.

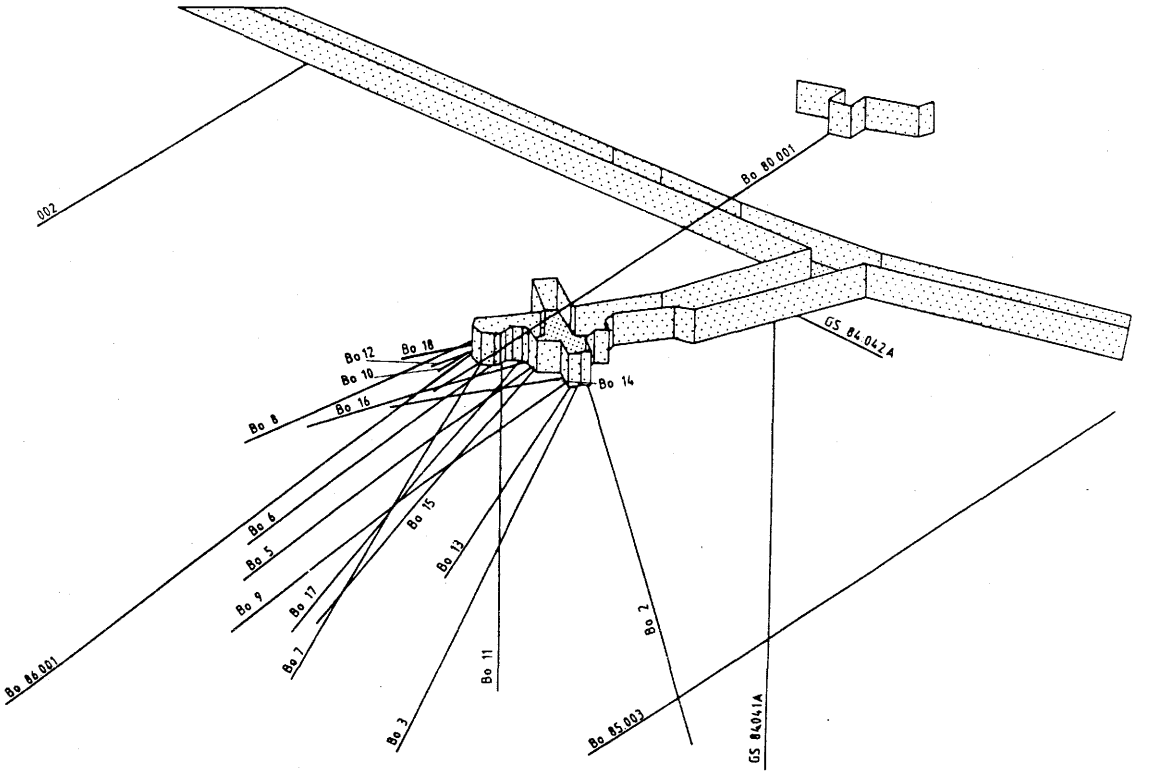

Fig. 9: Injection and observation boreholes in the Fracture System Flow Test area

During the first two drilling phases in 1985 and 1986, a total of 582.93 m were drilled. The geological features and the fractures encountered by these boreholes have been

described by BRÄUER et al. (1989). In a third phase of drilling, seven additional boreholes totaling 191.96 m were drilled in 1988 (Table 1).

Table 1: Data on the boreholes drilled in 1988 (third phase)

Borehole	ø mm	Depth m	Az/Dip Degree	Coordinates y	x	z	Drilling time
BK 88.012	86	4.85	310.1/ 8.7	413.88	222.81	1730.71	02.11.88
BK 88.013	86	29.20	309.4/58.1	414.45	209.12	1729.84	11.10.-17.10.88
BK 88.014	86	22.15	309.4/10.3	413.91	209.59	1730.69	05.10.-11.10.88
BK 88.015	86	41.25	308.7/48.9	415.65	214.67	1729.89	24.10.-01.11.88
BK 88.016	86	28.40	309.4/10.0	415.26	215.01	1730.76	11.10.-24.10.88
BK 88.017	86	48.78	311.0/50.4	424.74	218.61	1729.83	09.11.-22.11.88
BK 88.018	86	17.33	313.5/ 9.1	424.56	218.84	1730.79	03.11.-09.11.88

The objective of these boreholes was

- to acquire more comprehensive knowledge on the geological structure of the Fracture System Flow Test area,
- to confirm and supplement the information on the known fracture systems, and
- to localize open fractures belonging to certain fracture systems and to intersect water-bearing fractures.

To achieve these objectives, hydraulically significant fractures in the Fracture System Flow Test area were mapped in order to develop a fracture model as a basis for numerical calculations.

4.2.2 Mapping and Interpretation Methods

Like most of the other boreholes in the laboratory, the boreholes for the Fracture System Flow Test were drilled and cored using the conventional rotary drilling method. The boreholes for the Fracture System Flow Test are 86 mm in diameter; the diameter of the oriented cores is 72 mm. Core analysis, especially of the brittle structures, was done using the method described in NAGRA (1981).

To determine hydraulic relationships and identify the interconnected water-bearing fractures, packers and probes were installed during the drilling of further boreholes. Thus, permeable zones can be indicated by a reduction in pressure in the sections between packers in the boreholes.

4.3 Results of Geological Mapping

4.3.1 Description of the Rock Penetrated by the Test Boreholes

The third drilling phase in 1988 confirmed the geological information already available. The mostly mesocratic Central Aare Granite (ZAGr) in the Fracture System Flow Test area is predominantly medium-grained. In addition to melanocratic zones, the mostly equigranular rock also shows porphyritic zones. Massive zones alternate with intensely fractured zones (BRÄUER, 1990a).

Locally, hydrothermally altered granite was encountered, but no lamprophyre dikes. The geological description (BRÄUER et al., 1989) was supplemented by the following information obtained during the third drilling phase in 1988 (more detailed geological data are given in enclosures 1 to 7):

Borehole 88.012 (4.85 m, Enclosure 1):
The first ca. 1.60 m of the borehole penetrated mesocratic, medium-grained, massive granite. After a zone with a strong flow of groundwater in the next 0.20 m, the granite was massive to a final depth of 4.85 m.

Borehole 88.013 (29.20 m, Enclosure 2):
This borehole passes through leucocratic to mesocratic granite. Zones with a random mineral orientation alternate with zones of slightly to distinctly parallel texture. Zones showing slight hydrothermal alteration were penetrated from 2.2 m to about 3.0 m. There were relatively few open fractures. There was no significant flow of water from the borehole during drilling (Section 4.3.2).

Borehole 88.014 (22.15 m, Enclosure 3):
Slightly to distinctly foliated mesocratic and mostly massive ZAGr was penetrated in the first ca. 17.0 m. From there to the final depth of 22.15 m, however, the rock contained heavily fractured zones with discharge of groundwater into the borehole.

Borehole 88.015 (41.25 m, Enclosure 4):
The first ca. 25.0 m of the borehole penetrated massive to slightly fractured, mesocratic granite with slight indications of parallel texture. From there to about 25.3 m, a hydrothermally altered zone was encountered. Part of the granite here was cavernous, due to leaching of quartz. The larger cavities (max. 8 mm) were filled with granular chlorite and idiomorphic quartz crystals. In the remaining part of the borehole, slightly fractured granite alternated with heavily fractured zones, in parts showing shearing and mylonitization. Towards the final depth of 41.25 m, indications of tectonic deformation increased.

Borehole 88.016 (28.40 m, Enclosure 5):
Zones of massive, mesocratic, medium-grained ZAGr alternated with slightly fractured, partly kakiritized zones in the first ca. 17 m. Beginning at about 18 m, the number of fractures increased. To a depth of about 22 m the borehole passed through water-bearing zones. To about 26 m, the granite was heavily fractured and in parts mylonitized; towards the final depth of 28.40 m, it became increasingly massive.

Borehole 88.017 (48.78 m, Enclosure 6)
The first ca. 15.8 m of the borehole showed slight to heavy fracturing, including a quartz-chlorite-mylonite fault zone at 5 – 6 m. Massive granite was penetrated during further drilling to about 24 m. A zone with a strong flow of groundwater was encountered at about 24.7 m, followed by another quartz-chlorite fault zone. The zone between 28 and 29 m was also heavily fractured and probably contained water. From there to the final depth of 48.78 m, slightly fractured zones alternated with heavily fractured zones with a water-bearing zone at about 34 – 35 m.

Borehole 88.018 (17.33 m, Enclosure 7):
Slightly fractured zones alternated with heavily fractured zones in the ZAGr down to the final depth of 17.33 m. At a depth of 9.1 – 9.3 m, the granite showed hydrothermal alteration. Water-bearing zones were encountered at a depth of about 8.0 – 9.2 m and at various depths between 14 and 20 m.

4.3.2 Statistical Evaluation of Fracture Geometry

The distinct parallel texture observed in the Central Aare Granite and the Grimsel Granodiorite, and the various fracture systems crossing them, suggest that these rocks have

been subjected to several phases of tectonic activity. The geological interpretation of the fracture zones in brittle rock at the Grimsel Test Site was concentrated, therefore, mostly on assigning fracture systems to specific tectonic phases. According to recent studies, a division of the fractures into groups of shear planes (S) and groups of fracture planes (K) with differing orientation cannot always be applied to the Grimsel Test Site (BOSSART & MARTEL, 1990). When the fractures in the Fracture System Flow Test site were being mapped, for example, it was usually impossible to distinguish the orientations of the S1, S2, and S3 planes. However, some of the most important systems and their spatial orientation (Fig. 10) should be discussed so that a correlation with the classification of the fractures by KEUSEN et al. (1989) can be made within the scope of the geological description of the rock laboratory.

The geological evaluation of the boreholes of the first two drilling phases of the Fracture System Flow Test showed that circulation of water took place mainly in the fractures of the S1/S2 and K4 systems. The locations of the planes of these systems were known and to a certain degree also extrapolatable. The boreholes of the third drilling phase were oriented to pass through these planes for the subsequent hydraulic tests.

The data on the fractures in the additional boreholes show that – with the exception of borehole BK 88.013 – the boreholes pass through the planes of the S1/S2 and K4 systems as planned (Fig. 10). In addition to these planes, borehole BK 88.013 encountered a number of closed fractures in the K3 system. No significant flow of water into this borehole was observed during drilling, although a hydraulic connection

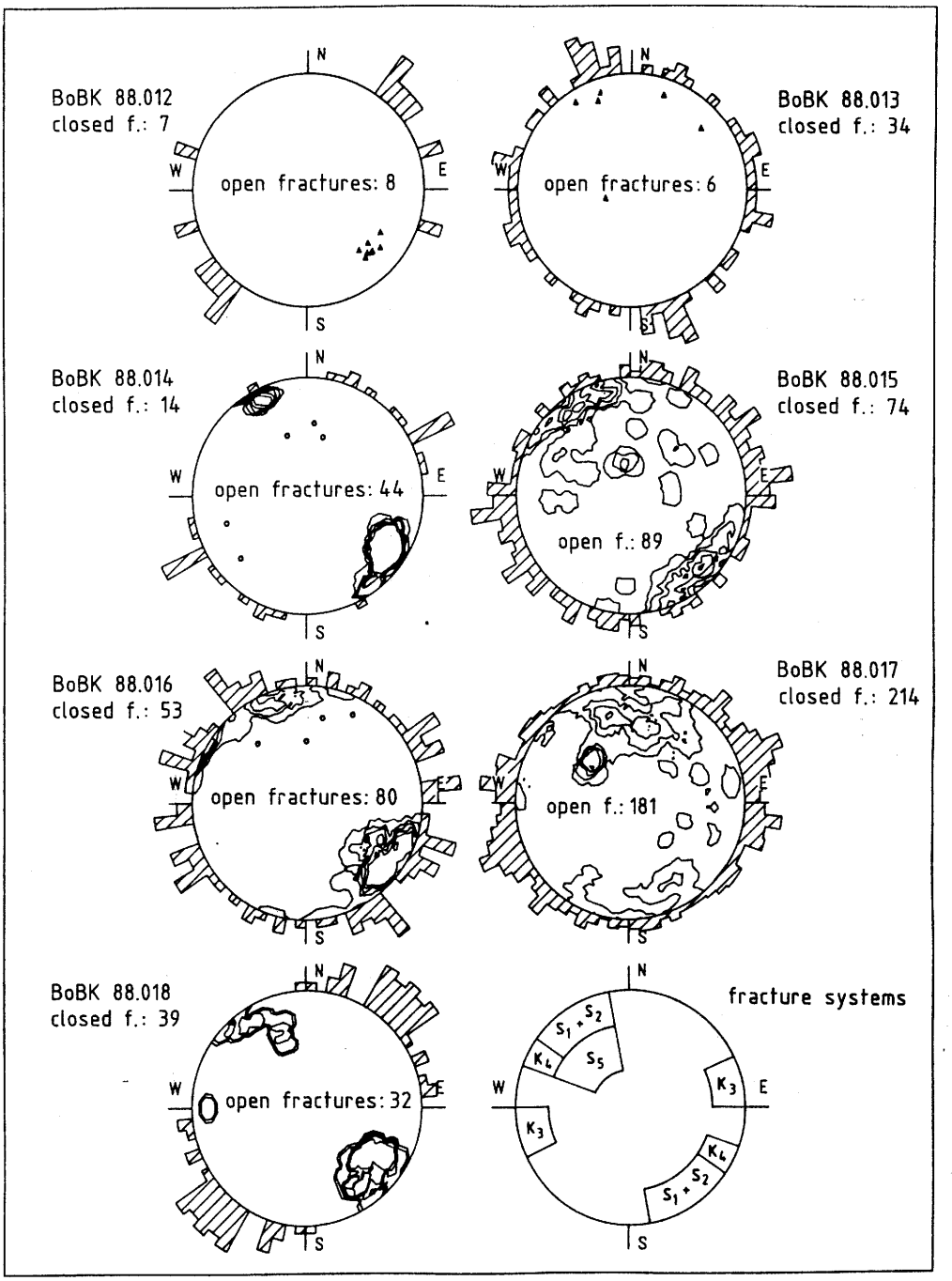

Fig. 10: Fracture orientation in the boreholes drilled in 1988 for the Fracture System Flow Test: Outside the circles: closed fractures (strike directions); Inside the circles: open fractures (Schmidt net, lower hemisphere projection; 1, 3, 5, 7 and 10% lines)

with other boreholes within the Fracture System Flow Test area was indicated later by a drop in water pressure in other boreholes. This is probably due to extensive connections between the fractures of the various systems (Fig. 11).

The water inflow in borehole BK 88.017, which was drilled to pass through the S1/S2 system, was about 7 l/min at a depth of about 24.0 to 28.7 m even before the fractures of the S1/S2 system were reached. In this section, open fractures of the relatively gently dipping S5 system were cut, which probably provided a hydraulic connection with the open fractures of the S1/S2 system within the Fracture System Flow Test area.

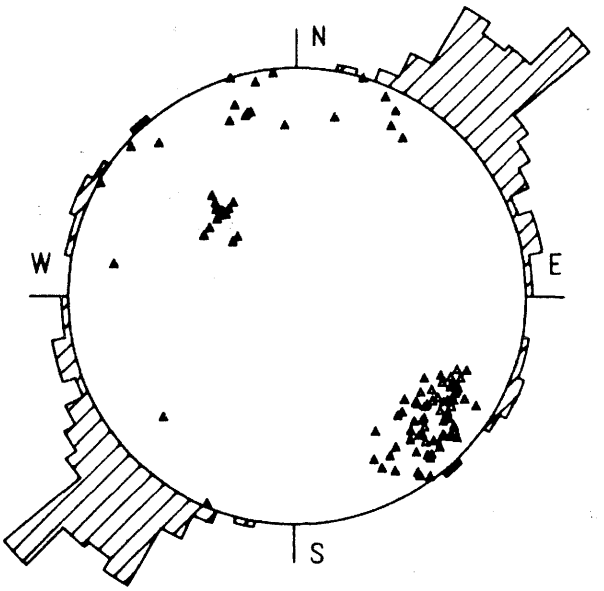

Fig. 11: Orientation of the water-bearing fractures in the boreholes drilled during the third phase (101 fractures, Schmidt net, lower hemisphere projection; strike directions also shown)

Evidence for a hydraulic connection with the fractures of the S1/S2 system at about 33.9 – 34.6 m was also provided by a pressure drop in other boreholes. A zone of S3 fractures was also encountered in this borehole.

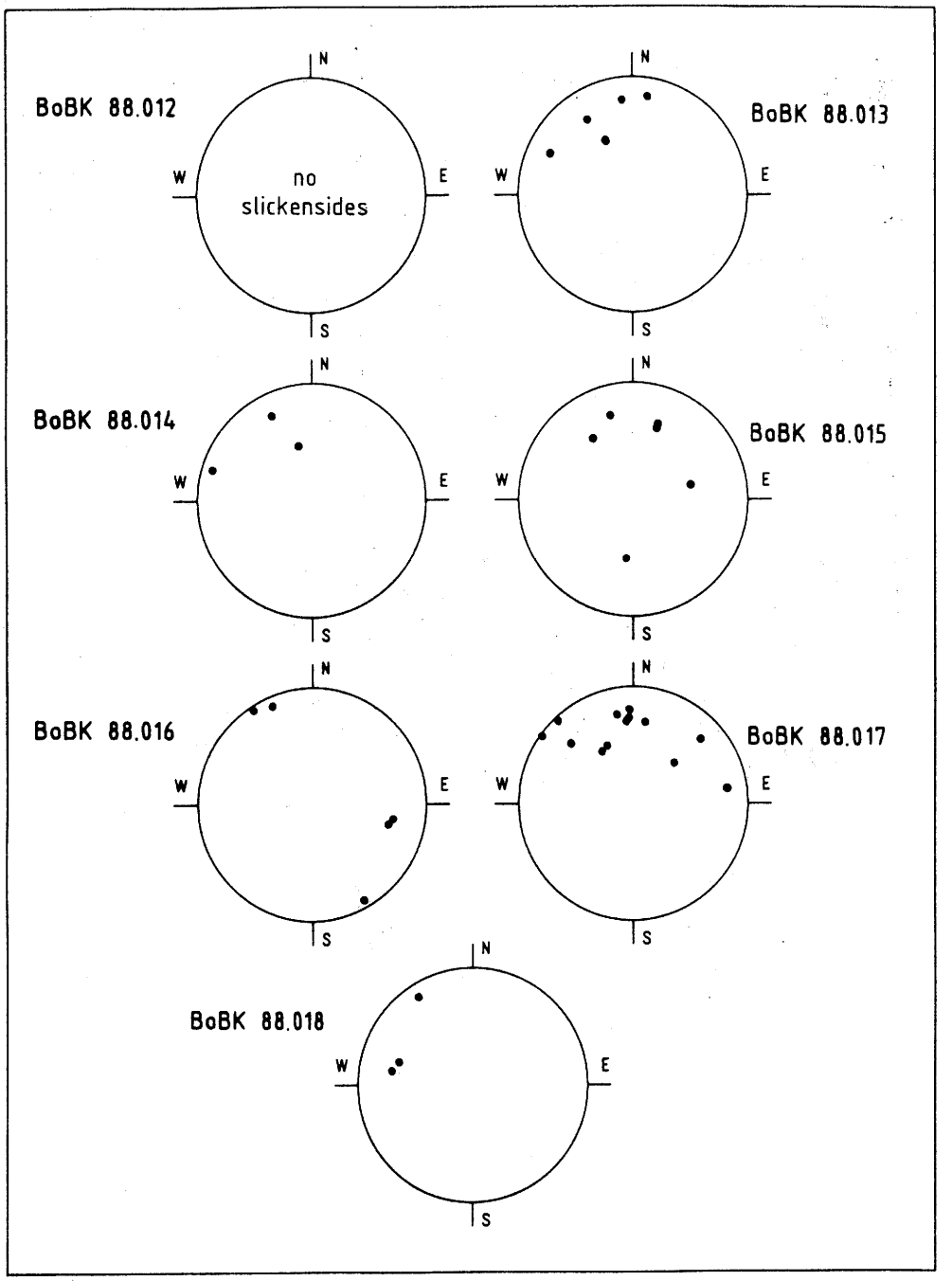

Fig. 12: Orientation of the slickensided planes encountered in boreholes drilled during the third phase (Schmidt net, lower hemisphere projection)

The aim to pass through mainly open fractures was achieved with the boreholes drilled in the third phase. This is reflected by the relatively small number of slickensided planes (35) that were encountered (Fig. 12), most of them following the main Alpine foliation. Because there were so few of them, the slickensided planes were not statistically evaluated. However, an analysis of the slickenside lineations using the data from the boreholes of the first two drilling phases was made by BRÄUER et al. (1989).

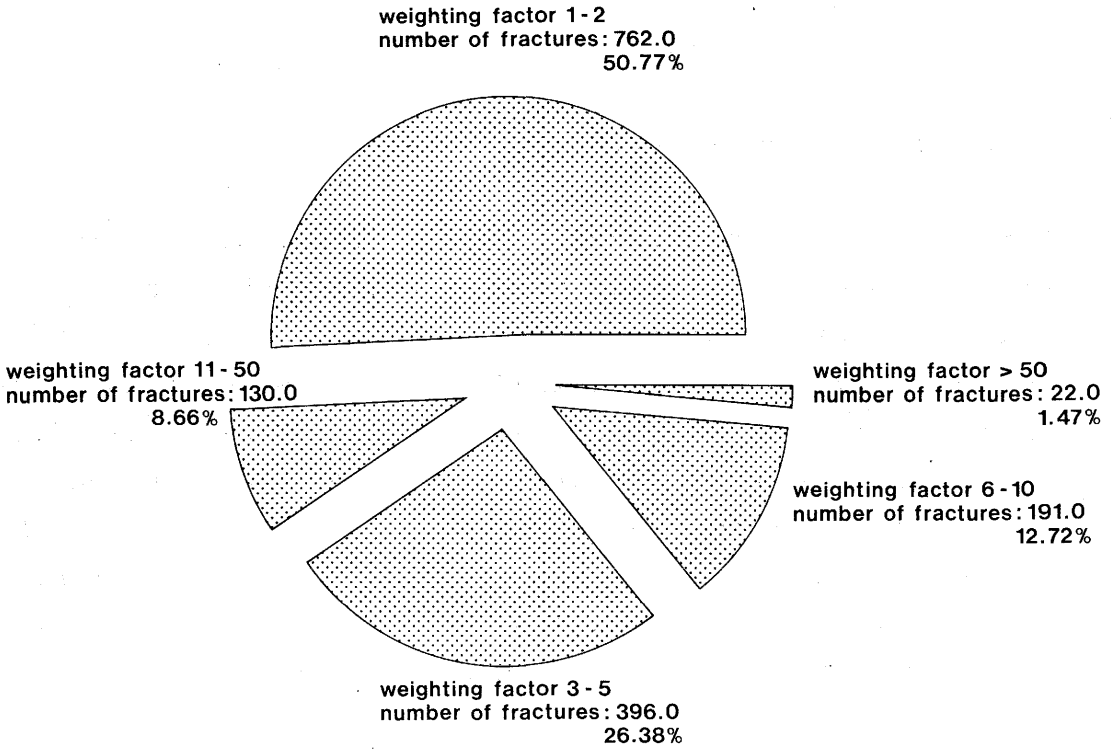

Fig. 13: Frequency distribution of the open fractures in the Fracture System Flow Test area according to weighting factor:

1 - 2:	fracture can be seen without a magnifying glass
3 - 5:	aperture <1 mm
6 - 10:	aperture about 1 mm
10 - 50:	several fractures of >1 mm
>50:	fracture zone several dm wide

The classification system for open fractures that was introduced in the first drilling phase to provide weighting factors for hydraulic analyses was used and refined during the third drilling phase (BRÄUER et al., 1989). This classification of the fractures was important for the initial estimation of the flow of water from the water-bearing fracture zones. The frequency of the fracture classes indicates that most of the open fractures had apertures of about 1 mm or less (weighting factors 1–2, 3–5, and 6–10) (Fig. 13). The rather high flow rate encountered in the Fracture System Flow Test area is, therefore, attributable almost exclusively to the clustering of these fractures in groups of sometimes more than 20 fractures.

4.3.3 Hydraulic Aspects

Before drilling was begun in 1988, all boreholes within the Fracture System Flow Test area were equipped with probes for measuring changes in hydraulic head in the rock and then sealed. Packers were installed in borehole sections chosen on the basis of geological aspects. In one case (BK 85.009), seven zones of open fractures were separated from each other. Drilling was started after sufficient hydraulic head had accumulated. Immediately after drilling, the borehole was equipped with a probe and then sealed to avoid further lowering of the hydraulic head in the fractures.

When the water-bearing zones were encountered, an initial inflow with a maximum 7 – 8 l/min was observed. The discharge rate then gradually decreased to a continuous rate of about 2 l/min.

Almost all of the packer sections in the observation boreholes showed a drop in pressure when water-bearing fractures were cut. Differences in fracture aperture and thus the permeability of individual fractures are indicated by the differences in the rate of the drop in pressure. As an example, Figure 14 shows the water pressure in the observation boreholes during the drilling of borehole BK 88.012. The probes measuring the pressure in boreholes BK 85.011, 88.014 and 88.016 showed a gradual drop in pressure when the water-bearing fracture zones were reached in BK 88.012. In boreholes BK 85.004, 85.005, and 85.006, this pressure drop was abrupt and was observed at the same time in all three boreholes, although they were at different distances from BK 88.012.

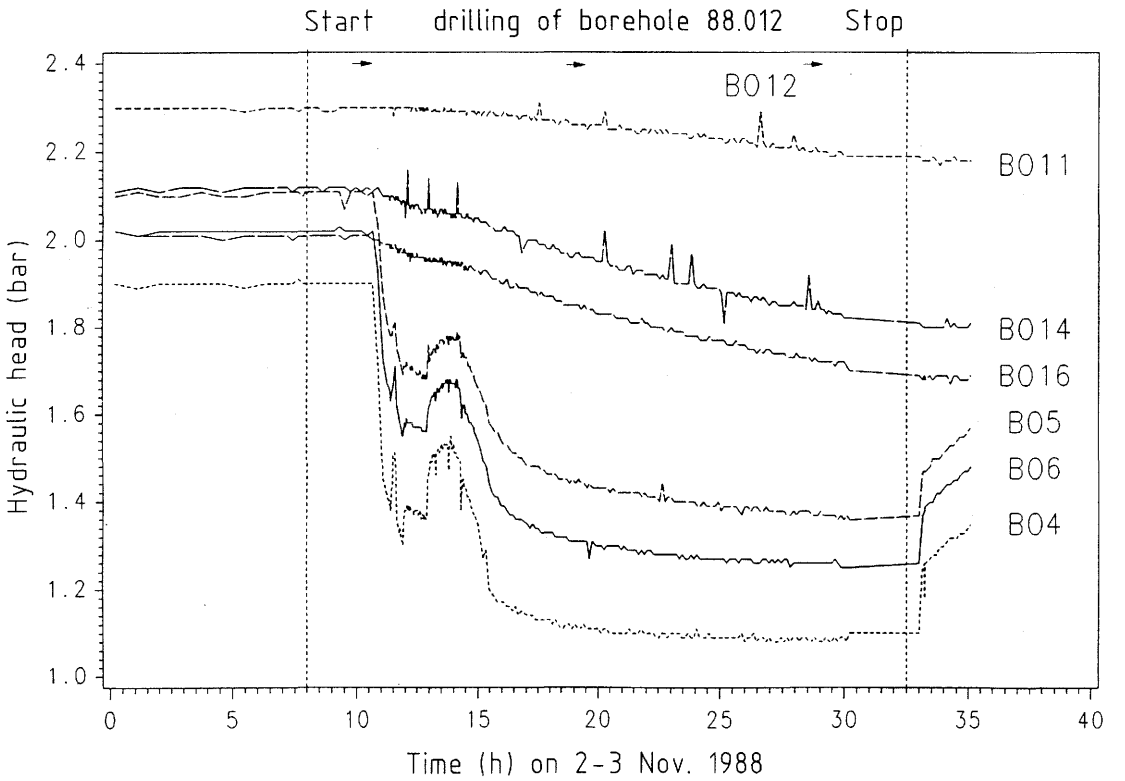

Fig. 14: Drop in hydraulic head in observation boreholes during the drilling of borehole BK 88.012 (BRÄUER, 1990b).

The variations in drilling fluid pressure (about 4.5 to 5.0 bar) in borehole BK 88.012 are reflected in the slight variations in the first part of the curves, suggesting a direct hydraulic connection between the observation boreholes and the borehole being drilled. After the drilling of BK 88.012, a packer was installed at the mouth of borehole. This resulted in immediate recovery of the water pressure in boreholes BK 85.004, 85.005 and 85.006.

Another example (Fig. 15) shows the pressure drop in boreholes BK 85.009 and 88.015 during the drilling of borehole BK 88.017. The pressure reductions recorded by the probes (S2 – S7) show clearly that borehole BK 88.017 penetrated two zones of open fractures at depths of about 24.5 and 34.0 m.

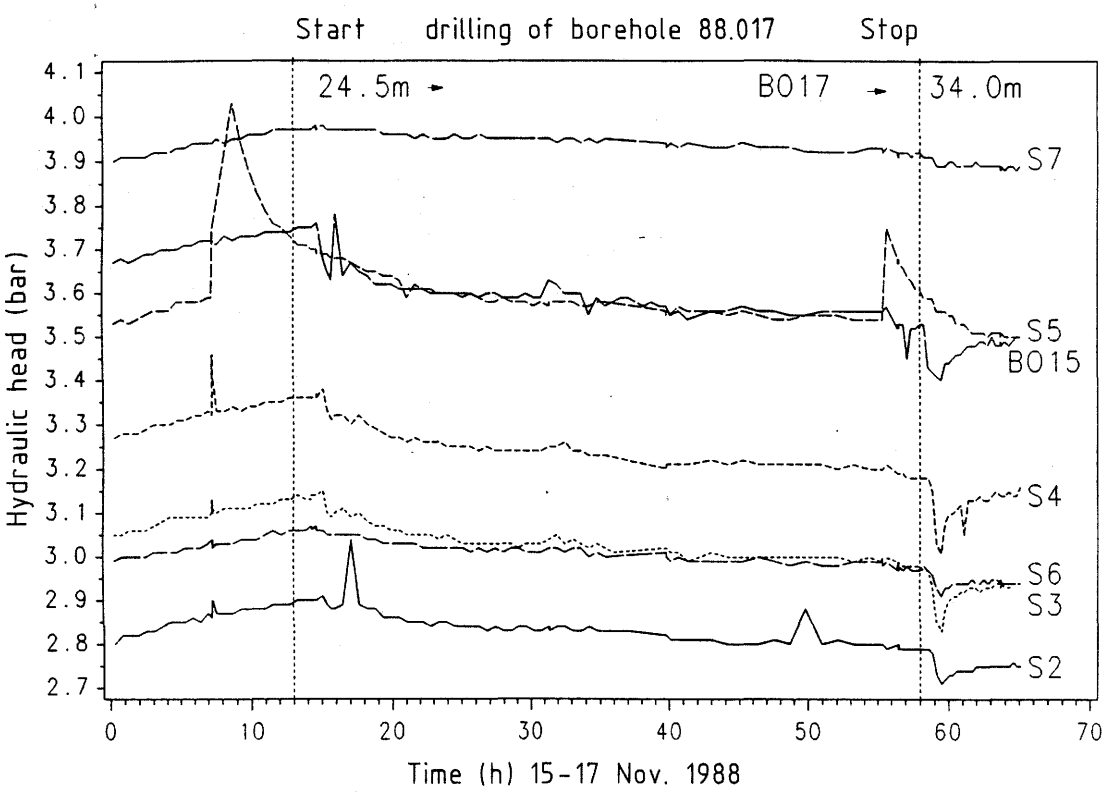

Fig. 15: Drop in hydraulic head in observation boreholes during the drilling of borehole BK 88.017 (BRÄUER, 1990b)

The hydraulic head measurements in the observation boreholes provided information on the location of water-bearing fractures, making it possible to estimate the size of the fractures in the Fracture System Flow Test area.

4.3.4 Correlation of the Geological Interpretation of the Core and Electrical Conductivity Tracer Tests (Fluid Logging)

When all of the boreholes had been drilled, electrical conductivity tracer tests (fluid logging) were carried out by NAGRA (KELLEY & FRIEG, 1990) and BGR (Section 5.2.1) to identify zones with open fractures.

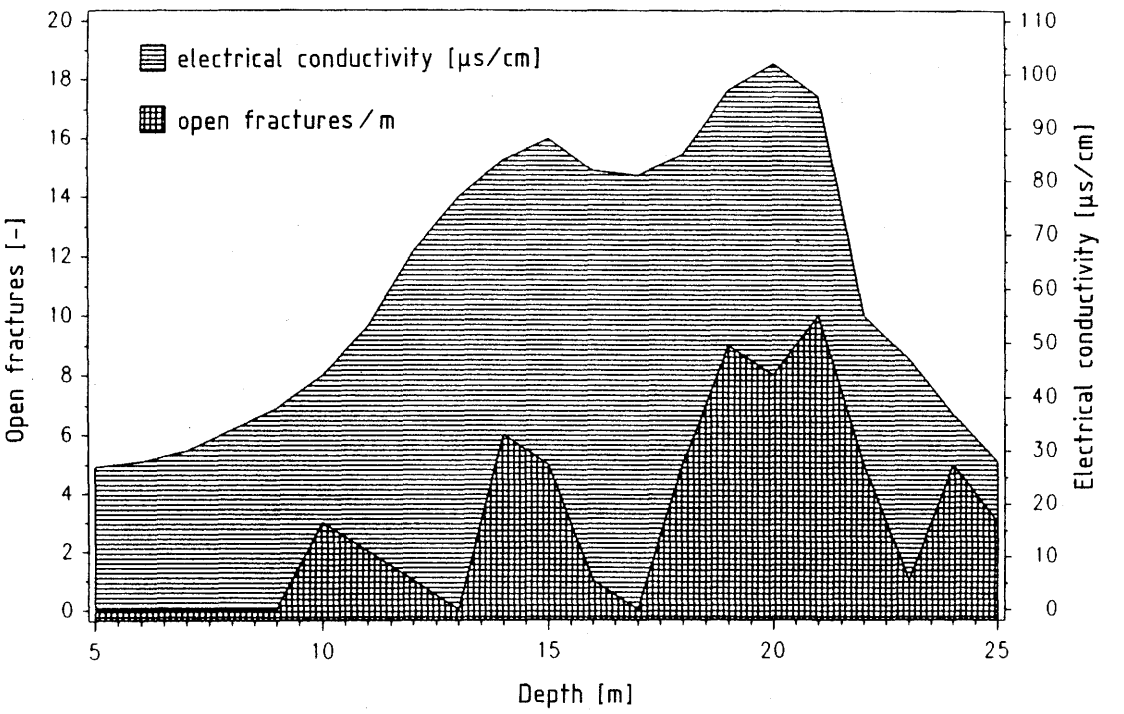

Fig. 16: Relationship between electrical conductivity and frequency of open fractures in borehole BK 85.010

After flushing the system with fresh water, a salt tracer was injected in one of the boreholes and conductivity logs were run in an observation borehole with a conductometer. An increase in electrical conductivity in the observation borehole provided information on the locations of open fractures.

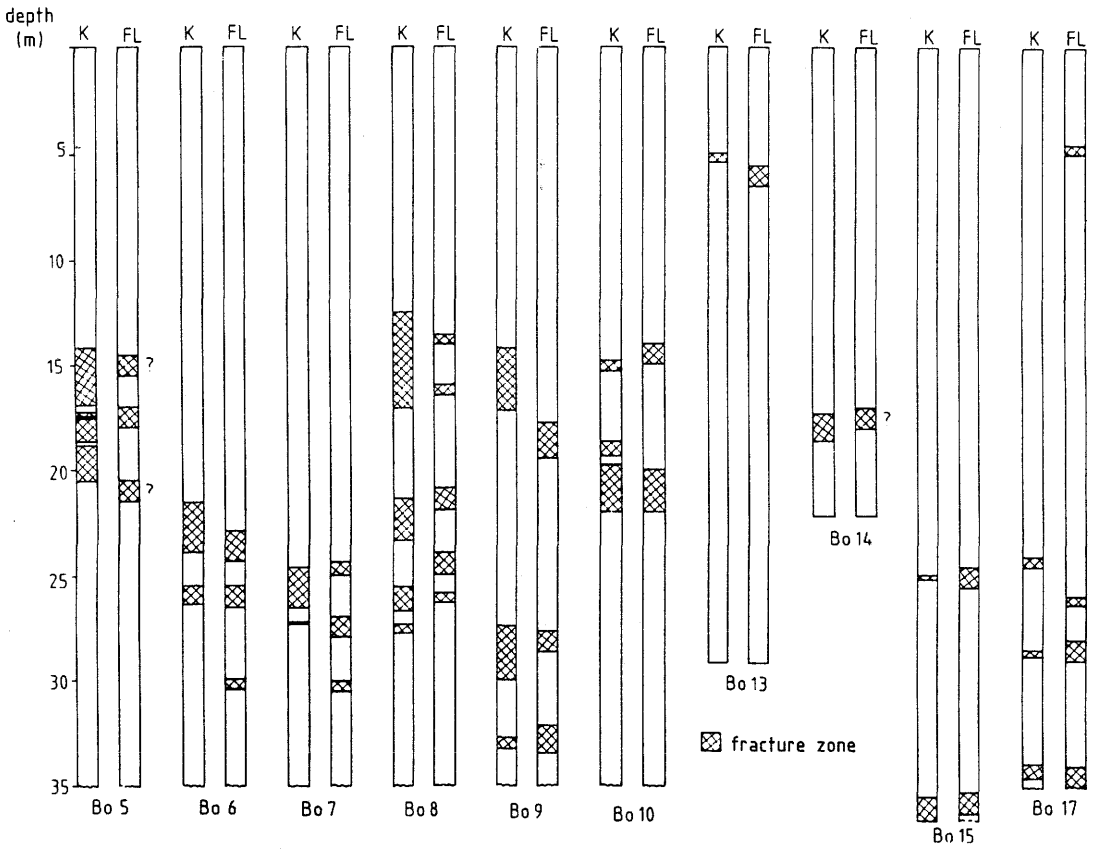

Fig. 17: Comparison of the results of the geological evaluation of cores (K) and fluid logging (FL) (⊠ indicates the location of the fracture zones identified by each method)

An example of fluid logging is shown in Figure 16 (borehole BK 85.010). Discharge of the salt tracer at about 20 m depth correlates directly with a zone of numerous open fractures. Another conspicuous increase in conductivity was observed at a depth of about 15 m. Here, too, the granite contains numerous open fractures.

Thus, it is clear that the geological evaluation of the cores, especially the identification of the zones with open fractures, is in general confirmed by the results of fluid logging. The geological evaluation shows in detail the distribution of the open fractures, whereas the fluid logs show only the places where the tracers reappear in the boreholes.

Using combined fluid/temperature logs it was also possible to locate zones of groundwater discharge that were not identified by an increase in conductivity (KELLEY & LOEW, 1991).

A comparison of the geological evaluation of cores and the results of fluid logging in the Fracture System Flow Test area mostly shows agreement (Fig. 17). It must, however, be taken into consideration for both fluid logging and pressure reduction measurements that injections were only made in one borehole and measurements in one observation borehole at a time. This explains the differences in the position of the water-bearing zones. The agreement in almost all boreholes indicates, however, that there are many connections between the fractures so that the water flows through the rock along various fractures at the same time. Therefore, fluid logging and temperature measurements are valuable supplementary methods for the geological evaluation of the cores. Due to their simplicity, these methods help to rapidly locate water-bearing fractures.

4.3.5 Hydraulically Significant Fracture Systems in the Fracture System Flow Test Area

The hydraulic connections of the fractures in the near-field of the Fracture System Flow Test area were reassessed on the basis of the information from the geological evaluation of the drill cores, the hydraulic conductivities of the fractures, the changes in water pressure in the rock during the last drilling phase, and the injection and conductivity tests. Fractures in individual zones at various drilling depths were classified according to orientation (mean azimuth and dip). Owing to the small amount of data for the boreholes of the first two phases, they were classified by comparison with, and extrapolation of, data from boreholes of the third phase (Table 2).

The distribution pattern of the water-bearing fracture systems developed on the basis of the data from the first two phases was refined using the new data. The complete analysis of the geology and hydraulic conditions on the basis of the results of the third drilling phase, together with the results of the fluid logs, was used to develop a simple fracture model for the calculation and simulation of the flow paths in the Fracture System Flow Test area (Section 5.4).

Table 2: List of zones of open fractures in the boreholes in the central part of the Fracture System Flow Test area (b = orientation opposite to that of the unmarked fracture systems, az = dip azimuth, hydr. = hydrothermal alteration, FL = fluid logging)

Borehole No.	depth (m)	System	mean az/dip	number of fractures	cored	Fluid Logging
85.004	2.6- 4.4	S1/S2 b	312/65	7	x	no FL
	6.8- 7.4	S1/S2 b	321/73	7	x	no FL
	7.8- 8.2	S1/S2 b	339/77	5	x	no FL
	8.7- 9.3	S1/S2 b	323/69	4	x	no FL
85.005	14.1-17.0	K4 b	295/71	16	x	x
	17.2-17.5	S1/S2 b	308/73	8	x	x
	17.5-18.7	K4 b	295/67	7	x	
	18.8-21.0	S1/S2 b	317/78	9	x	x
85.006	21.4-24.0	S1/S2 b	307/70	12	x	x
	25.4-26.4	K4 b	293/78	8	x	x
85.007	24.6-27.0	K4 b	296/65	5	x	x
	27.2-27.6	S1/S2 b	320/78	2	x	x
	30.0-30.5	ZK	311/23	1	x	x
85.008	12.4-14.4	S1/S2 b	313/58	4	x	x
	15.8-17.1	S1/S2 b	309/60	2	x	x
	21.6-21.8	S1/S2 b	327/68	1	x	x
	25.5-25.7	S1/S2	146/86	2	x	x
	27.1-27.8	S1/S2	162/90	8	x	(x)
85.009	14.2-15.2	K4 b	302/66	2	x	
	14.2-15.2	S1/S2	143/76	2	x	
	18.3-19.3	S1/S2	145/81	2		x
	27.48	S1/S2 b	306/68	1	x	
	27.8-28.5	S5 hydr.	131/53	>15	x	x
	30.04	K4 b	302/68	1	x	
	32.8-33.3	ZK hydr.	154/21	4	x	x
85.010	14.8-15.3	K2	198/76	6	x	x
	18.7-19.4	K4 b	290/71	5	x	x
	19.8-22.0	hydr.		>15	x	x
85.011	6.0- 8.0	S6	295/51	5	x	no FL
88.012	1.6- 1.8	S1/S2 b	314/64	7	x	no FL
88.013	5.1- 5.3		219/48	2	(x)	(x)
88.014	17.3-18.6	K4 b	300/68	21	x	(x)
88.015	25.0-25.1	S1/S2 b	317/70	1	x	x
	35.4-36.7	S1/S2 b	320/76	11	x	x
88.016	19.3-21.8	S1/S2 b	314/75	13	x	no FL
88.017	4.5- 5.0	K2	203/77	4	(x)	x
	24.0-24.5	S5	137/41	12	x	
	26.0-26.5					x
	28.5-28.8	S5	131/38	9	x	x
	33.9-34.6	S1/S2	168770	4	x	x
88.018	8.0- 9.3	S1/S2 b	319/71	10	x	no FL
	14.0-16.0	K4	302/65	6	x	no FL
	16.0-16.5	S1/S2 b	318/74	1	x	no FL

5. Hydrogeological Studies

5.1 Hydrogeology of the Test Site

Borehole SB 80.001 was drilled at a low angle from the main drift to explore the rock in which the BK gallery was driven later. A zone with a flow of about 1 – 4 l/min was encountered at a depth of about 82 m in the borehole. This increased to 24 l/min when the borehole reached a depth of about 94 m (NAGRA, 1981). This high rate of flow rapidly dropped to a constant 1.5 – 2 l/min. Interpretation of the fracture zones in brittle rock in the drill cores showed that the water-bearing fractures were mostly S2. On the basis of this information, the Fracture System Flow Test gallery was located so that the water-bearing fractures could be used for hydraulic tests. When this zone was approached during the excavation of the gallery, water seeped from fractures in the roof and walls. When water also began to flow from boreholes drilled for blasting, further advance was stopped to avoid draining of the rock.

The rock was immediately mapped geologically, revealing a network of closed fractures of varying orientation in the part of the gallery near the access drift. Further into the gallery, however, open fractures were mapped. From a number of these, a weak to strong flow of water was observed. The drill cores obtained later confirmed that the water-bearing fractures were mainly S1 to S3.

During phases I and II of the Fracture System Flow Test, tests were conducted in zones I, II, and IV (Fig. 2), which have no hydraulic connections with each other that are relevant to the test. The original hydraulic head of about 40 bar, corresponding to a cover of rock 400 m thick, was

considerably reduced when the gallery was driven and the boreholes were drilled – the water flowing off through the access drift. Strictly speaking, this means that all tests were carried out under more or less transient conditions.

The highest hydraulic conductivities were observed in the heavily fractured test area I, the central part of the Fracture System Flow Test area (see Section 5.3.1), in which 16 boreholes were drilled: BK 85.004, 85.005, 85.006, 85.007, 85.008, 85.009, 85.010, 85.011, 88.012, 88.013, 88.014, 88.015, 88.016, 88.017, 88.018, and SB 80.001. Most of the fractures are interconnected. However, there are individual neighbouring parallel fractures which, over considerable distances, have no identifiable hydraulic connection with each other. From this it can be derived that the permeability of the rock matrix is negligible in comparison with the permeability of the fractures. In some cases, the connection between two fractures was created only when the borehole was drilled. For in-situ tests, these artificial connections have to be eliminated by packers to avoid misinterpretations.

In the central part of the Fracture System Flow Test area, the rock in the neighbourhood of the gallery is almost completely drained if one of the boreholes remains open over a period of several weeks. Eventually, the discharge rate approaches about 2 l/min. Additionally, there is a discharge of about 0.5 l/min from the walls of the gallery. When all the boreholes are closed, the hydraulic head rises only very slowly. The maximum values reached within 2 months are less than 10 bar. During this time the discharge in the gallery increases to about 1 l/min. Drainage of the rock may also occur through the gravel bed beneath the concrete floor via boreholes BK 85.007 and 85.011; during a test, however, this can be avoided by packers.

Observations indicate that the rock surrounding the gallery is almost saturated with water when all the boreholes are closed. When the hydraulic conditions change, all the above-mentioned boreholes – as well as borehole SB 80.001 in the roof of the gallery, which has been sealed with a packer since 1988 – react with virtually no delay. When boreholes were closed in the central Fracture System Flow Test area, no reaction (i.e. increase in discharge or hydraulic head) was detected in the neighbouring test areas (i.e. on the other side of the shear zones shown in Fig. 2) or in more distant zones which, in principle, might offer possibilities for discharge. This means that the discharge of about 2 l/min that is prevented when all boreholes are closed comes mostly from the fractures of the central Fracture System Flow Test area, for which a volume of several cubic meters can be calculated.

Test area II is penetrated by borehole BK 86.003, drilled from the Fracture System Flow Test gallery (see Section 5.3.2). The rock, which in the deeper part of the borehole is heavily fractured and hydrothermally altered, shows a connection to borehole US 85.003; the exact geometry of this connection, however, is not known. Above the shear zone in this borehole, there is no seepage of groundwater. When these two boreholes are open, their discharge rates are both about 2 l/min. When one of the boreholes is closed, the hydraulic head in that borehole (at the level of the laboratory gallery) rises to 12 – 13 bar within a few weeks. At the same time, the discharge rate in the other borehole rises to 4 l/min. When both boreholes are closed for a long time, the pressure rises to more than 40 bar. In this case, borehole BK 86.002, which ends before the shear zone begins, shows a very subdued reaction.

Test area III, on the other side of the lamprophyre shear zone (Fig. 2), penetrated by boreholes BK 86.001, 85.008, 85.010, and possibly borehole US 85.002, has not yet been included in the tests.

Another test area (IV) was included in the Fracture System Flow Test program using the 191m vertical borehole GS 84.041A, drilled within the scope of the Rock Stress (GS) project (Section 5.3.3). Hydraulic connections with the central Fracture System Flow Test area or one of the other Fracture System Flow Test boreholes were not found. During 1987 and 1988, borehole GS 84.041A was constantly open; the discharge rate was less than 0.1 l/min.

5.2 Fundamental Considerations

5.2.1 Basic Ideas on Rock Hydraulics

Various models can be used to describe flow in rock:

- porous medium (flow only in the matrix),
- fractured medium (flow only in the fractures),
- double-porosity medium (flow in matrix and fractures).

If a sufficiently large observation section ("representative elementary volume") is chosen, the assumption of quasi-homogeneous flow leads to a continuous model of the rock with possibly anisotropic permeability (SNOW, 1965). If the rock zone to be studied does not allow homogenization, flow in the individual fractures must be considered. This must be done by taking two-dimensional flow in parallel plates as a basis. For complicated three-dimensional fracture zones consisting of individual, randomly distributed, intersecting fractures, however, exact solutions are not possible. Thus, if it is assumed that the rock is discontinuous (LOUIS, 1967) the hydraulic system in this case can be modeled only with numerical calculation methods. The DURST finite-element program system (Chapter 3), developed within the scope of the Fracture System Flow Test project, is being used for this purpose. A special case occurs if the water flows preferably along linear channels within a two-dimensional frac-

ture and especially at intersections of fractures. The fact that "parallel plate flow" becomes "pipe flow" greatly simplifies numerical calculations. The assumption of laminar flow which in general is valid for porous media is not always justified for fractured rock. A linear relationship between pressure and flow rate, which is to be expected if Darcy's law is valid, is only seldom observed in in-situ injection tests. There are many reasons for this. A more rapid increase in the flow rate than the increase in injection pressure, for example, may be due to expansion of the fractures caused by the increased pressure, i.e. caused by the test conditions. If the increase in flow rate is slower than the increase in pressure, this is not definite proof of turbulent flow conditions, since especially during short-term tests this may be caused by non-ideal geometry of the flow paths in the fractured rock. When in-situ tests are evaluated, it may be assumed on the basis of the Reynold's number that turbulent conditions prevail in the immediate vicinity of the injection zone, but that at some distance and after longer periods of time the flow becomes laminar. Therefore, complicated flow laws are normally not applied for model calculations.

The granite formation being investigated in the Fracture System Flow Test project is a typical fractured aquifer and is suitable for studying the possibilities and problems of discontinuous modeling. Knowledge of the structure of the rock is a prerequisite. To obtain this knowledge, comprehensive geological and hydraulic investigations are necessary. Evaluation methods for determining parameters for a qualitative assessment of rock permeability or for numerical simulation calculations are generally based on continuous models and use geometric idealizations. Therefore, section 5.4 deals with the uncertainties and confidence intervals resulting from these simplifying assumptions. In principle, however, numerical methods, e.g. simplified two-dimensional models adapted to the special case, can also be used for

closing the gap between simple models and complicated three-dimensional model calculations. An increasing number of attempts have been made to use models based on rock hydraulics for quantitative calculations on transport in fractured rock. Although many of the fundamental physical phenomena are in principle well known, difficulties arise in practice because, compared to merely hydraulic modeling, the number of the unknown factors increases. Thus it is necessary to describe the rock as exactly as possible. Such rock mechanics models can be developed in one of two different ways: (i) The transport in very precisely known individual fractures is described in great detail or (ii) the three-dimensional propagation of substances in the rock over large distances is modeled by random mechanisms. Studies are conducted at the Grimsel Test Site within the scope of the Fracture System Flow Test to determine whether three-dimensional discontinuous modeling is possible for transport in fracture zones that are rather precisely known but for which statistical simplifications must be made.

The most important terms, which are not uniformly used in the literature, are briefly listed here. Since theoretical considerations are generally based on the assumption of a porous medium, they can be applied to fractured rock only with some restrictions. A distinction must be made between hydraulic conductivity and storage capacity on the one hand and parameters for describing the transport of dissolved substances on the other hand.

a) Description of hydraulic properties

The term hydraulic conductivity, k_f (length/time), is used as a measure of permeability (as applied to the rock and fluid together). It gives the volume Q of a fluid with a given kinematic viscosity ν that flows in a porous medium with a hydraulic gradient of 1 through a cross section A of 1 m^2.

A porous medium has an intrinsic permeability constant k of 1 m^2 if 1 m^3 of a fluid with a kinematic viscosity ν of 1 m^2/s flows with a hydraulic gradient of 1 through an area of 1 m^2 (applied to the rock alone).

$$k = k_f \cdot \nu / g,$$

where g is the gravity constant and the units of k are length^2.

Transmissivity T gives the volume Q of a fluid with a given kinematic viscosity with a hydraulic gradient of 1 that flows through a cross section A with a 1 m with and a height equal to the total water-saturated thickness of the aquifer (applied to the system rock and fluid). It equals the product of the hydraulic conductivity k_f and water-saturated thickness m:

$$T = k_f \cdot m,$$

where the units of T are length^2/time.

Accordingly, transmissibility T* can be defined (applied to the rock) as follows:

$$T^* = T \cdot \nu / g,$$

where the units of T* are length^3.

Transmissivity and transmissibility are suitable parameters when aperture and distance between fractures are unknown. In general, the evaluation of an in-situ test with standard methods yields a transmissivity value from which the hydraulic conductivity can possibly be derived.

Assuming a hydraulic head Δh and a surface A, a water volume V can be pumped from or stored in an aquifer. The ratio of these quantities is the storage coefficient S (which is unitless):

$$S = V/A \cdot \Delta h$$

It is equal to the integral of the storage coefficient S_o over the thickness of the aquifer m. When S_o is constant,

$$S = S_o \cdot m.$$

In general, the storage coefficients of confined and unconfined groundwater differ by several orders of magnitude.

The description of flow in a porous or fractured medium based on a finite-element model (GÄRTNER, 1987; WOLLRATH & ZIELKE, 1990) is obtained by combining the law for the conservation of mass

$$S_o \frac{\partial h}{\partial t} + \text{div } \underline{v} = q \qquad (1)$$

and a flow law

$$\underline{v} = -\underline{K} \ (\text{grad } h)^a = \underline{K} I^a. \qquad (2)$$

The result can be written as follows:

$$\begin{pmatrix} v_x \\ v_y \\ v_z \end{pmatrix} = \begin{pmatrix} k_{xx} & k_{xy} & k_{xz} \\ k_{yx} & k_{yy} & k_{yz} \\ k_{zx} & k_{zy} & k_{zz} \end{pmatrix} \cdot \begin{pmatrix} \frac{\partial h}{\partial x} \\ \frac{\partial h}{\partial y} \\ \frac{\partial h}{\partial z} \end{pmatrix}$$

Equation (1) states that in the velocity field $\underline{v}$ the sum of the water quantities flowing across the model boundaries and to and from the sources and sinks (represented by the function q) in the steady-state case (i.e. flow does not change with time) is equal to zero and in the non-steady-state case (i.e. flow changes with time) equals the stored amount of water in the modeled area.

Table 3: Compilation of flow laws for fractures (after LOUIS, 1967)

Flow Conditions	Resistivity law		$\underline{v} = k_f \cdot \lvert\underline{I}\rvert^{\alpha-1} \cdot \underline{I}$	
	according to	formula	k_f	α
parallel flow: $\frac{k}{D_h} \leq 0{,}032$				
hydraulically smooth fracture surfaces laminar flow	POISEUILLE	$\lambda = \frac{96}{Re}$	$g \cdot \frac{(2a_i)^2}{12 \cdot \nu}$	1
hydraulically smooth fracture surfaces ($\frac{k}{D_h} = 0$) turbulent flow	BLASIUS	$\lambda = 0{,}316 \cdot Re^{(-1/4)}$	$\left[\frac{g}{0{,}079} \cdot \left(\frac{2}{\nu}\right)^{(1/4)} \cdot (2a_i)^{(5/4)}\right]^{(4/7)}$	$\frac{4}{7}$
rough fracture surfaces turbulent flow	NIKURADSE	$\lambda = \frac{1}{4 \cdot \left(\log \frac{k/D_h}{3{,}7}\right)^2}$	$4 \cdot \sqrt{g} \cdot \log\left(\frac{3{,}7}{k/D_h}\right) \cdot \sqrt{2a_i}$	$\frac{1}{2}$
nonparallel flow: $\frac{k}{D_h} > 0{,}032$				
laminar	LOUIS	$\lambda = \frac{96}{Re}\left[1 + 8{,}8 \cdot \left(\frac{k}{D_h}\right)^{1{,}5}\right]$	$\frac{g \cdot (2a_i)^2}{12 \cdot \nu \cdot \left[1 + 8{,}8 \cdot \left(\frac{k}{D_h}\right)^{1{,}5}\right]}$	1
turbulent	LOUIS	$\lambda = \frac{1}{4 \cdot \left(\log \frac{k/D_h}{1{,}9}\right)^2}$	$4 \cdot \sqrt{g} \cdot \log\left(\frac{1{,}9}{k/D_h}\right) \cdot \sqrt{2a_i}$	$\frac{1}{2}$
filled fracture				
laminar	DARCY		k_f	1

$\underline{v}$ = flow rate vector
k_f = hydraulic conductivity
$\underline{I}$ = grad h, hydraulic head gradient
k/D_h = relative roughness of fracture walls
D_h = $4a_i$, hydraulic diameter
$2a_i$ = average fracture aperture
λ = Darcy coefficient
Re = vD/ν Reynold's number
v = mean flow rate in the direction of the flow
ν = kinematic viscosity of the fluid

Equation (2) is valid for flow according to Darcy's law (porous media) and for flow in open as well as filled fractures. This equation says that the velocity field can be calculated from the permeability parameter $\underline{K}$ and the hydraulic gradient grad h = $-\underline{I}$. In a porous isotropic medium, the permeability tensor $\underline{K}$ reduces to the scalar hydraulic conductivity k_f; in the case of anisotropy, it includes the permeability of the medium as a function of direction.

The hydraulic conductivity of the fractures depends on the flow regime. Laminar flow in fractures with a constant aperture and smooth walls can be derived from the equations of Navier and Stokes. Empirical flow laws were formulated for turbulent flow in fractures; in this case, the hydraulic conductivity of the fractures is a function of the gradient of the hydraulic head, and equation (2) becomes nonlinear. This means that for porous media the Darcy coefficient k_f, and for fractured rock $k_f \cdot |\underline{I}| \cdot \alpha^{-1}$, are included in the permeability tensor $\underline{K}$. If equation (2) is set in equation (1), a differential equation with hydraulic head h as unknown is obtained.

b) Description of the transport properties

Several different terms are used to describe flow in geologic media: The Darcy velocity is the ratio of the cross section through which the water flows and the flow rate and is a parameter for Darcy's law. In comparison, the porespace velocity refers to the apparent cross section of the free pore space. The actual velocity is the ratio between the actual flow path and traveltime and describes the actual flow rate of a water molecule through the pore space. The tracer velocity is the ratio of the straight-line distance between two observation points and the time required by a water molecule to cover this distance. In the mathematical formulation of the transport equation, the tracer velocity is shown as a ratio of Darcy velocity and effective porosity n_e. If, instead of a porous medium, discrete fractures are modeled, the tracer velocity corresponds to the Darcy velocity ($n_e = 1$).

In a tracer test, it is not possible to determine the tracer velocity exactly because even tracer injected at a single point is dispersed throughout the rock and therefore arrives at the observation point over a period of time. On the basis of a typical tracer curve (Fig. 18), various tracer velocities can be defined in terms of first arrival time, the curve maximum, the "50 %" arrival time, or the centroid of the area below the curve. Since the form of the curve is influenced by various factors (e.g. the time needed to inject the tracer), the first arrival time is considered as most important for the following test evaluation.

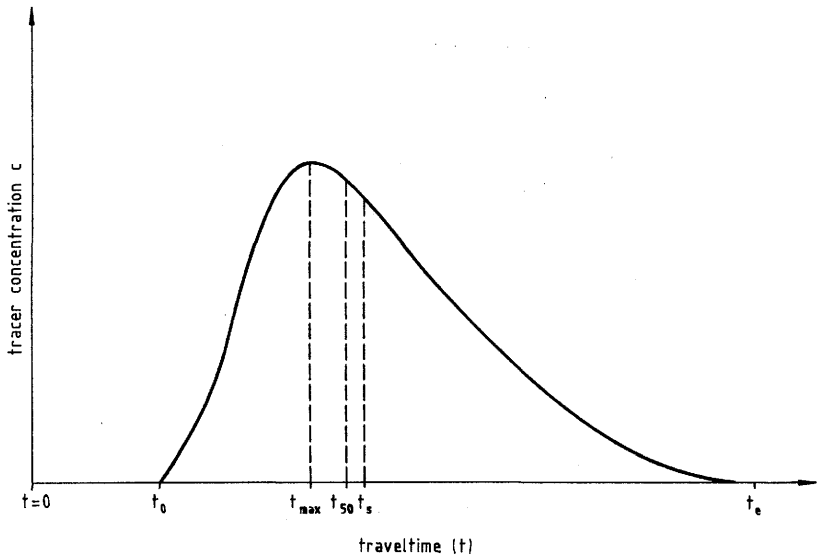

Fig. 18: Typical tracer curve

Various physical phenomena must be considered in connection with the transport of matter dissolved in water. BROWNian movement is the basis for molecular diffusion, which takes place when miscible fluids of differing concentrations come into contact with each other (e.g. freshwater and salt water). However, this effect is negligible with respect to hydrodynamic dispersion if the fluids move at a certain minimum velocity, e.g. through a geologic medium. More relevant is the mixing resulting from differing velocities in the individual pore spaces or, in the case of laminar flow, in the cross section through which the water flows. Owing to local differences in the hydraulic conductivity of the fractures, there is macroscopic dispersion also in fractured media.

In the DURST finite-element program (GÄRTNER, 1987; KRÖHN & ZIELKE, 1990), the diffusion flow parameter $\underline{w}$ is needed for the three-dimensional calculation of transport:

$$\underline{w} = -\underline{D} \cdot \text{grad } z$$

This can be written as follows:

$$\begin{pmatrix} w_x \\ w_y \\ w_z \end{pmatrix} = \begin{pmatrix} D_{xx} & D_{xy} & D_{xz} \\ D_{yx} & D_{yy} & D_{yz} \\ D_{zx} & D_{zy} & D_{zz} \end{pmatrix} \cdot \begin{pmatrix} \frac{\partial z}{\partial x} \\ \frac{\partial z}{\partial y} \\ \frac{\partial z}{\partial z} \end{pmatrix} \qquad (3)$$

For a mathematical treatment of this process, a distinction is made between the longitudinal dispersion coefficient and a (normally smaller) transversal dispersion coefficient (whose units are length²/time). In the simplest case, these coefficients can be represented as the product of aquifer parameters and flow as follows:

$D_L = \alpha_L \cdot v$ and $D_T = \alpha_T \cdot v$, respectively,

where α_L and α_T are called longitudinal and transversal dispersivity (in units of length), respectively.

Diffusion is an irreversible thermodynamic process. Therefore, the diffusion tensor $\underline{D}$ must be symmetrical and accordingly have three real, positive eigenvalues λ_1, λ_2 and λ_3 which means that a matrix $\underline{Q}$ can be written with the property $\underline{Q}^{-1} = \underline{Q}^T$ and

$$\underline{D} = \underline{Q}^T \cdot \underline{\Delta} \cdot \underline{Q}, \qquad \underline{\Delta} = \text{diag}\,(\lambda_1, \lambda_2, \lambda_3) = \begin{pmatrix} \lambda_1 & 0 & 0 \\ 0 & \lambda_2 & 0 \\ 0 & 0 & \lambda_3 \end{pmatrix} \qquad (4)$$

Thus, equation (3) can be written as follows:

$$\underline{w} = -\underline{Q}^T \cdot \underline{\Delta} \cdot \underline{Q} \cdot \text{grad } z \qquad (5)$$

Multiplying the left side by Q, one obtains

$$w_\xi = -\lambda_1 \frac{\partial z}{\partial \xi} \qquad (5a)$$

$$w_\eta = -\lambda_1 \frac{\partial z}{\partial \eta} \qquad (5b)$$

$$w_\zeta = -\lambda_1 \frac{\partial z}{\partial \zeta} \qquad (5c)$$

This is associated with a main axis system with the coordinates ξ, η, and ζ, where

$$\begin{pmatrix} \xi \\ \eta \\ \zeta \end{pmatrix} = \underline{Q} \cdot \begin{pmatrix} x \\ y \\ z \end{pmatrix}$$

For the individual cases, it will be important to define a main axis system for equations 5a, b and c. The diffusion tensor $\underline{D}$ is then fixed relative to the global Cartesian x,y,z coordinate system.

A commonly used approach is based on the assumption that the ξ-axis is tangent to the direction of flow, i.e. the direction of the tracer velocity v (or opposite to it). Accordingly, the η or ζ axes are normal to the streamline. In the direction of flow, as well as perpendicular to it, a velocity-dependent dispersion is defined so that the longitudinal dispersivity α_L and the transversal dispersivity α_T multiplied by the velocity yield the dispersion coefficient for the ξ,η,ζ coordinate system. If these coefficients are within the order of magnitude of the molecular diffusion, the diffusion coefficient D can simply be added (model 3). If not, molecular diffusion is neglected (model 2). Accordingly, three diffusion/dispersion models can be formulated:

Model 1: molecular diffusion

$\lambda_1 = \lambda_2 = \lambda_3 = D$

Model 2: velocity-dependent dispersion

$\lambda_1 = \alpha_L |v|$

$\lambda_2 = \alpha_T |v|$

$\lambda_3 = \alpha_T |v|$

Model 3: dispersion/diffusion according to SCHEIDEGGER

$\lambda_1 = \alpha_L |v| + D$

$\lambda_2 = \alpha_T |v| + D$

$\lambda_3 = \alpha_T |v| + D$

Except for an irrelevant degree of freedom, the matrix $\underline{Q}$ can be determined as a function of vector $\underline{v}$, and thus operation (2) can be carried out using the λ_i of one of the three models.

5.2.2 Basics of the Test Evaluation

In-situ tests can be classified on the basis of various aspects, for example:

a) active tests	- passive tests
b) short-term tests	- long-term tests
c) single-borehole tests	- multi-borehole tests
d) injection tests (pressure build-up)	- pumping tests (pressure reduction)
e) hydraulic tests	- tracer tests

The tests can be illustrated best by graphs of injection pressure and flow rate as a function of time. Some typical injection tests (active tests) are shown in Figure 19.

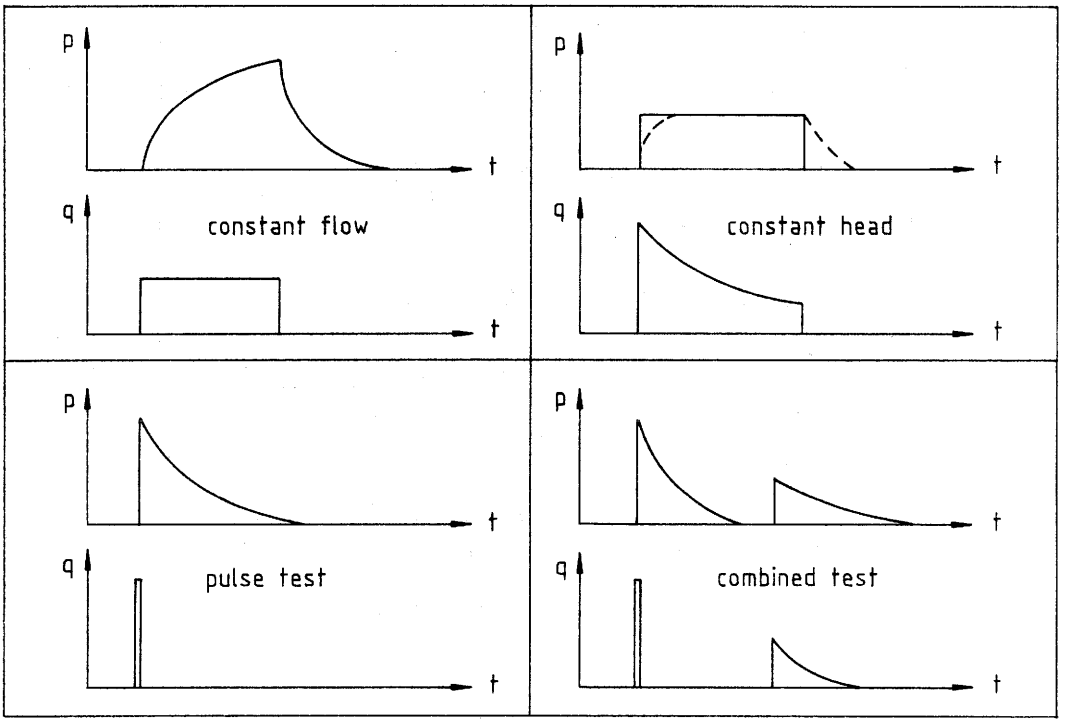

Fig. 19: Injection pressure p and flow rate q as a function of time

Which kind of test is best suited depends mainly on the range of the permeability expected. In the Fracture System Flow Test area, in which the permeability is high, mainly tests with a constant flow rate are conducted. Pulse tests and combined tests are recommended for low permeabilities; slug tests or drill stem tests can be used for studying areas with average permeabilities. Figure 20 shows various types of tests as a function of permeabilitiy (WILSON et al., 1979).

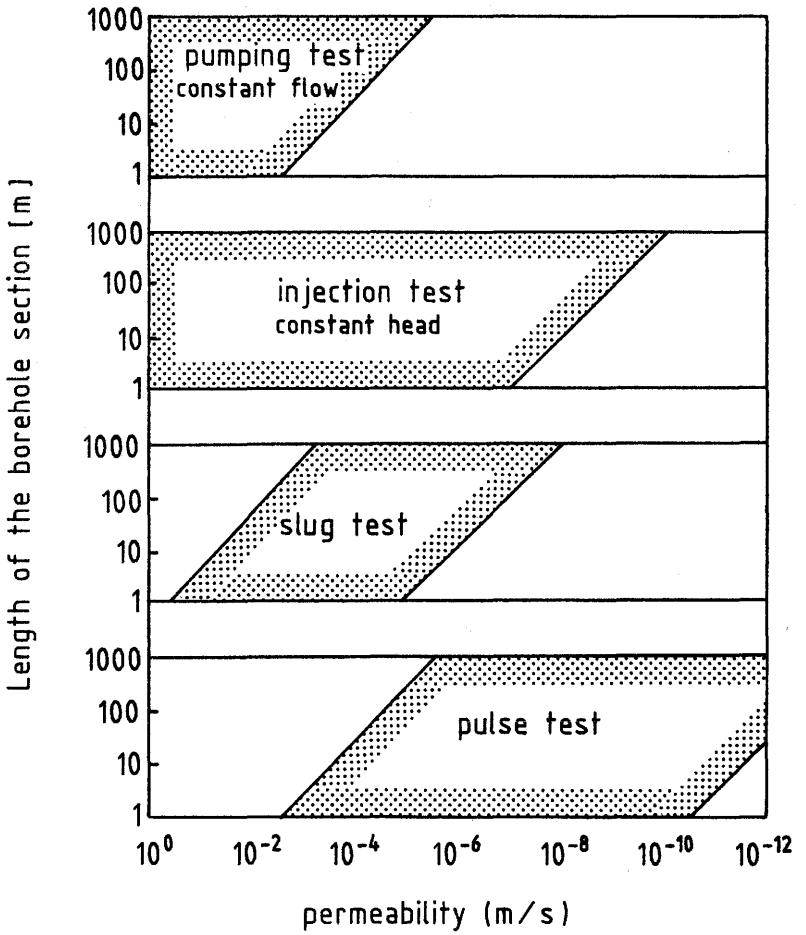

Fig. 20: Suitability of several types of tests with respect to permeability of the rock (according to WILSON et al., 1979)

The following types of tests are used within the Fracture System Flow Test project:

- pressure recovery tests,
- short-term injection tests in one-meter sections to determine the permeability distribution in a borehole (index tests),
- hydraulic interference tests to determine the major flow paths,
- injection tests with constant flow rates (several hours, days, or weeks) to determine hydraulic parameters in fracture zones showing high permeability,
- tracer tests to locate fractures in open observation boreholes (fluid logging),
- dipole tracer tests to determine tracer velocities (mostly several tracer test phases over a period of several hours during a longer injection test).

In contrast to the active tests, no additional fluid is injected in passive tests. Pressure recovery tests are passive tests; to measure flow rate, however, it may be necessary to actively influence the test conditions, for example, by keeping the discharge constant.

A rough characterization of the permeability can be made using simple standard tests. For the well-known Lugeon test, specific borehole sections are sealed using single or double packers; fluid is injected at constant pressure into these sections over short periods of time. Assuming steady-state flow conditions, an approximate transmissivity value T or a hydraulic conductivity k_f can be obtained (e.g. HEITFELD & KOPPELBERG, 1981; recommendation no. 9 of workshop 19 of the DGEG, 1984). Comparable index tests were conducted in 1-m sections of boreholes at the Grimsel Test Site to determine the permeability distribution (BRÄUER et al., 1989).

The length of the injection or observation sections between two packers can be set on the basis of various criteria. Assuming that this length corresponds to the "water-saturated thickness" of the aquifer being tested, the transmissivity in a 1-m section can be equated with the average permeability. Moreover, short sections allow more detailed information to be obtained on the exact position of fractures of hydraulic relevance. On the other hand, long observation sections are useful for assessing the integral permeability of rather large rock zones. Lastly packers can be used to separate fracture zones from each other to conduct interference tests to study hydraulic connections. The length of the individual sections is of secondary importance for this test method, which puts emphasis on quantitative aspects.

To describe the effectiveness of crystalline rock as a hydraulic barrier, the permeability over a long period of time is of special importance. Therefore, in-situ tests within the scope of the Fracture System Flow Test project are conducted over at least several days or weeks so that conclusions can be drawn with respect to the non-steady-state flow conditions and comparisons with short-term tests (e.g. Lugeon tests) be made; their evaluation is based on steady-state conditions.

Injection tests to determine hydraulic parameters are conducted with a single borehole. Most of the tests during project phase BK II, however, were conducted using two boreholes (dipole tracer tests). Strictly speaking, this means that it is not possible to evaluate the hydraulic data with standard methods.

Tracer tests are necessary to study the spread of substances dissolved in water because the hydraulic reaction in fracture systems takes place within a much shorter period than the chemical reaction (e.g. changes in the concentration). This means that hydraulic tests are not sufficient to assess the transport of a substance in the rock mass.

Common salt (NaCl), a conservative tracer, was used for the tracer tests. Salt changes the electrical conductivity of water.

The following electrical conductivity values are typical (HÖLTING, 1989):

rain water	5 – 30 µS/cm
fresh water	30 – 2,000 µS/cm
sea water	45,000 – 55,000 µS/cm

The electrical conductivity of the groundwater at the Grimsel Test Site is 80 – 90 µS/cm, that of the surface water used for the tests is 15 – 25 µS/cm. Experiments in the rock laboratory provided information on the relationship between the amount of dissolved NaCl and the electrical conductivity of the salt solution. The straight line (base value = 25 µS/cm, corrected to 25 °C) shown in Figure 21 agrees very well with measurements by SHEDLOVSKY + SHEDLOVSKY (1971).

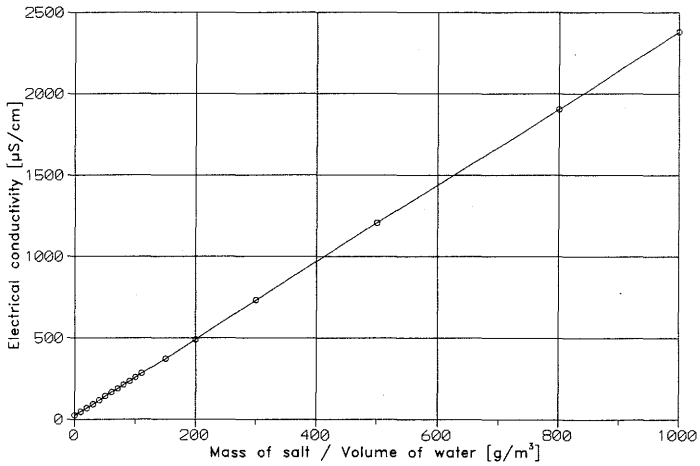

Fig. 21: Electrical conductivity as a function of salt concentration

The main properties of salt that make it suitable as a tracer are chemical stability, little or no adsorption, easy identification, no effect on flow, simple handling, low cost and nontoxicity (HILL, 1984).

5.3 Test Results

5.3.1 Central Fracture System Flow Test Area

The basis for in-situ hydraulic tests in rock is the engineering-geological mapping of the drill cores. The frequency of fractures in the cores (for example, from borehole BK 85.005, Fig. 22), provides a first impression on the permeability of the rock. However, the emphasis is shifted if the fractures are assigned a weighting factor on the basis of their hydraulic significance.

A more detailed characterization is possible using short-term injection tests. For these index tests, which are comparable to Lugeon tests, injections are made in 1-m intervals using several pressure increments. The approximate transmissivity of the rock can be derived from the relationship between injection pressure and flow rate assuming steady state conditions (Fig. 22). In the example considered here, a comparison with the fracture frequency shows sufficient agreement, since the maximum values occur at the same places (here for example at depths ranging from 17 to 20 m or 31 to 33 m) in borehole BK 85.005.

On the basis of the short-term tests and the fracture frequencies from the drill cores, an initial hydraulic model of the fracture system can be developed. Interference tests can be used to study the hydraulic connections in the rock in more detail. For this purpose, the individual fracture systems are separated from each other by installing packers in the boreholes. Probes monitor the hydraulic reactions in the observation sections between the packers. The large number of observation points available in the fracture system means that every in-situ test is, in principle, an interference test.

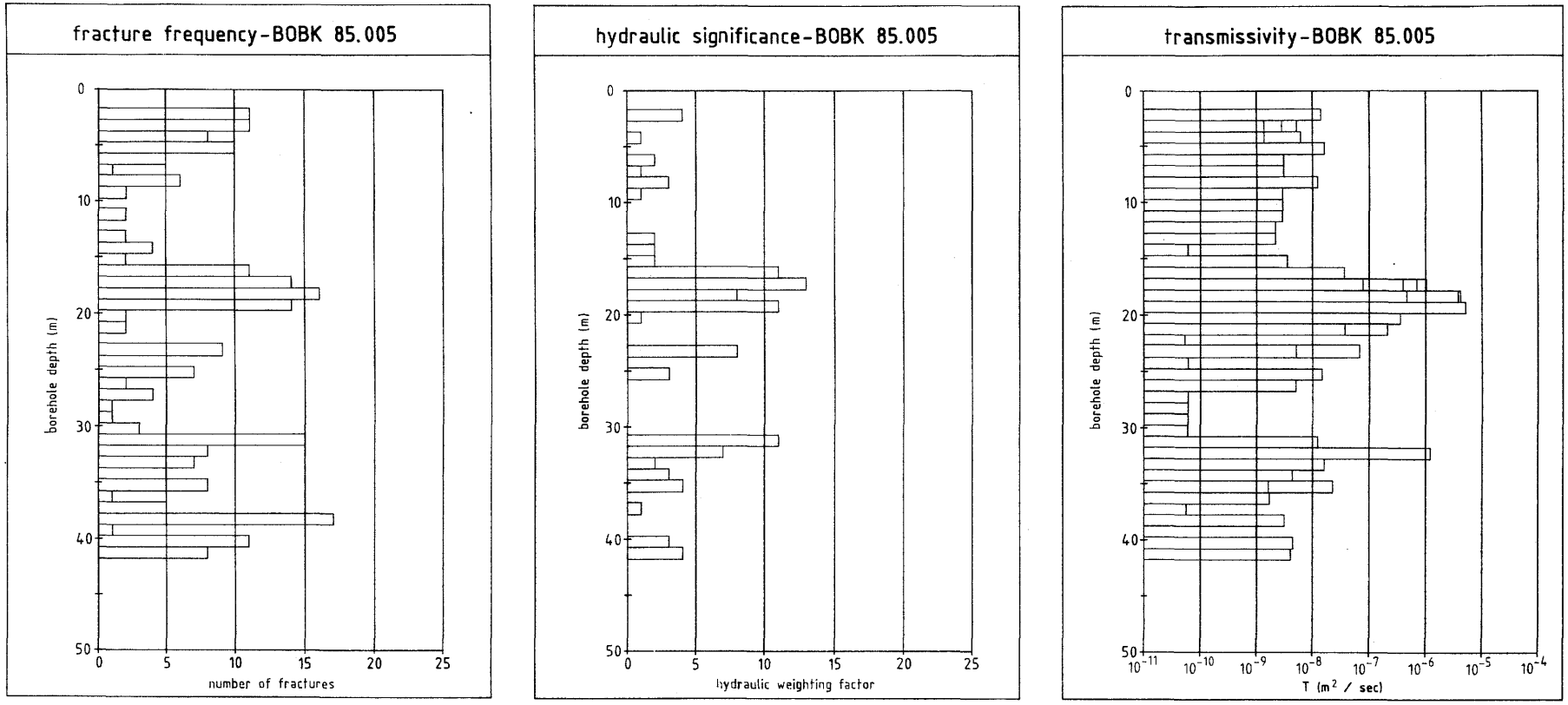

Fig. 22: Fracture frequency distribution, hydraulic weighting factors and transmissivity as a function of depth in borehole BK 85.005

A series of interference tests was conducted at the beginning of 1990. Fluids were injected in borehole BK 85.004 for tests at constant flow or constant pressure. On the basis of the prior information, several borehole intervals were used for injection to a depth of about 45 m, a zone which shows a wide range of permeability.

Test VE 457, planned in cooperation with NAGRA (KELLEY & FRIEG, 1990), is taken as an example (injection section of 6.7 to 10.7 m in a zone containing a fracture with particularly high hydraulic conductivity). The locations of the probes and packers are given in Table 4. The duration of the test was 24 hours and the average injection rate was about 7 l/min. Figures 23 and 24 show the pressures in the center left fan of boreholes BK 85.005, 88.015 and 88.016 and the center right fan of boreholes BK 85.004, 85.007, 85.011 and 88.012. Hydraulic reactions were also recorded in boreholes BK 85.008, 85.010 and SB 80.001.

It can be seen that the pressure build-up rates at the end of each injection phase are rather similar: 0.06 bar/h in the section in which the fluid was injected and in most of the observation sections. The slightly slower pressure rise in the upper (closer to the mouth of the borehole) section of borehole BK 85.005 as well as in borehole BK 85.011 is due to leakage at the mouth of the borehole or in the gravel bed below the concrete floor of the gallery. However, low values were also observed in boreholes BK 85.008 and 85.010 further away. Conspicuous is a pressure build-up rate in the bottom interval of borehole BK 85.006 (0.07 bar/h) that is greater than that of the injection pressure. This was also observed in other tests and can be interpreted as a concrete indication of the existence of a no-flow boundary.

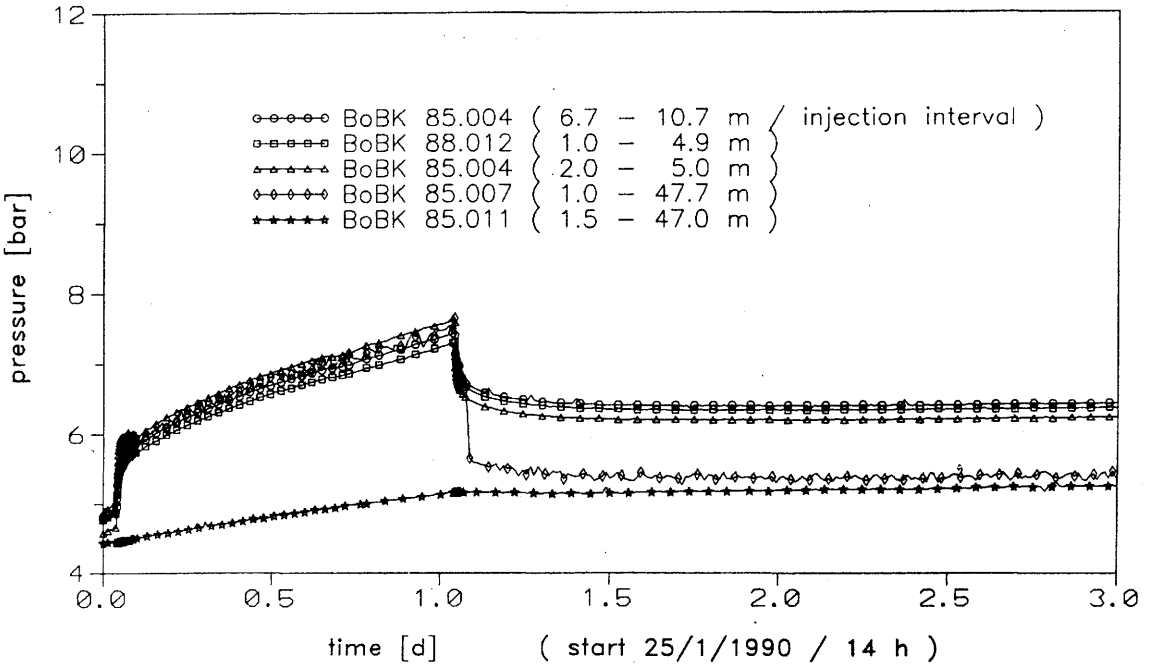

Fig. 23: Pressure in boreholes BK 85.004, 85.007, 85.011 and 88.012 as a function of time during test 457

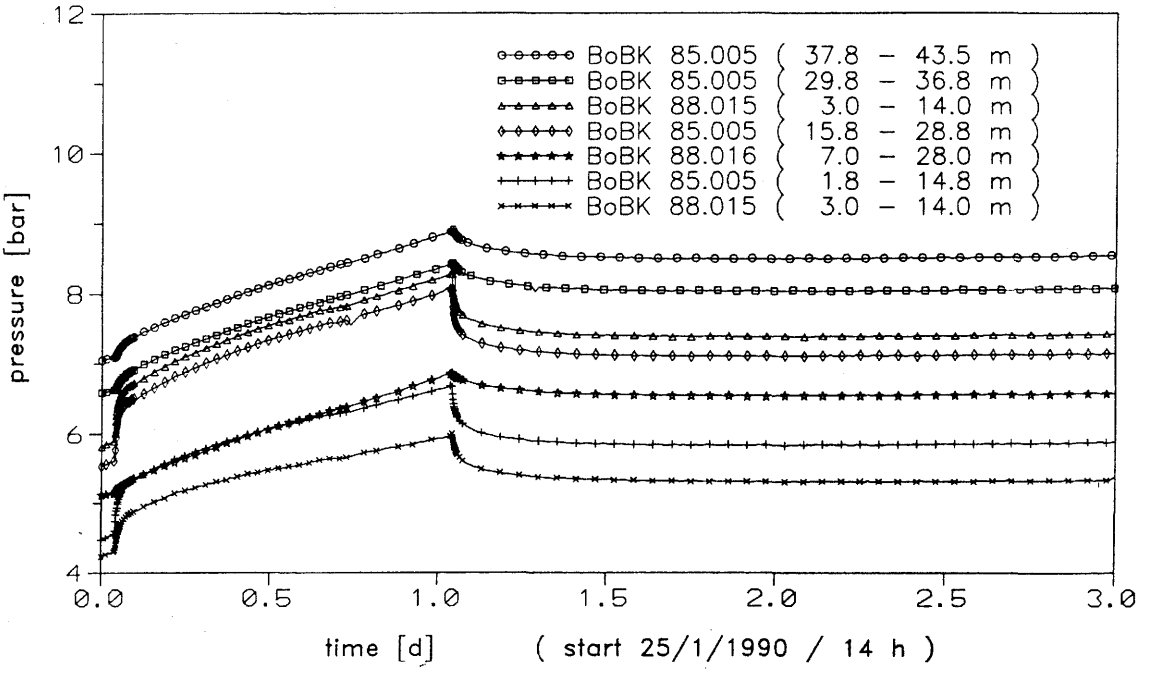

Fig. 24: Pressure in boreholes BK 85.005, 88.015 and 88.016 as a function of time during test 457

Table 4: Position of the probes during test 457

Borehole	Interval	Measurement interval (m)	Depth of probe in borehole (m)	Depth relative to BK-area level (m)
86.002		1.0 - 49.0	BK-area	-0.5
86.003		1.0 - 68.0	BK-area	-0.5
85.004	i1	2.0 - 5.0	BK-area	-0.5
	i2	6.7 - 10.7	BK-area	-1.6
85.005	i1	1.8 - 14.8	2.3	1.3
	i2	15.8 - 28.8	16.3	9.3
	i3	29.8 - 36.8	30.3	17.4
	i4	37.8 - 43.5	38.3	22.0
85.006	i1	2.0 - 11.0	42.5	1.4
	i2	12.0 - 19.0	12.5	7.2
	i3	21.0 - 27.0	27.5	15.8
	i4	28.0 - 45.0	28.5	16.3
85.007		2.0 - 48.0	2.5	2.0
85.008		1.0 - 49.0	BK-area	-0.5
85.009		3.0 - 49.0	3.5	2.5
85.010		1.0 - 43.0	BK-area	-0.5
85.011		2.5 - 45.0	3.0	3.0
88.012		1.8 - 5.0	2.3	1.8
88.013		3.5 - 29.0	4.0	2.3
88.014		11.0 - 22.0	11.5	3.1
88.015	i1	3.0 - 14.0	3.5	2.8
	i2	15.0 - 41.0	15.5	12.4
88.016		7.0 - 28.0	7.5	2.0
88.017	i1	2.0 - 11.0	2.5	2.0
	i2	12.0 - 21.3	12.5	10.0
	i3	22.0 - 49.0	22.5	18.0
88.018		3.0 - 17.0	3.5	0.9

Distinct differences between individual packer sections were observed immediately after pumping was stopped. The two upper intervals in BK 85.005, for example, show a much more prominent reaction than the two lower intervals, which lie outside the S1/S2 fracture system (Fig. 24). The reactions in boreholes BK 85.009, 88.013 and 88.014, as well as BK 85.008 and BK 85.010, are relatively weak.

VE 465 can be taken as an example of a passive pressure recovery test in the central part of the Fracture System Flow Test area. This test was followed by a constant-flow period (VE 466) at a discharge rate Q of 2 l/min in the 6.7 – 10.7 m interval in BK 85.004. The selected flow rate is about equivalent to a yield of Q = 2.2 l/min, which is reached a considerable time after a borehole is opened in the central BK area. With a duration of four and two weeks, respectively, both tests can be regarded as typical long-term tests.

The natural pressure rise (0.1 bar/day) takes place much more slowly than in the injection test (VE 457) described above. This means that for the calculation of results of an active test, the natural pressure build-up can be neglected in most cases. The pressure in the above-mentioned interval in BK 85.004 is plotted versus flow rate in Figure 25. After four weeks no decrease in the rate of pressure build-up can be detected, thus making extrapolation impossible. The pressure recovery is much more uniform than in the active test VE 457. The pressure behaviour is practically the same in all observation sections; it rises uniformly throughout the central test area. Even in the period immediately following the opening of the discharge interval, the reactions at the different observation points were very similar (BK 85.005 in Fig. 23, for example).

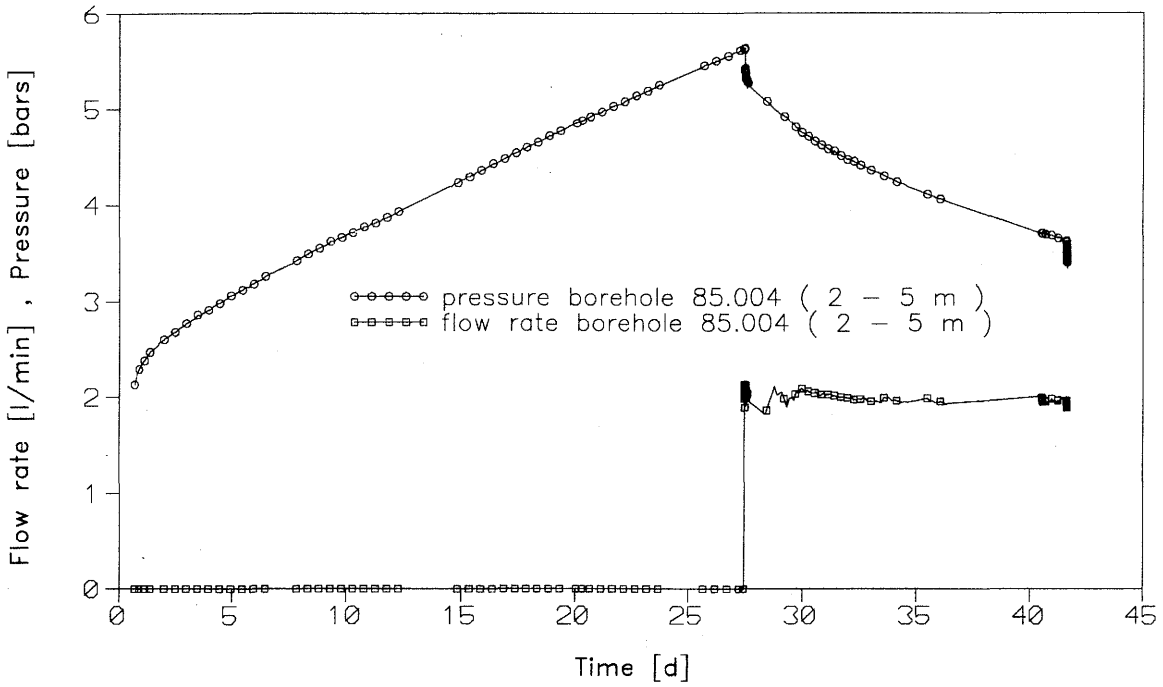

Fig. 25: Pressure build-up test (VE 465) and pressure recovery test at constant withdrawal rate (VE 466) in borehole BK 85.004

Results of tracer tests

Tracer tests using NaCl were conducted with various objectives in the central testing area. Some results of the different types of tests are discussed in the remainder of this chapter:

a) fluid-logging tests,
b) tracer tests with an open observation borehole (dipole tests) and
c) tracer-pulse tests with closed observation borehole.

A series of fluid-logging tests were conducted in collaboration with NAGRA and GEOTEST at the beginning of 1990 to localize tracer pathways between a selected injection borehole and various observation boreholes.

NaCl solution with a conductivity of 10 μS/cm was injected in BK 85.004 in the interval between 6.7 and 10.7 m over a period of 11 days. A low injection rate of 0.5 l/min was chosen to ensure that the natural flow conditions were disturbed as little as possible, but was high enough to ensure that the reaction would be observed in the open boreholes within a few hours after being opened. Because the hydraulic heads or differences in hydraulic head in this highly permeable part of the rock are rather rapidly reduced after a borehole is opened, the observation boreholes could be tested one after the other over a short period of time. In contrast, the pressure build-up resulting from injection or natural influx occurs in this part of the rock mass relatively slowly and does not produce any significant change in the flow field during logging. The traveltime of a tracer from an injection borehole to an observation hole was irrelevant in this series of tests.

The results from BK 85.005 and 85.006 are given here as an example of the seven holes investigated. Figure 26 shows electrical conductivity logs run at different times after borehole BK 85.005 was opened. It displays a prominent peak between 17 and 18 m. With increasing displacement of the freshwater initially present in the borehole, this peak widens toward the mouth of the borehole. The electrical conductivity gradually increases to a value of slightly more than 1 μS/cm; this is considerably less than the conductivity of the injected brine. The irregularities in the curves between 18 and 21 m suggest that inflow in the observation borehole occurs at several places. The electrical conductivity logs for BK 85.006 show a relatively long section (about 23 – 27 m; Fig. 27) along which the tracer enters the borehole. The irregular curve suggests that there are several fractures in this section.

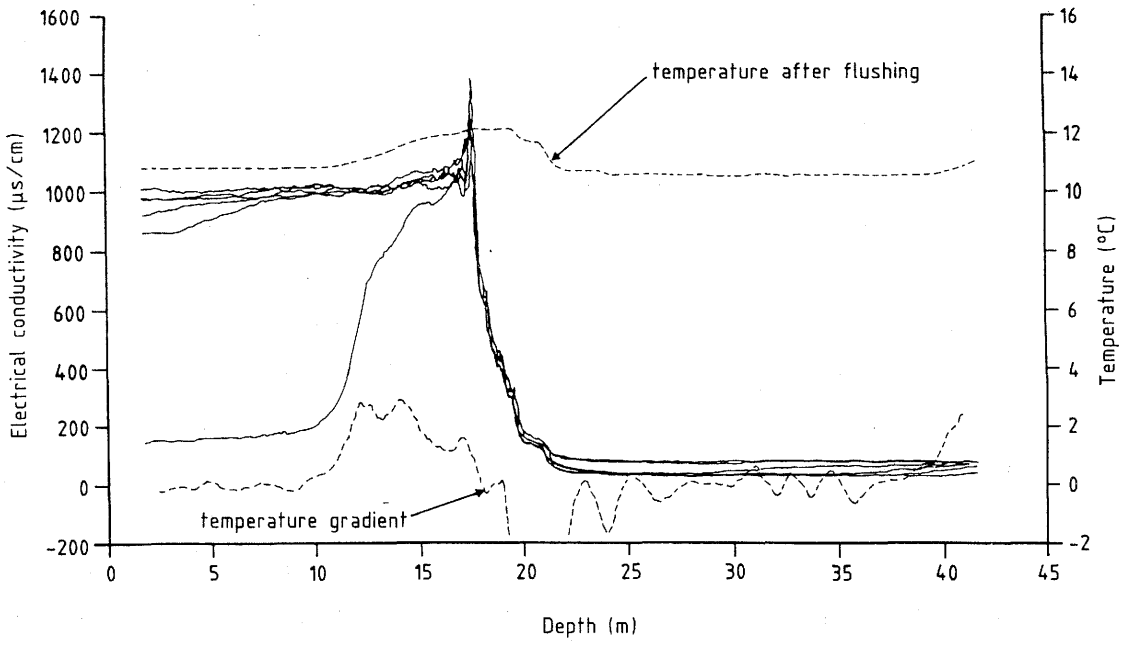

Fig. 26: Electrical conductivity logs run in borehole BK 85.005 on 13 Feb. 1990 (test 462) (KELLEY & LOEW, 1991)

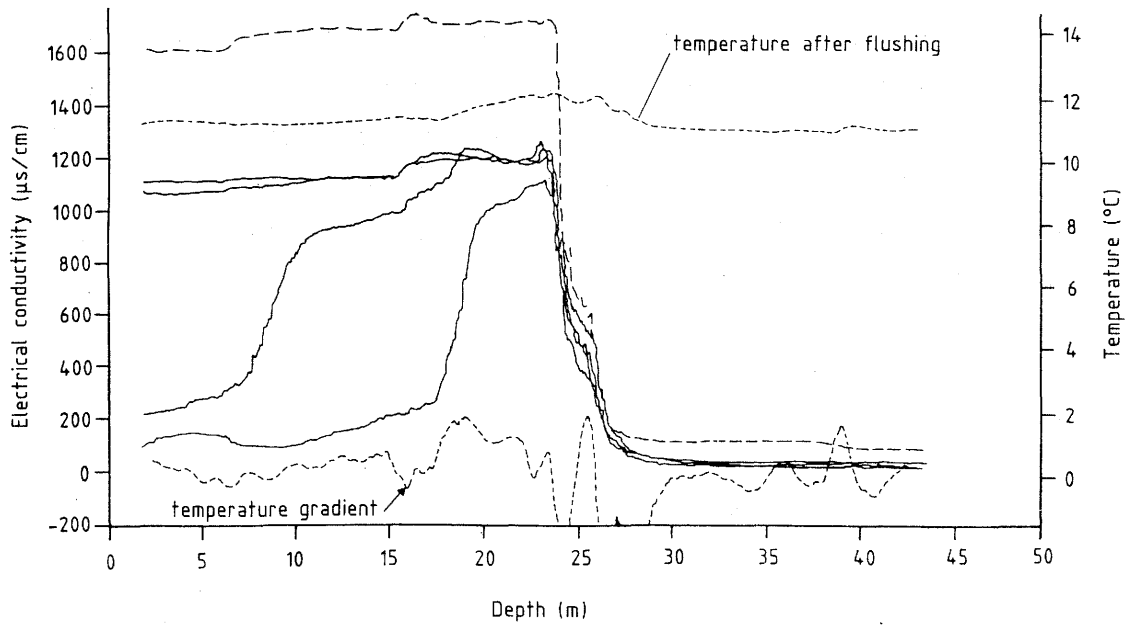

Fig. 27: Electrical conductivity logs run in borehole BK 85.006 on 12 Feb. 1990 (test 459) (KELLEY & LOEW, 1991)

Because of the movement of the probe in the borehole, mixing of the water cannot be completely prevented; thus the position of the fractures can be determined with a precision of only a few centimeters. Any mixing due to density effects (sinking of the relatively dense salt water flowing out of a fracture) could be neglected for the concentrations and test periods involved. The results generally show good agreement with the fracture analysis carried out on the drill cores. It becomes clear that unambiguous information about connecting pathways for fluids in the rock mass can be obtained only by using tracer tests. For example, no connection was found during fluid logging between the injection section in BK 85.004 and the section in BK 85.005, in which a high fracture frequency and permeability was observed at about 31 m (Figs. 22 & 26). During the dipole tracer test, simplified conductivity logs were run in several boreholes using conductometers from the firm WTW; these results agree very well with those obtained by fluid logging. Thus, tracer-bearing fractures can also be localized using simple instruments.

Figure 28 shows the results of a typical tracer test which displays three nearly identical breakthrough curves. In test 300 in BK 85.009, the tracer was injected between depths of 28 and 29 m at a constant flow rate of 15 l/min and an almost constant injection pressure of about 12.5 bar (steady--state flow field). The observation borehole was BK 85.004, which was isolated by a packer at a depth of 4 m. The tracer flowed only from a highly permeable zone at 3 – 4 m depth (fracture system S1/S2). Assuming a straight-line distance of 20 m, a mean traveltime of as little as one hour was obtained for the tracer; this is due to the high hydraulic gradient.

In project phase BK II, improvements in the probe-packer system used in the boreholes permitted long-duration tests to be conducted at lower injection rates of 0.5 – 5 l/min. At these injection rates, the flow conditions were little changed. The variations in electrical conductivity were

recorded both by probes at different depths and by WTW conductometers at the mouths of the boreholes. The probes were positioned on the basis of existing information about the location of fractures.

In the dipole tracer tests VE 433 and 434, injection took place in BK 85.005 at a depth of between 18 and 19 m (Fig. 29). The discharge was recorded in BK 85.006 by probes and conductometers; all other boreholes were sealed. The injection rates of about 5 l/min (VE 433) and 2.5 l/min (VE 434), the injection pressure and the discharge rate in the observation hole can be obtained from Figure 30. Concentrations of initially 200 μS/cm and then 800 μS/cm were selected for tracer phases of five hours each. At an injection rate of 2.5 l/min (VE 434), this concentration turned out to be too low to permit the traveltime to be determined unambiguously. Figure 31 shows the reaction in BK 85.006 recorded by a probe installed at a depth of 9 m. For an injection rate of 5 l/min (VE 433), a traveltime (first arrival time) of three hours was obtained for the tracer (Fig. 31).

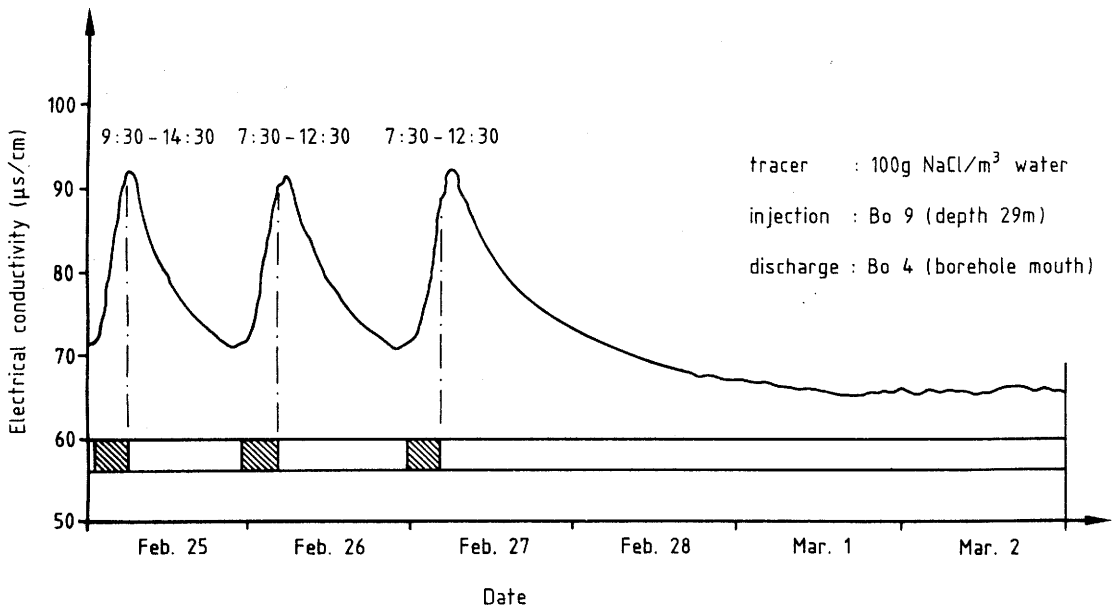

Fig. 28: Electrical conductivity during tracer test VE 300: NaCl tracer (100 g/m^3 water) injected at a depth of 29 m in borehole BK 85.009 and measured at the mouth of borehole BK 85.004; the shaded parts of the bar at the bottom of the graph indicate the times of injection.

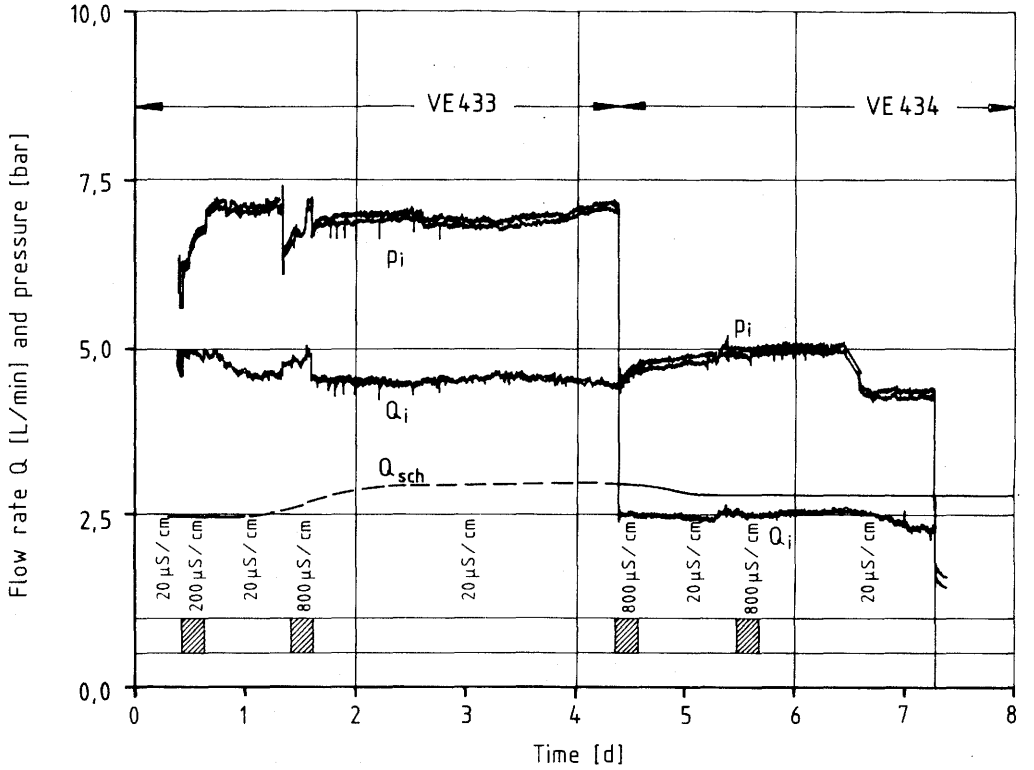

Fig. 29: Discharge from borehole BK 85.006, injection in borehole BK 85.005 (tracer tests VE 433 and 434)

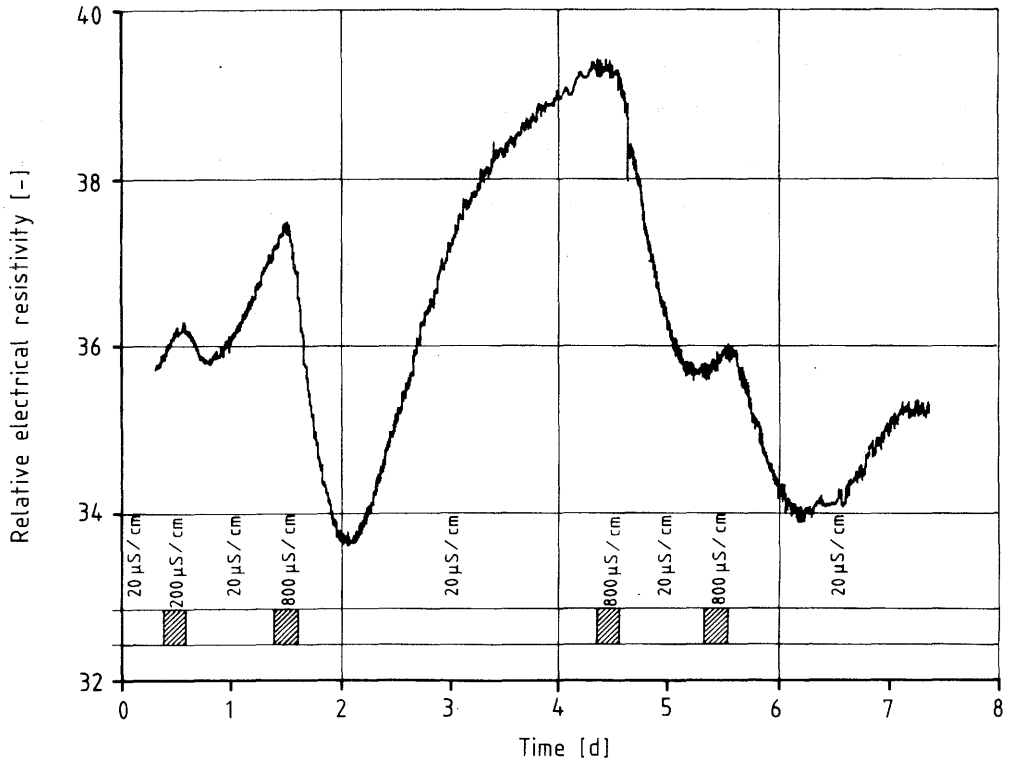

Fig. 30: Example of the reaction of a probe in borehole BK 85.006, injection in borehole BK 85.005 (tracer tests VE 433 and 434)

In later tests the tracer appeared at a depth of about 24 m in BK 85.006 (fracture system S1/S2). In this case, the traveltime within the fracture system was about 2.5 hours over a direct distance of about 10 m. Figure 32 shows the connection between the values obtained from the probe and the electrical conductivity recorded at the mouth of the borehole by means of a conductometer. The curves obtained by these two methods can be seen to have opposite gradients.

In order to localize the tracer discharge point in the observation borehole BK 85.006 more precisely, a probe was positioned at a depth of 16.5 m for test VE 444. The tracer was then injected at a rate of 2.5 l/min for 5 hours at a relatively high conductivity of 3000 μS/cm. In the target borehole a distinct reaction was observed 3.5 hours after the injection began (Fig. 33). The subsequent irregular part of the curve can be interpreted as a breakthrough of salt water in a secondary fracture superposing the breakthrough of freshwater in the primary fracture.

This effect was investigated in more detail in test VE 449. A special double-packer element was installed in BK 85.006 in order to enable water discharged from between 26 and 27 m depth to be withdrawn from the borehole separately. Figure 34 shows that, as was expected, the tracer appeared much later in this section than in the section up to 25 m. In this case the injection rate was 0.5 l/min for a period of five hours, the conductivity of the salt solution was 7500 μS/cm.

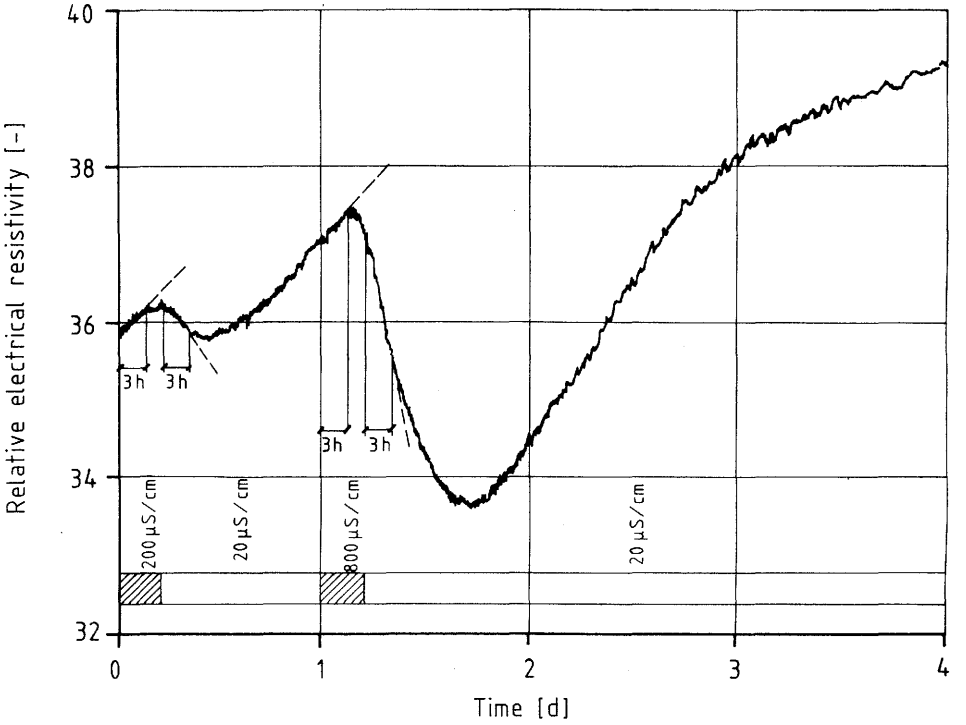

Fig. 31: First arrival times for the curve shown in Fig. 29

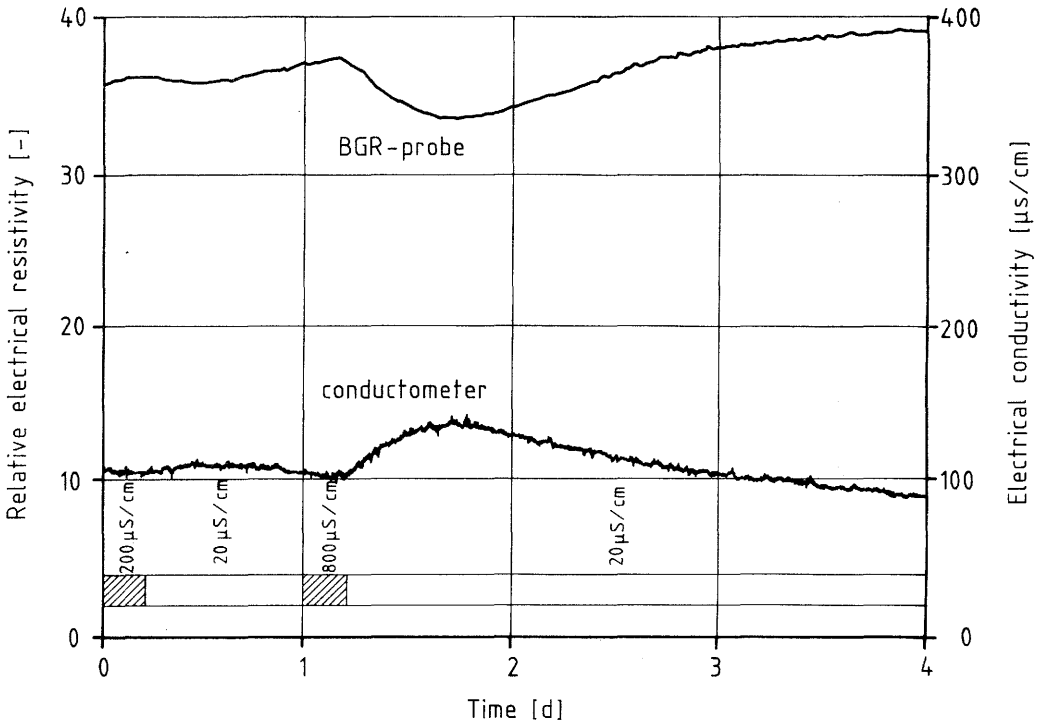

Fig. 32: Comparison of the data from a probe with that from a conductometer (tracer test VE 433)

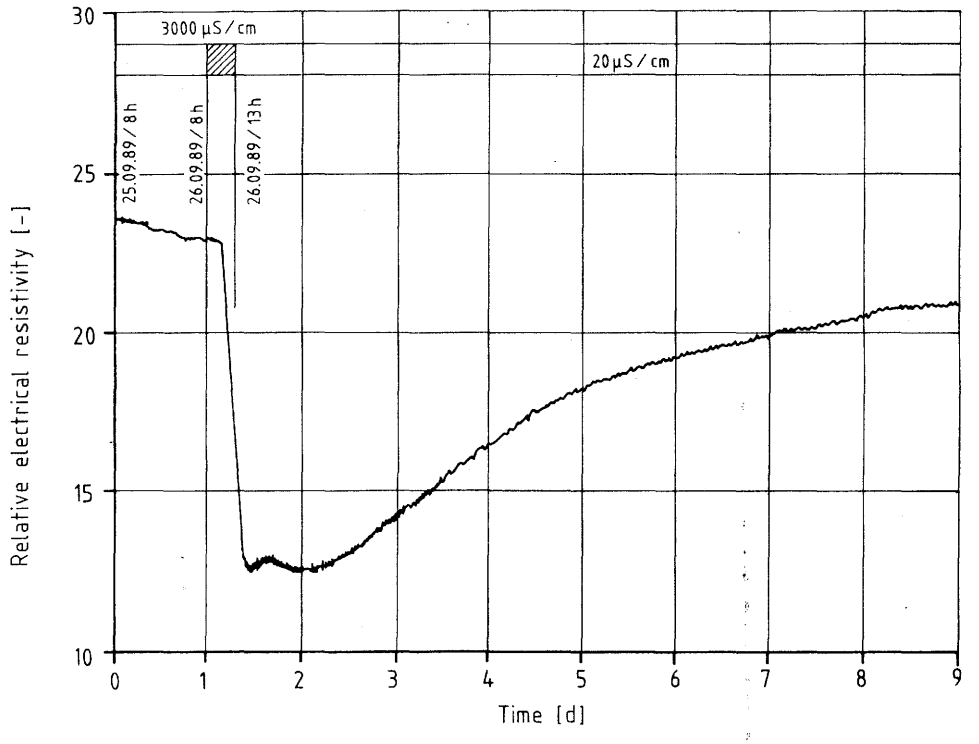

Fig. 33: Changes in tracer concentration in borehole BK 85.006 during tracer test VE 444

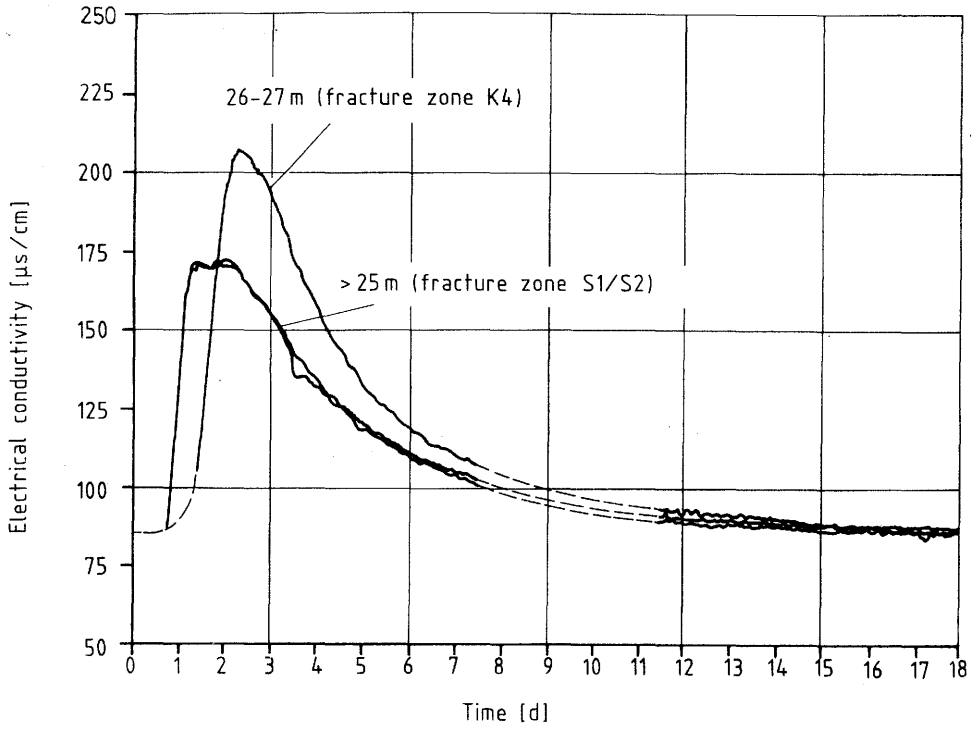

Fig. 34: Changes in tracer concentration in borehole BK 85.006 during tracer test VE 449

5.3.2 Area around BK 86.003 and US 85.003

A large number of tests were carried out in test area II, in which a connection exists via the fracture system between boreholes BK 86.003 and US 85.003.

Figure 35 shows the transmissivities calculated from the short-term injection tests, the fracture frequency and the hydraulic weighting factors, all plotted against depth in borehole BK 86.003. The highest transmissivity is observed between 63 and 65 m depth; this interval was therefore chosen for the tracer tests carried out in 1988.

The results of a typical injection test (VE 471) are shown in Figure 36. A single packer was positioned at a depth of about 4 m, enabling the whole length of the borehole to be used for injection. The computer-controlled test VE 473 was carried out in the same hole as a pressure-reduction test at constant withdrawal rates of 2 or 3 l/min (Fig. 37).

In 1988 a series of dipole tracer tests was conducted in this part of the rock mass using an injection interval in borehole BK 86.003 from 64 - 65 m which was sealed by double packers. Injection pressure and water flow rate during tests VE 380/381 and 390A/390B are shown as examples in Figures 38 and 39 as a function of time. It became clear that the pressure in this part of the rock mass, in spite of the fact that observation hole US 85.003 was open, rose considerably more rapidly than in the central area and that, using comparable injection rates, pressures were attained within a few days or weeks which were equivalent to the head of water from the surface.

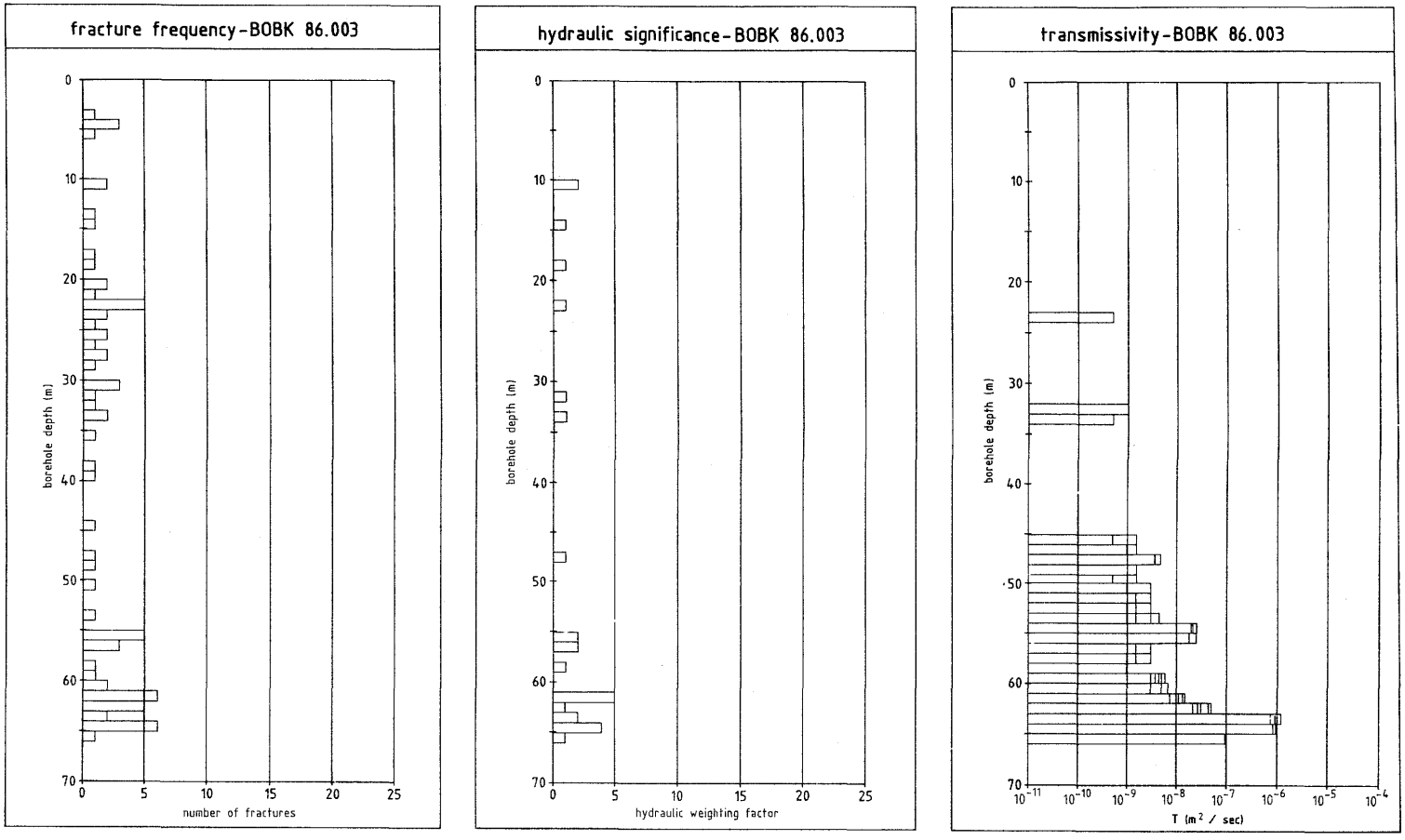

Fig. 35: Fracture frequency distribution, hydraulic weighting factors and transmissivity as a function of depth in borehole BK 86.003

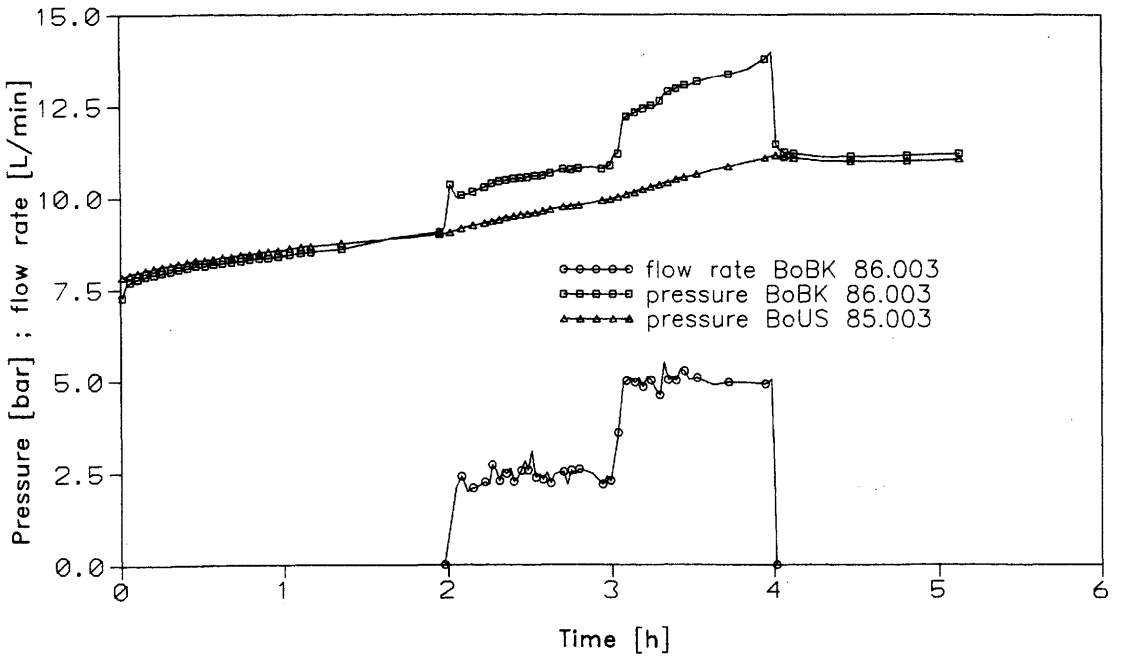

Fig. 36: Reaction in borehole US 85.003 to injection in borehole BK 86.003 (test 471)

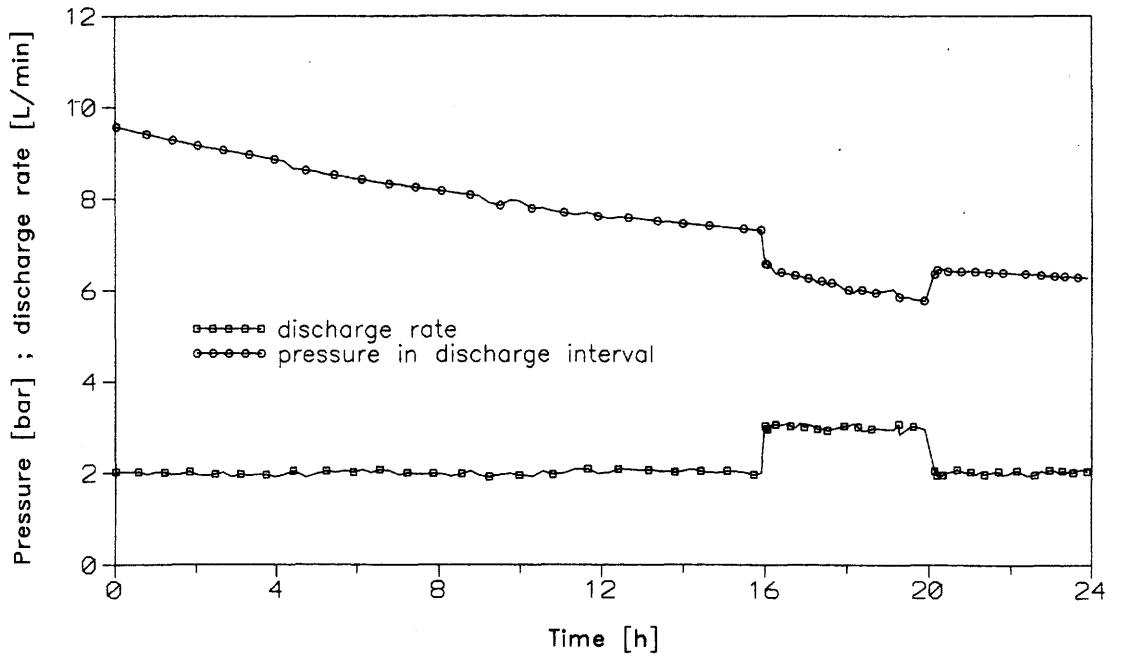

Fig. 37: Pressure drawdown test in borehole BK 86.003

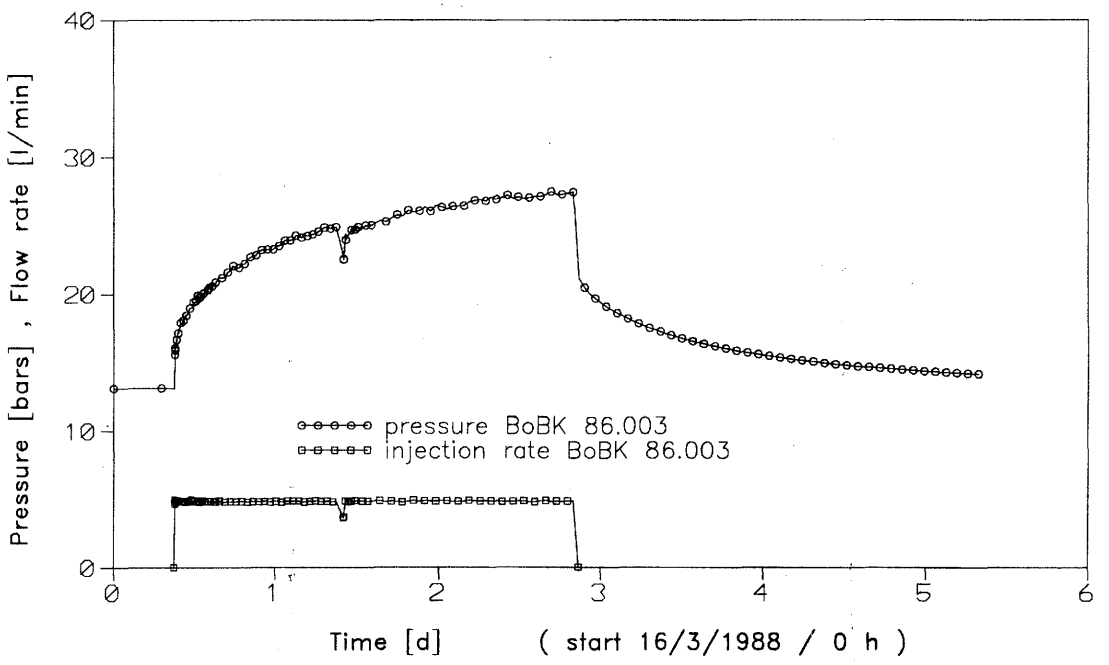

Fig. 38: Tests 380 and 381 in borehole BK 86.003; injection section: 64 - 65 m

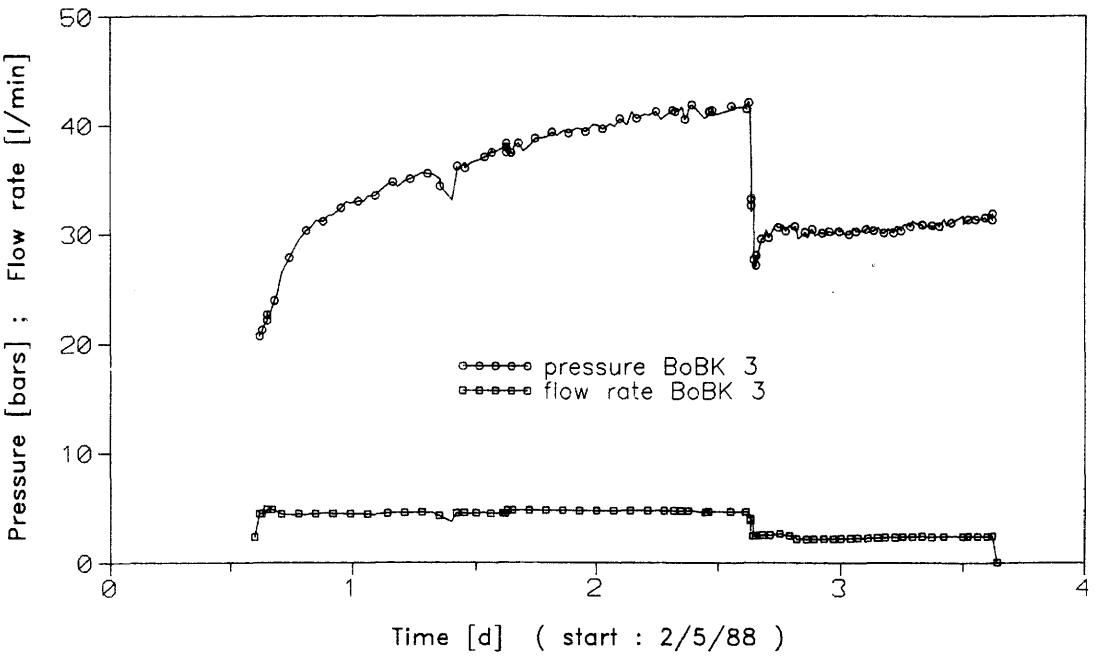

Fig. 39: Tests 390 A & B in borehole BK 86.003; injection section: 64 - 65 m

The abnormally rapid rise in pressure in the initial phase of test 390 is due to the fact that the pressure had already been increased during a previous test. One might suspect that, as a result of the numerous previous tests, the hydraulic conductivity of the fractures had been modified by the deposition of "foreign" particles in them. Later tests showed, however, that this effect is reversible.

A series of tests were conducted in US 85.003 to determine flow paths within the fracture system. Temperature logs showed that the main water influx occurred at about 109 m and 119 m. To determine unambiguously whether connections also existed between the upper part of the borehole and BK 86.003, which would possibly mean shorter flow paths, a conductivity log was run until a depth of 100 m was reached. The fact that the electrical conductivity measured at different times remains constant shows that no tracer entered this part of the borehole (Fig. 40). This flow path between BK 86.003 and US 85.003 has a length of at least 25 m. Computer simulations suggest that actual flow paths might be considerably longer.

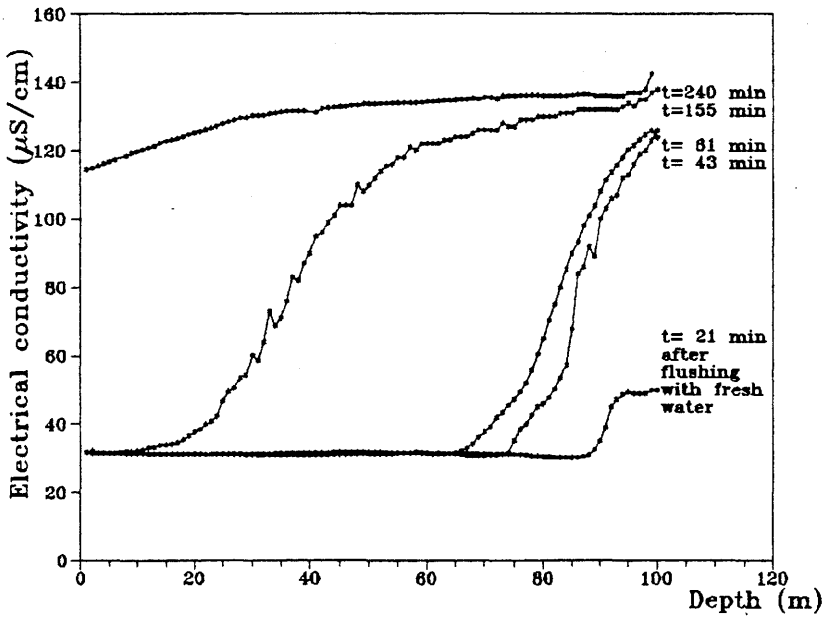

Fig. 40: Conductivity logs in borehole US 85.003

The results of a tracer test between these two boreholes are given in Figure 41. Over a period of several weeks, BGR probes were positioned in the US borehole at depths of 75 m and 86 m and a WTW conductometer at the mouth of the borehole; the electrical conductivity was monitored as a function of time with the conductometer and the electrical resistivity was monitored by the probes in the borehole. Injection rates of 2 – 3 l/min produced first-arrival times of 18 – 24 hours. This leads to a maximum flow rate of 1.5 m/h, assuming the water followed the shortest path.

5.3.3 Area around GS 84.041A

In this part of the test site, long-term pressure recovery measurements were carried out at the suggestion of NAGRA to investigate the behavior of deep-lying rock. Drill core logs had demonstrated that the permeability would vary considerably in the borehole. For this reason four test series were conducted in which a total of eight sections were tested (section 5.5):

VE 422	11.5 – 12.5 m	and 14.0 – 191.3 m
VE 423	11.5 – 59.0 m	and 60.5 – 191.3 m
VE 431	61.5 – 108.5 m	and 110.0 – 191.3 m
VE 440	91.5 – 138.5 m	and 140.0 – 191.3 m

BGR probes were installed below the packer to measure the pressure recovery, and additional high-pressure lines were laid between the drift and the observation section in the borehole so that pressures in the boreholes could be also measured outside the borehole.

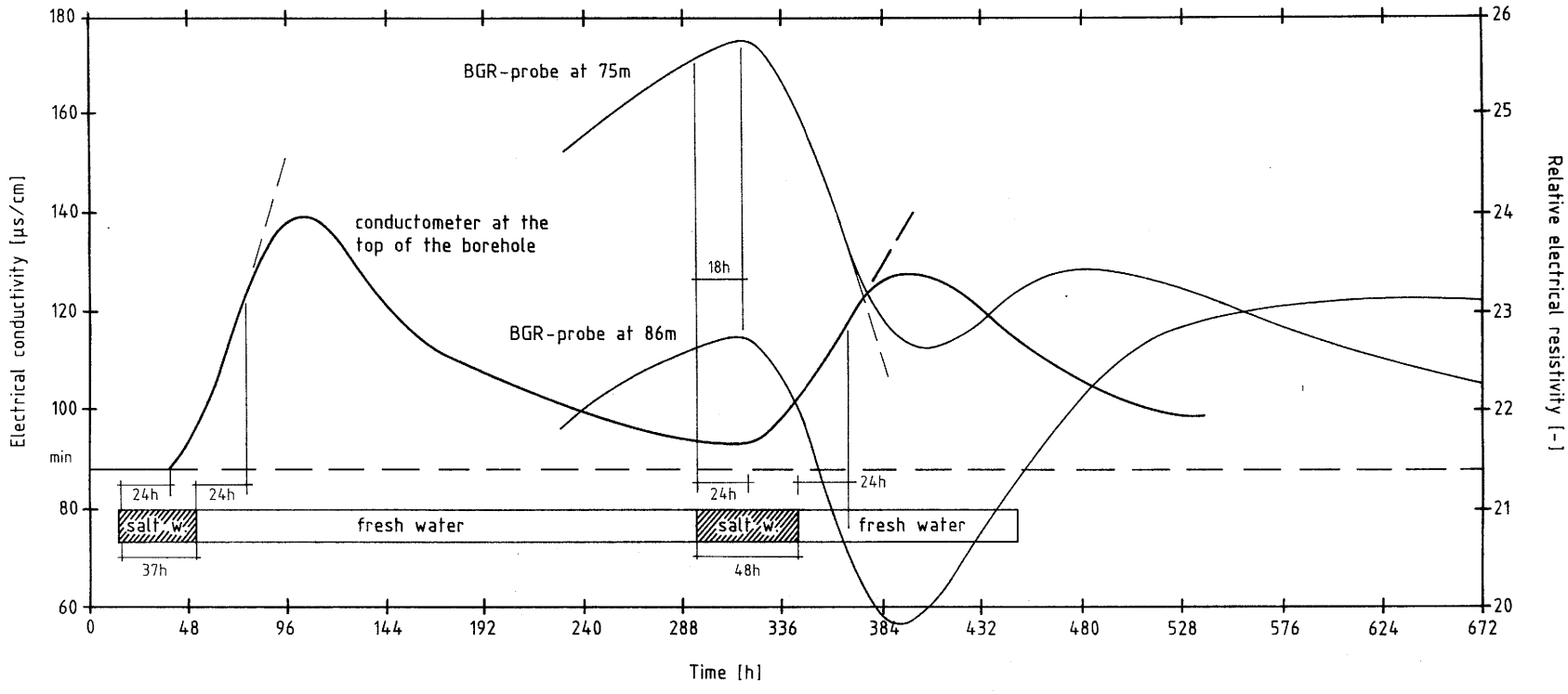

Fig. 41: Dipole tracer test: boreholes BK 86.003 and US 85.003
a) conductometer at borehole mouth
b) probe at 75 m
c) probe at 86 m

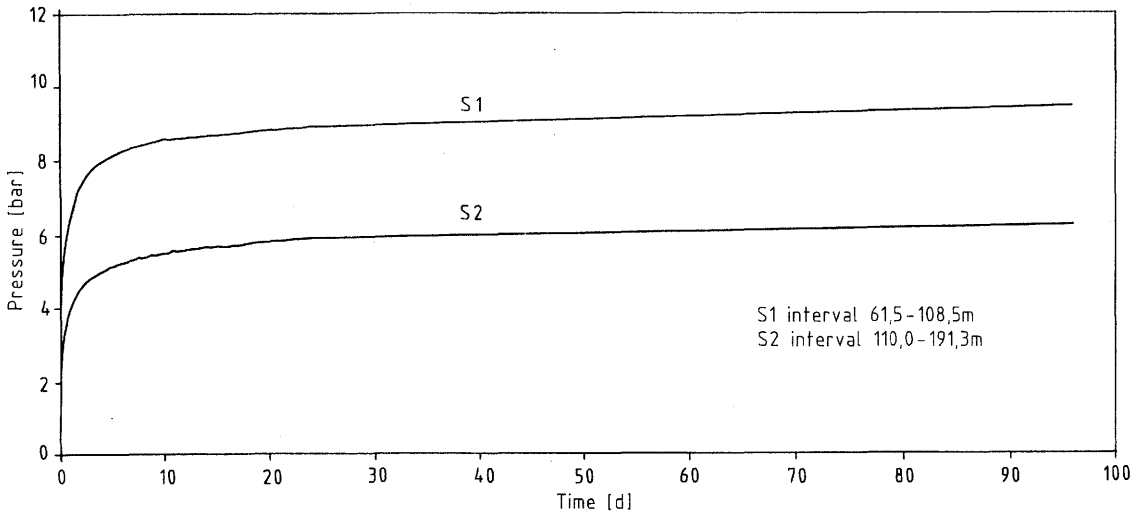

Fig. 42: Pressure recovery test in borehole GS 84.041A

The pressure build-up curves for the third test series (20 March to 23 June 1989) are shown in Figure 42 as an example. The curves are largely affine; however, the pressure difference of about 3 bar is not equivalent to the 50 m vertical distance between the two probes. In the second test series, higher pressures were obtained, even in the upper section toward the mouth of the borehole. Extrapolation of the pressure build-up curve shows that in all parts of the rock mass, one can expect a pressure rise over a long period to a maximum of 10 – 12 bar. However, no leakage from the walls of the drift was observed during the tests. In all cases the hydraulic conductivities were relatively low.

5.4 Interpretation of the Test Results

Analytical and numerical procedures are used to evaluate the test results. In the simplest case, analytical solutions are based on steady-state flow conditions, i.e. the storage capacity of the geological medium is neglected. The classical method for interpreting pumping-test data is THIEM's well-known equation:

$$h_2 - h_1 = \frac{Q}{2 \cdot \pi \cdot m \cdot k_f} \cdot \ln(r_2/r_1),$$

where the height of the water table (piezometric head) in the well can be used as a first approximation for h_1 and the radius of the well for r_1.

In the case of non-steady-state flow conditions, closed solutions are not possible. In the THEIS method, therefore, the measured curve is compared with the theoretical THEIS curve to obtain transmissivity T:

$$T = \frac{Q}{4 \cdot \pi \cdot s} \cdot W(u)$$

and the storage coefficient S:

$$S = \frac{4 \cdot t \cdot T}{r^2} \cdot u \ ,$$

where

$$W(u) = \int_o^\infty \frac{e^{-u}}{u} \, du \ .$$

The theoretically based assumptions demonstrate that even a mathematically exact description of a phenomenon yields only an approximate solution when applied in practice, the assumptions being:

- the aquifer is confined,
- flow to and from boreholes is radial,
- the aquifer has an infinite extent,
- the aquifer is homogeneous and consists of an isotropically porous medium,
- the water table is horizontal,
- the water flows horizontally to the well,
- the pumping rate is constant.

Owing to the practical importance a realistic interpretation has for the petroleum industry or the water supply, for example, it was necessary to develop evaluation methods that use theoretical curves that take special boundary conditions into consideration (e.g. KRUSEMANN & DE RIDDER, 1973; LANGGUTH & VOIGT, 1980). Irregular aquifer geometries, however, can be realistically dealt with only by using numerical methods. Even then it often turns out that the transient reaction of a medium through which a fluid is flowing under variable hydraulic conditions provides more reliable information than tests carried out under steady-state conditions. On the other hand, the uncertainties in the parameter values do not result from the fact that the interpretation is made difficult by complicated geometrical and hydraulic boundary conditions, but from the fact that we do not have a detailed knowledge of these boundary conditions.

Interpretation procedures based on the assumption of a porous medium can be applied to fractured rock only if a representative elementary volume with no preferred flow paths is considered. For this reason, more effort is being put into determining the influence of fractures or fracture systems (STRAYLE, 1983; STOBER, 1985; KOPPELBERG, 1986; SCHNEIDER, 1987; DOE et al., 1987; etc.).

The examples of the quantitative evaluation of the tests given here are mostly results from test area II (Fig. 2), i.e. boreholes BK 86.003 and US 85.003, in which the hydraulic conditions are relatively accurately known (no leakage into the drift).

Injection test VE 471 (Fig. 36) was evaluated using the THEIS method. This is shown in Figures 43 (VE 471A) and 44 (VE 471B). A BASIC-program was used (Fig. 7) to iteratively fit the empirical curve to a theoretical curve derived from the test data. Borehole US 85.003 was closed a few days before the test: thus, a pressure increase (approaching steady-state) which took place independently of injection in BK 86.003 had to be taken into account. Since the pressure in US 85.003 rose almost parallel to that in the injection hole BK 86.003, only the pressure measured in the latter was considered. A borehole radius of 0.043 m was used for the sake of simplicity, the radius of the borehole theoretically has no influence on the transmissivity. This means that it is hardly possible to give any reliable information about the storage capacity. A transmissivity T of 1×10^{-6} m²/sec was obtained for both test phases (injection rates of 2.5 l/min and 5.0 l/min in an injection section about 60 m long). From this a hydraulic conductivity of $k_f = 10^{-3}$ m/s can be calculated for a joint with an aperture of 1 mm as an example assuming porous medium flow.

Although this evaluation led to clear results, the uncertainty associated with the applied assumptions is difficult to estimate. It is not possible to use THIEM's method to evaluate this clearly non-steady-state test curve. The transmissivities derived from the 1986 short-term tests using THIEM's method and assuming steady-state conditions are certainly too large (Figs. 22 & 35).

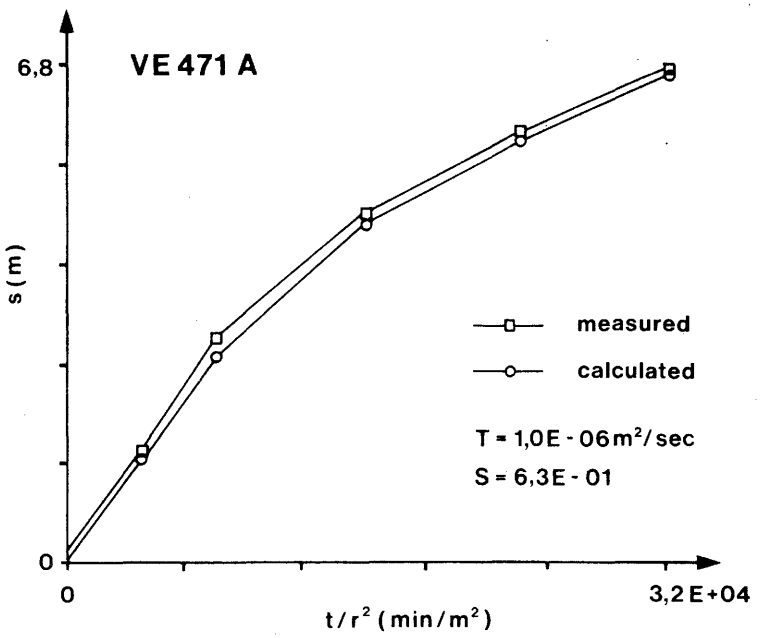

Fig. 43: Test 471A: THEIS method

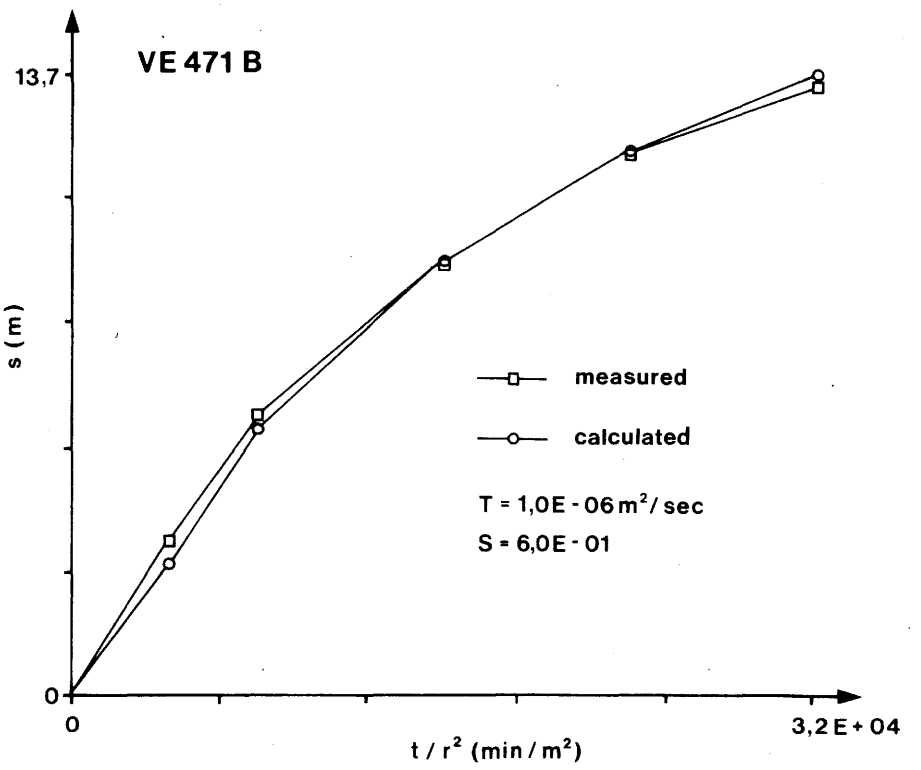

Fig. 44: Test 471B: THEIS method

As a comparison, the 1988 dipole tracer tests were evaluated using THEIS' method (Figs. 45 & 46). For a 1-m injection section between 63 and 65 m, transmissivities of 6×10^{-8} – 2×10^{-7} m²/sec were obtained; these can be considered to be limiting values. Strictly speaking, the THEIS method is not applicable to these tests, since basic assumptions are invalidated by the open borehole US 85.003. A realistic evaluation is possible in such cases only by using numerical methods.

Measurements made in borehole US 85.003 during pressure build-up were evaluated using the recovery method of THEIS & JACOB (Fig. 47). The borehole was left open for a considerable time before the test began, resulting in a distinct drawdown cone. The duration (t_o) of this drawdown phase was varied (i.e. 500 h, 1000 h, and 2000 h) so that a plot of the hydraulic pressure against the normalized time $(t_o+t)/t$ produces different curves which, however, give results of the same order of magnitude. Extrapolation yields a hydraulic head at equilibrium of about 450 m and for Q = 4 l/min a transmissivity of 10^{-7} m²/sec.

A finite-difference program for numerical calculations was used to estimate the storage coefficient from these values. A single horizontal fracture was modeled with a fixed pressure at the boundaries equal to the measured pressure head. Taking the results of the previously conducted tests into consideration, the pressure curves shown in Figure 48 are obtained for storage coefficients S of 0.002 and 0.005. However, it is a general rule that calculation of a storage coefficient from pressure recovery measurements in a single borehole is subject to a considerable degree of uncertainty of at least one order of magnitude.

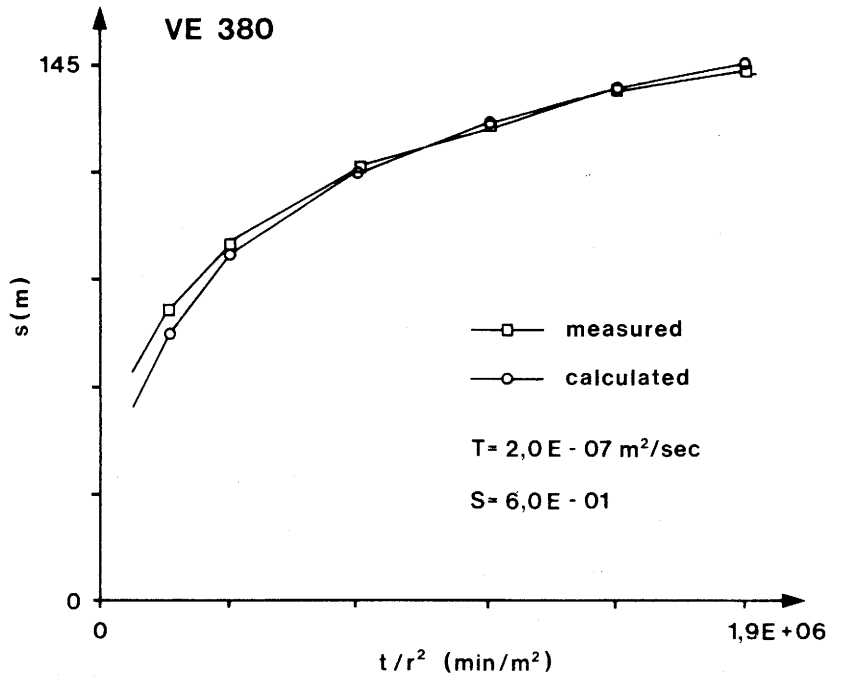

Fig. 45: Test 380: THEIS method

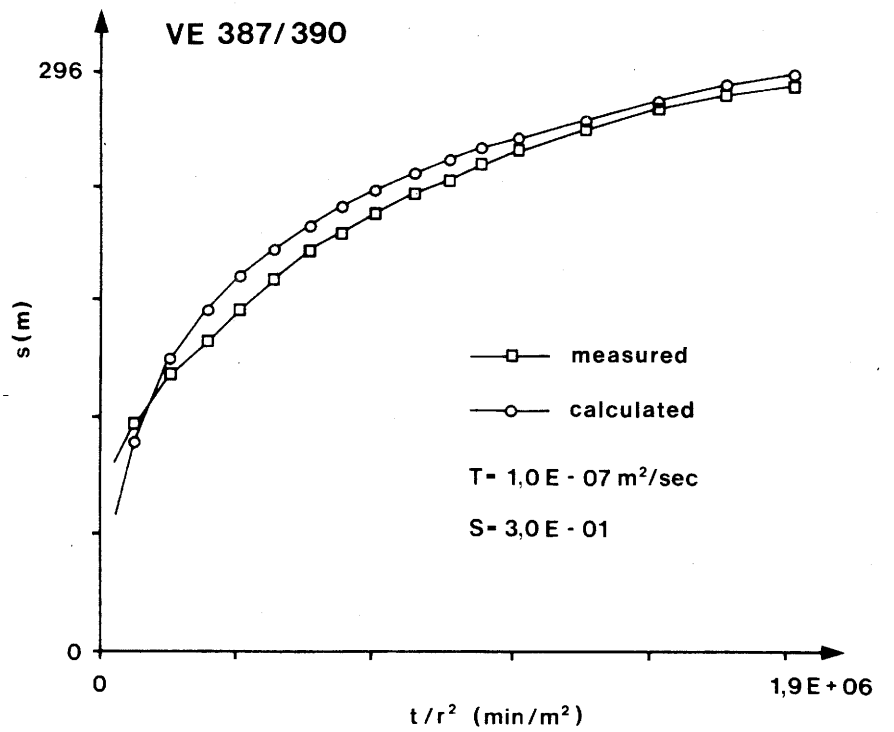

Fig. 46: Tests 387 & 390: THEIS method

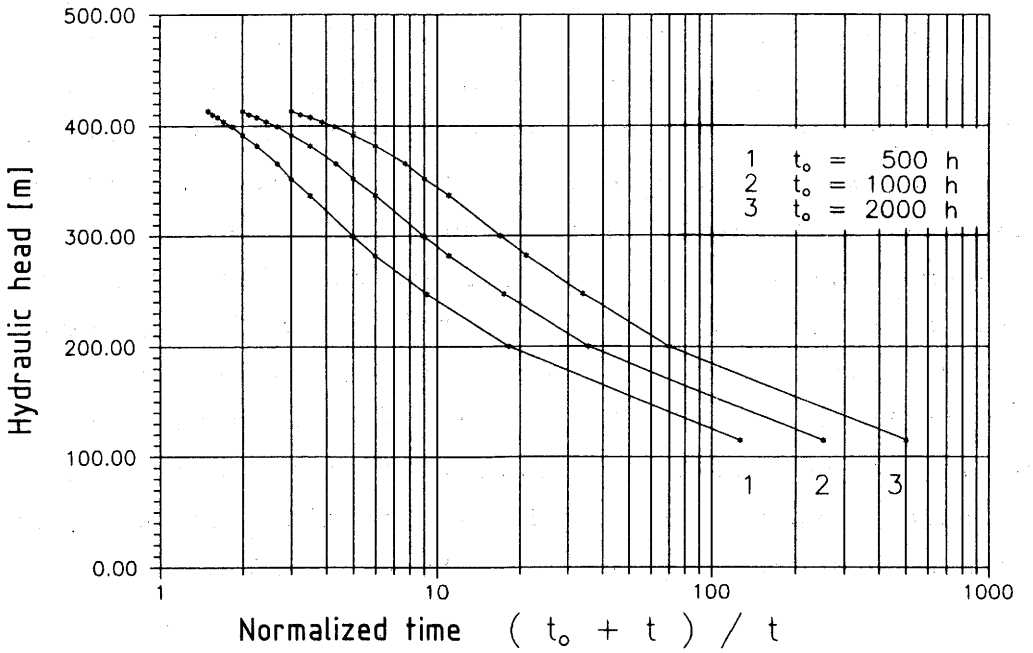

Fig. 47: Pressure recovery test in borehole US 85.003: COOPER & JACOB method

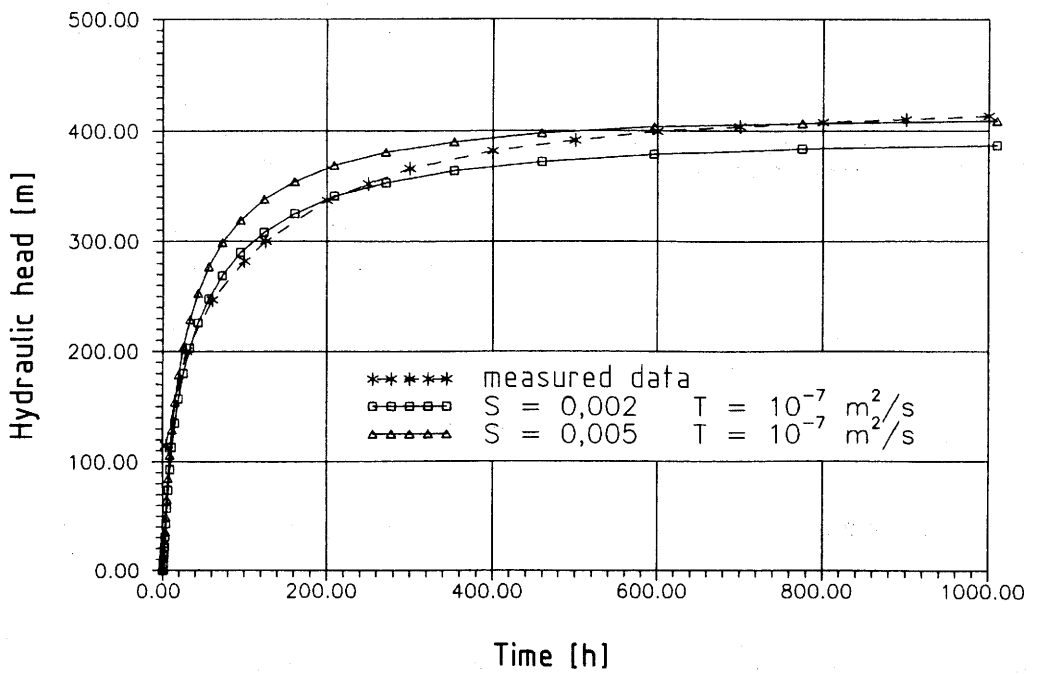

Fig. 48: Pressure recovery test in borehole US 85.003: finite differences program (2-D)

The straight-line method of COOPER & JACOB is normally used to evaluate pressure recovery tests. This is a plot of hydraulic head as a log function of time (COOPER et al., 1946). A plot of the first phase of test VE 473 in BK 86.003 shows that an approximately straight line for the hydraulic head is attained after several hours (Fig. 49).
A transmissivity of 2×10^{-7} m²/sec was calculated for the following period (p = 2.5 bar within a logarithmic decade on the time axis). At the beginning of the test the flow field appeared to be linear (short-term test); a large drawdown cone formed only gradually (long-term test). Curves of similar shape to that in Figure 49 were obtained for all comparable pressure recovery tests at the US-BK site.

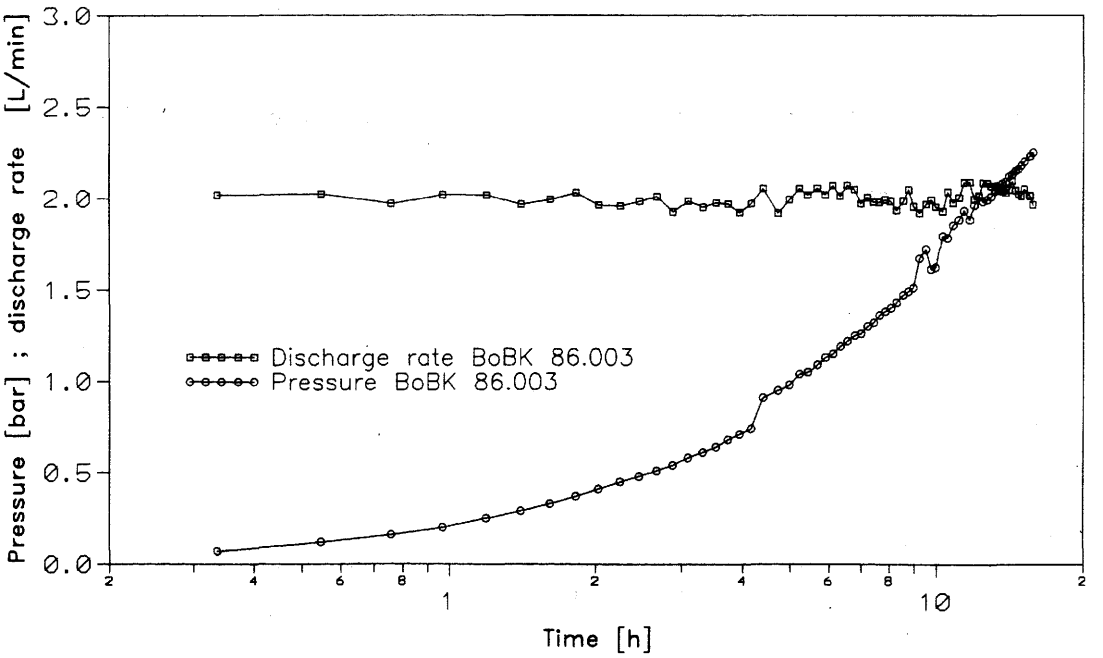

Fig. 49: Computer-controlled pressure recovery test 473

Evaluation of the test data is facilitated by use of "diagnostic" plots, which provide clues about the geometry of the flow field. If pressure is plotted as a function of time at various scales, then it is possible to distinguish between radial, linear, or spatial (3-D) flow conditions (Figs. 50 – 53, modified after ERSHAGI & WOODBURY, 1985).

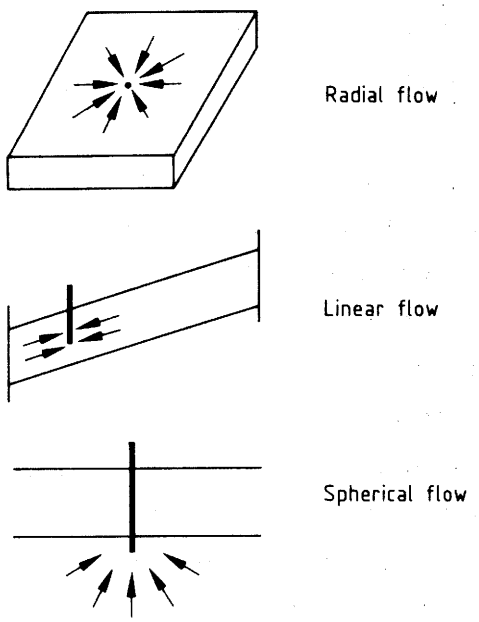

Fig. 50: Idealized flow models

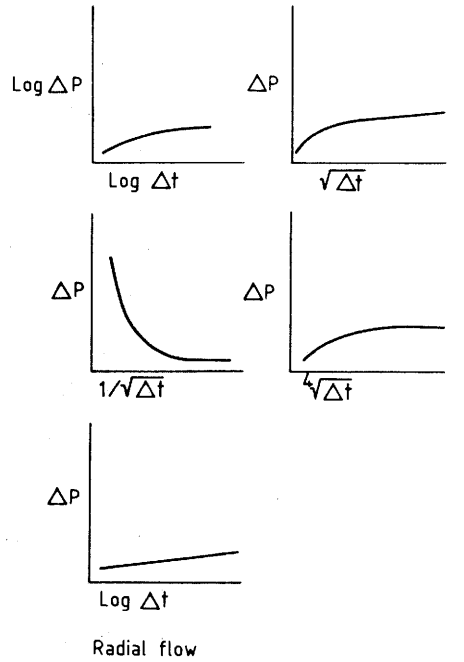

Fig. 51: Radial flow field: diagnostic plots

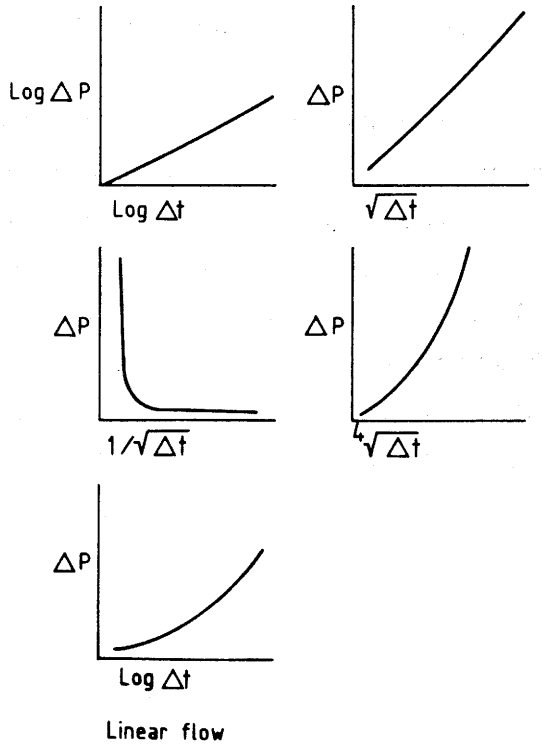

Fig. 52: Linear flow field: diagnostic plots

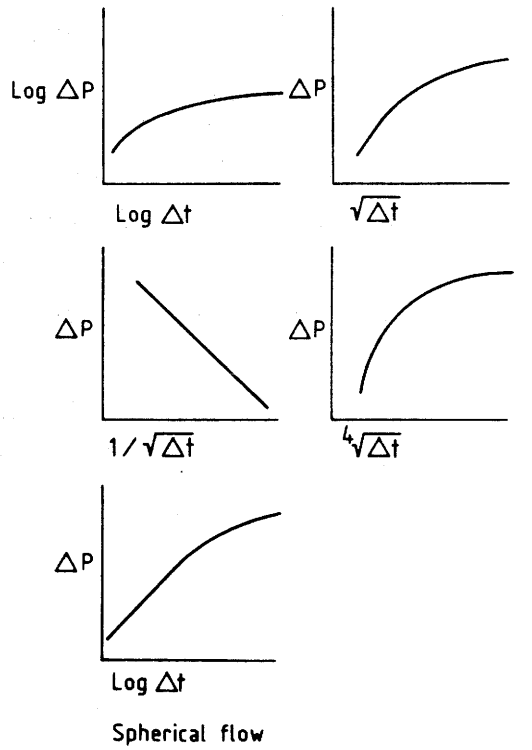

Fig. 53: Spatial flow field: diagnostic plots

Since ideal geometry does not exist in nature, in cases where the curve is ambiguous it is not possible to determine which assumption is invalid. In particular it is possible that due to the overlapping of special conditions (boundary, skin, wellbore storage, etc.), a pressure-time curve is obtained which fortuitously resembles the typical curve for a special set of conditions. When several boreholes are present, this problem could be solved by interchanging the injection and observation holes. When the curves qualitatively agree, it can be assumed that the flow geometry between the two points does not vary significantly. For the first phase of test VE 473, a close approximation of a straight line is obtained in a log-log plot of pressure versus time as well as in a plot of pressure versus the square root of the time (Figs. 54 & 55). This means that the main flow towards the open borehole is not radial but linear, i.e. movement of the water in the fractures therefore took place along paths of elevated permeability.

Similar results were obtained, for example, in test 465/466 in BK 85.004, which is in the central part of the Fracture System Flow Test area (Fig. 25). The transmissivity calculated using THEIS' method would thus be considered an estimate. We conclude that hydraulic parameters should be determined using several different methods in order to estimate the uncertainties in the methods. Further tests in the third phase of the project have been planned to investigate this phenomenon in detail.

The quantitative evaluation of tracer tests will not be dealt with until later, since in the tests conducted so far some uncertainties in the geometric and hydraulic boundary conditions have become apparent. The factor which contributes to the difficulties in the central part of the test site are loss of tracer due to leakage into the drift, which as a whole cannot be estimated. In some cases, NaCl concentrations were measured where water was dripping from the roof or walls of the drift that were higher than in the observation borehole. In future tracer tests it is planned to incorporate some of these leaks as observation points.

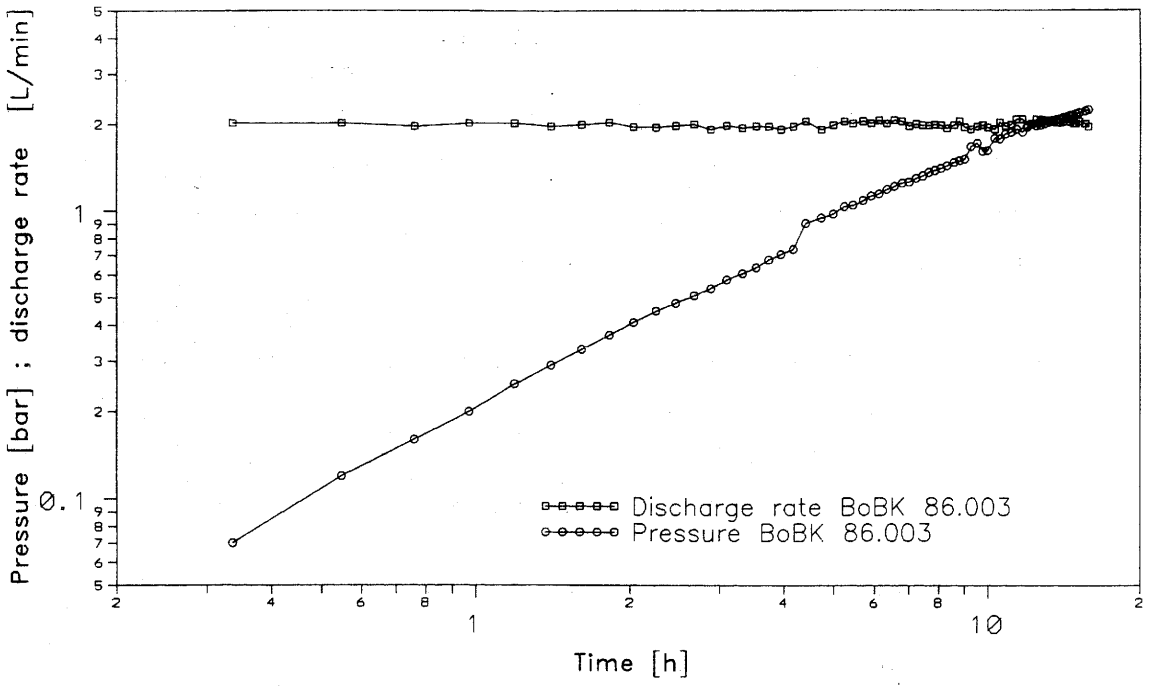

Fig. 54: Computer-controlled pressure drawdown test 473 in borehole BK 86.003 as a logarithmic function of time

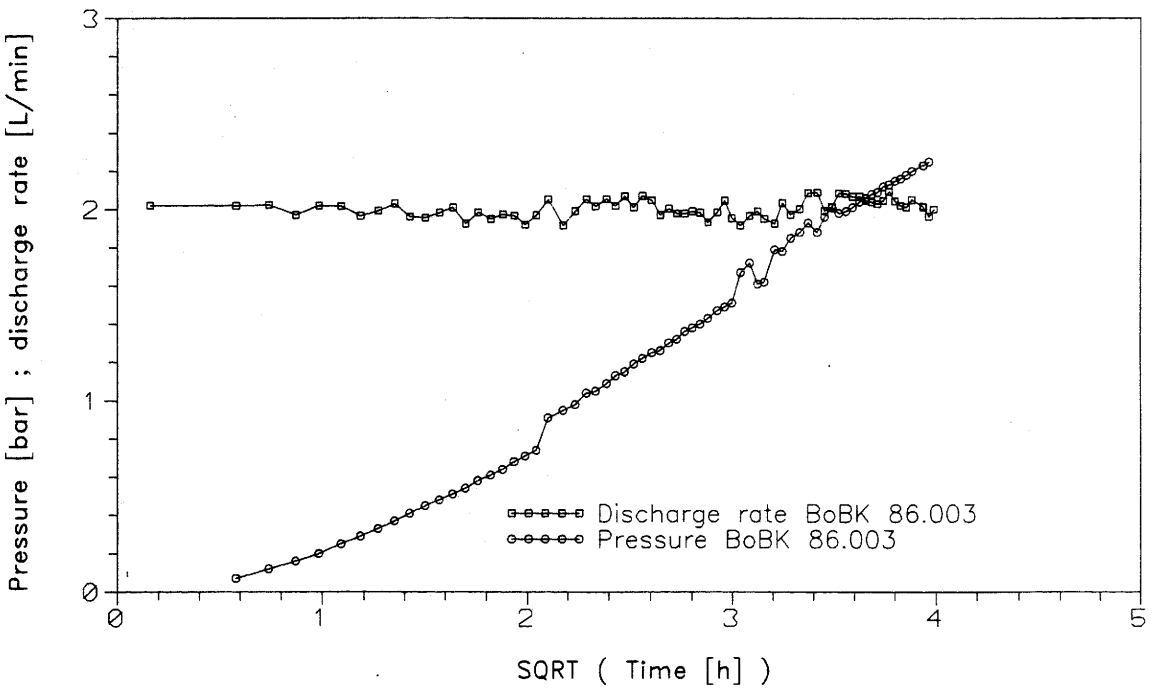

Fig. 55: Computer-controlled pressure recovery test 473 in borehole BK 86.003 as a square-root function of time

5.5 Numerical Calculations using the Finite-Element Method

5.5.1 Procedures

The following procedure was used for hydraulic modeling:

- idealization of the sets of fractures using a simulation model,
- definition of the parameter values and boundary conditions,
- solution of the system of simultaneous equations,
- interpretation of the results.

It should be borne in mind that the permeability tests yield transmissivities that apply only to the section of a borehole which is isolated with packers. Only the tracer tests provide permeabilities of individual fractures or fracture zones, based on the calculated first arrival times. Tracer velocities are then obtained by numerical calculations.

The following three conditions must be fulfilled in the model calculations:

- the mass balance is maintained (law of mass conservation),
- the boundary conditions must be equivalent to those of the in-situ tests (hydraulic head, nodal flux, storage coefficients),
- the traveltimes of the tracer (flow rates) must be of the same order of magnitude as the empirical values.

The variation of the hydraulic head and nodal flux as a function of time is put into the model as boundary conditions. The non-steady-state flow behavior within the rock mass requires an exact knowledge of the storage coefficient, which, like the permeability in the various elements, can take local differences into account.

The third condition is verified by the following calculation using the transport model. The agreement between the measured and calculated first arrival times, as well as the shape of the conductivity curve, is evidence for the correctness of the assumed dispersion coefficients, i.e. the size of the rock mass represented by the fracture model.

The modeling method we used will be illustrated by taking four typical calculations as examples:

- mass (tracer) transport in borehole US 85.003,
- mass transport in a fracture in the central part of the Fracture System Flow Test site,
- calculation of hydraulic head in the central part of the Fracture System Flow Test site,
- mass transport in peripheral area II (Fig. 2) of the Fracture System Flow Test site.

The above calculations are based mainly on the geological and geohydraulic analysis of the site as a whole as described in report NTB 88-37 (Sections 4 & 5.1). The results described here are confined to the modeling of individual fractures by rectangulated plate models with any spatial orientation. Previous model calculations for intersecting fractures or sets of fractures are not considered here. One reason for this is that, according to the numerous tests carried out in 1989/90, the assumptions made for the calculations are no longer compatible with present knowledge. The other reason is that the DURST-GP graphics program has been improved and permits a considerably better representation of the results than was possible previously. We plan to validate these calculations, which we have so far considered as preliminary, by using improved fracture models.

5.5.2 Mass Transport in Borehole US 85.003

In the fluid logging tests (Section 5.3.2), the concentration distribution was determined after flushing; the slope of the decrease in concentration was found to become flatter with time (Fig. 56). This decrease may have been due to the presence of a relatively large dispersion coefficient. On the other hand, it is not impossible that there was an influx of water from the rock mass (with a salt concentration different from that of the water used for flushing).

To examine this possibility, a 114-m-long interval of borehole US 85.003 was flushed with freshwater (with a conductivity of 31 μS/cm) and salt water with a conductivity of about 1000 μS/cm was injected into borehole BK 86.003. Then the concentration of the salt water discharged from borehole US 85.003 was measured five times. The water entering borehole US 85.003 from the surrounding rock had a conductivity of about 135 μS/cm, at least during the test period. It flowed from the borehole at a rate of 4 l/min.

The decreasing concentration found during the test was numerically simulated using the program DURST. The model consisted of 115 pipe elements each 1 m long. The flow field was determined with DURST-SM; the associated geometric boundary conditions were used as the initial conditions for variation of the dispersion coefficient with the program DURST-TM.

The calculated (smooth) curves using a diffusion coefficient D of 0.01 m^2/s are in good agreement with the measured (irregular) curves (Fig. 56), taking the disturbing influence of the conductivity measurements themselves into account (see, for example, the first two curves, t = 21 min and 43 min).

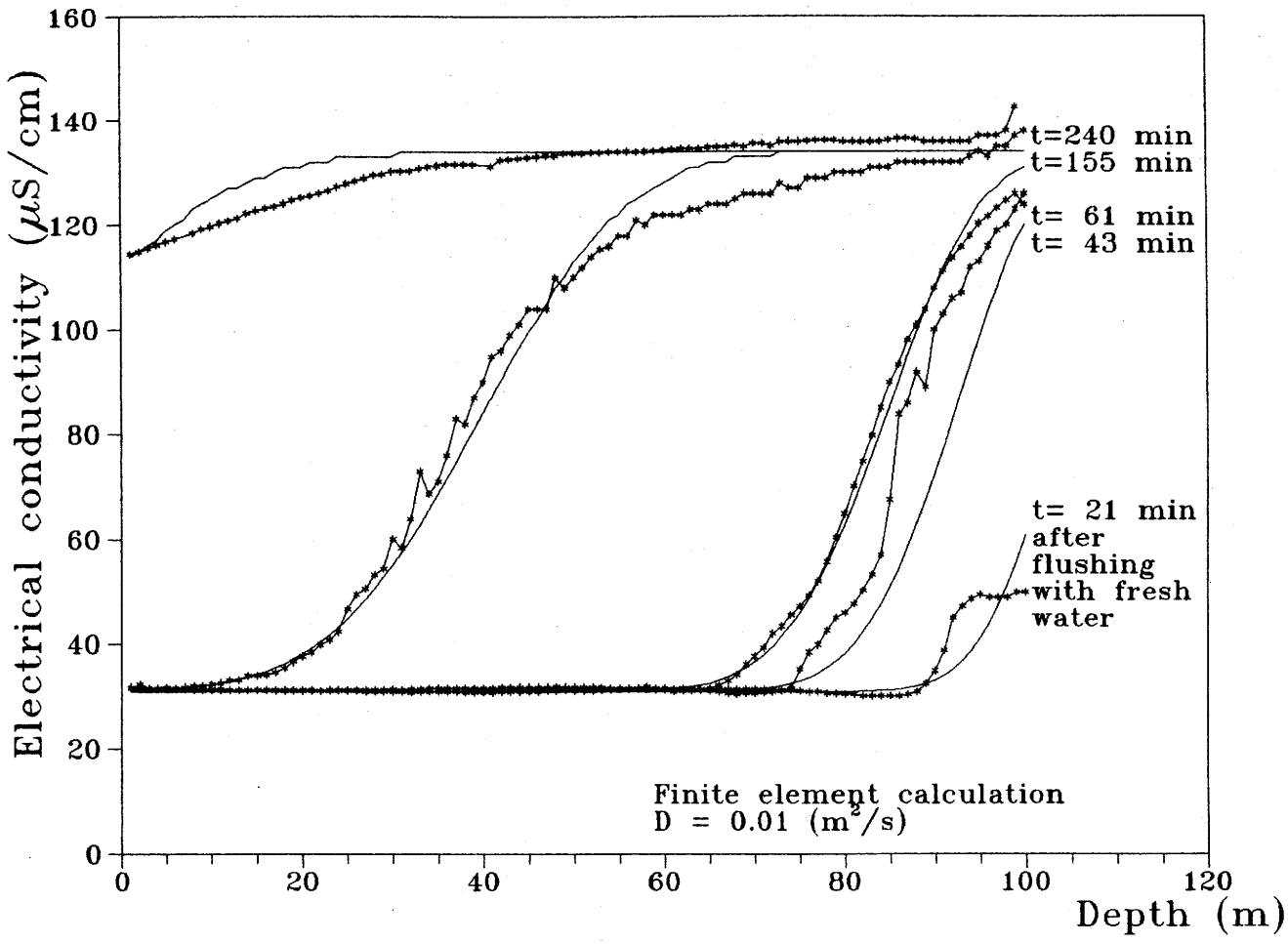

Fig. 56: Electrical conductivity as a function of depth in borehole US 85.003: comparison of the measured data and the results of the finite element computations using a dispersion coefficient of 0.01 m^2/s

The increase in the values at a depth of 100 m shows that the concentration of the incoming water varies. Later measurements down to the bottom of the hole will help to explain this effect.

5.5.3 Mass Transport in a Fracture in the Central Part of the Fracture System Flow Test Site

Tracer tests were conducted to determine the flow rate in the main fractures. The injection interval for this series of tests was between 28 and 29 m in borehole BK 85.009. The injection rate was about 15 l/min. During the tests all boreholes except one were sealed with pneumatic packers, so that most of the injected salt water could escape from the rock via the open borehole. The first arrival times and dispersion coefficients were determined by alternately injecting salt water and fresh water. The following three different kinds of tests were used:

I. The injection time (brine) in borehole BK 9 was three hours (Fig. 57). This was followed by 22 hours of injection of freshwater to flush the salt from the fractures. The concentration of the brine issuing from the neighbouring borehole BK 85.005 was recorded at the mouth of the borehole and by probes at several locations within the borehole. The data from one of the probes in the borehole is shown in Figure 58 as an example. The salt took about 20 minutes to travel the 9 m flow path. The pressures of the injected and discharged water were more or less constant throughout the test. For this reason, steady-state flow conditions were assumed.

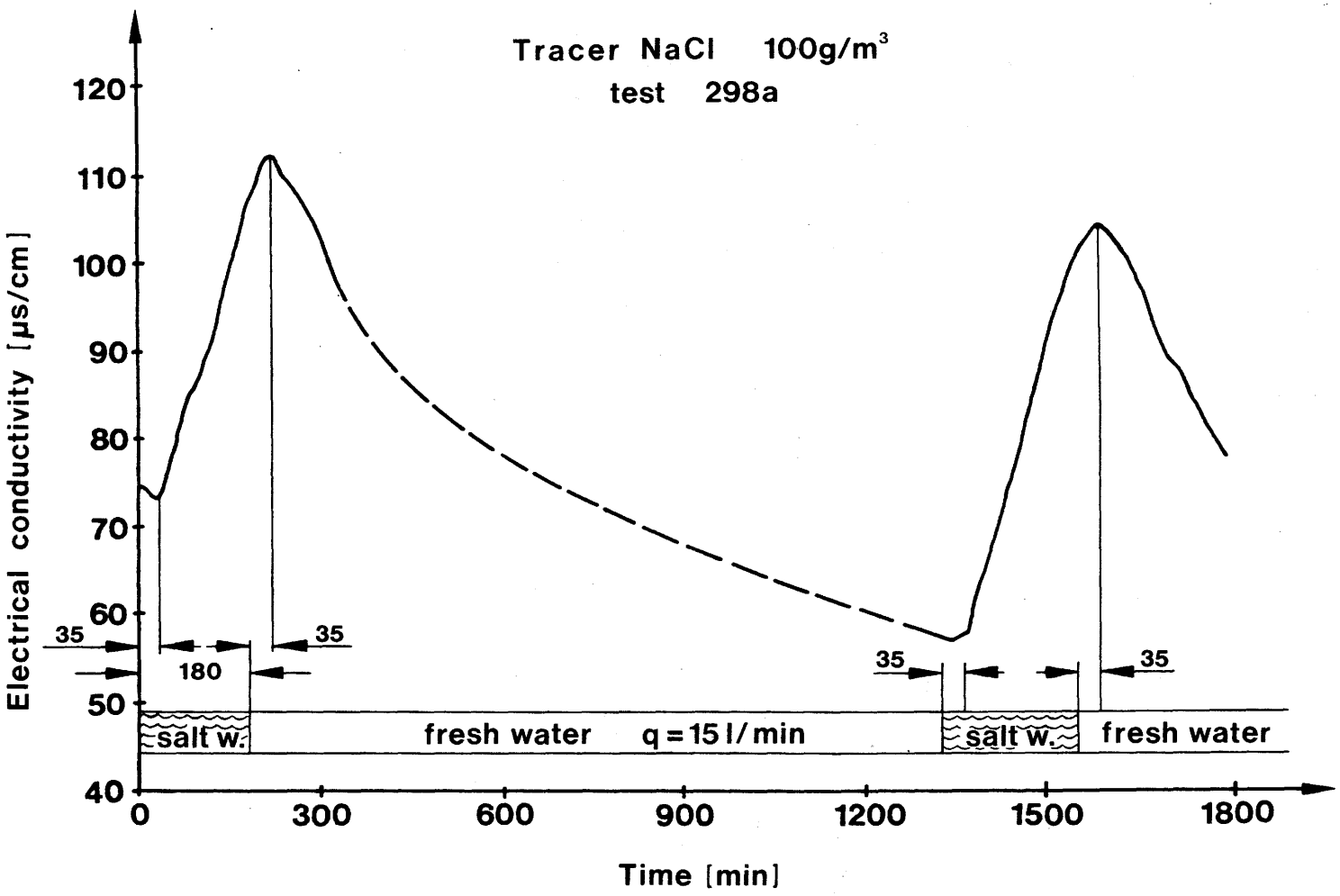

Fig. 57: Electrical conductivity as a function of time at the mouth of borehole BK 85.005 (test 298A)

II. The second series of tests was carried out under the same hydraulic conditions. The injection interval, the injection rate and the pressures were the same as in series I. The electrical conductivity of the injected fluid was alternately 180 μS/cm (salt water) and 14 μS/cm (fresh water). The salt concentration was changed at intervals of an hour. The first arrival times for these rapidly alternating tests could be determined only by the change in the slope of the concentration curve. The first arrival times measured at the mouth of the borehole were between 26 and 28 minutes (Fig. 59).

III. Borehole BK 85.005 was closed with a pneumatic packer during the third series of tests so that the injected brine could discharge only from a fracture at a depth of about 4 m in borehole BK 85.004. The lower part of BK 85.004 and all other boreholes were closed. The injection times were 5 hours for the brine and 19 hours for the fresh water. This cycle was repeated three times and then the rock mass was flushed with fresh water for several days (Fig. 28). The water discharged after the flushing phase had a lower conductivity (60 – 70 μs/cm) than that of the naturally occurring groundwater at the site (70 – 90 μS/cm). The first arrival times were 80 $\pm$ 20 minutes. Figure 60 shows the first cycle as an example.

A finite-element model was set up for hydraulic calculations. It consists of an idealized plate, 48 m square. The number of finite elements was either 132 or 1296 isoparametric 2-D elements. A close-spaced grid was required for the mass transport calculations. The injection point and the discharge location are called source and sink, respectively. They are placed along one diagonal. The edges of the finite element grid are 12 m and 16 m from the source and sink, respectively. It was assumed that the rock and fractures were saturated with water.

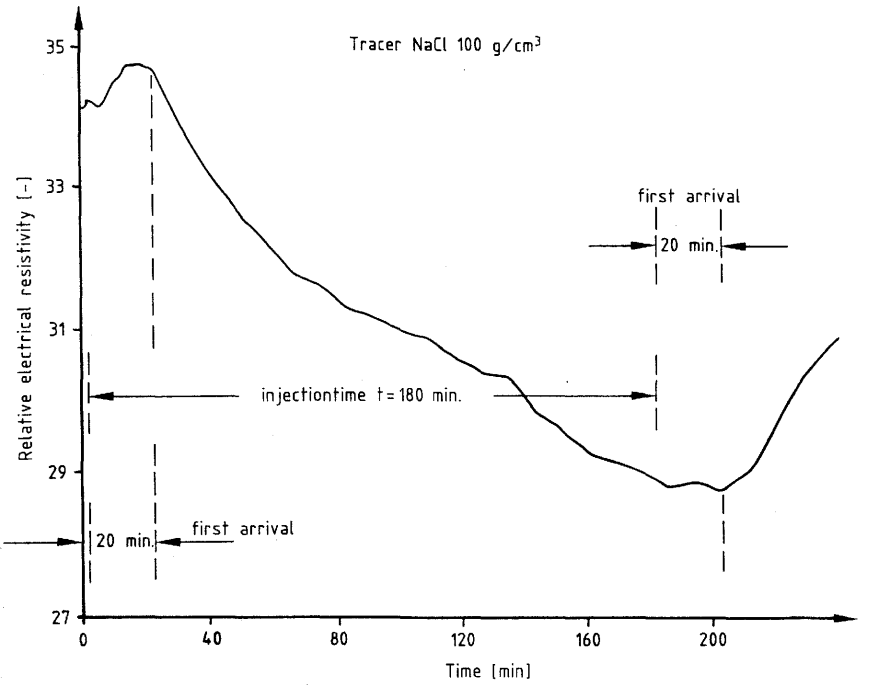

Fig. 58: Reaction of probe 39 (borehole depth 19 m) (test 298A)

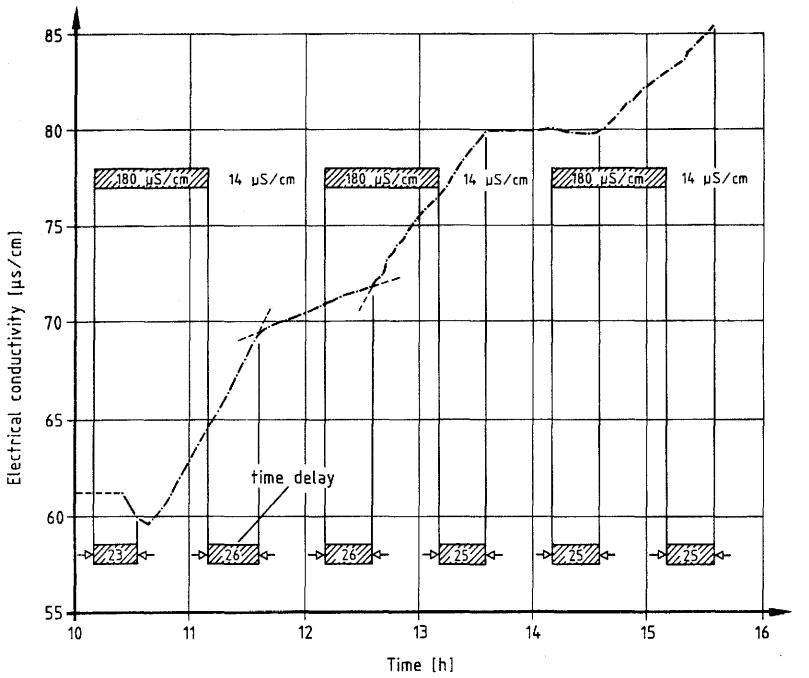

Fig. 59: Dipole tracer test: injection periods of one hour seperated by one-hour intervals

A fracture thickness of 2.2 mm (porosity n_e = 1) was obtained by comparison of the measured first arrival times and integration of the flow rate while varying the hydraulic conductivity and element thickness. The hydraulic head was constant at 80 m at the source and 0 m at the sink. The calculated hydraulic heads are shown in Figure 61, as viewed from two different directions. The steep hydraulic gradients around the boreholes show close agreement with the measured data. The flow velocities were calculated for the four integration points per element; however, for reasons of simplicity only one has been plotted per element in Figure 62. The calculated and empirical flow rates along the shortest flow path from borehole BK 85.009 to BK 85.004 are given in Figure 63.

The flow field as obtained above is a prerequisite for the mass transport calculations described below. Model 1 described in Section 5.2.1 was used for these calculations.

For steady-state flow, the Courant number (Eq. 6) and the Grid-Peclet number (Eq. 7) are necessary for the transport calculations. Simplified, the following formulas can be written for the Courant number and the Grid-Peclet number:

$$C_o = |\Delta t \cdot u/\Delta x_i| \leq 1, \qquad (6)$$

where Δt = time difference,
u = absolute value of the velocity vector $\underline{u}$,
$\underline{u} = (u_x, u_y, u_z)$, and
Δx_i = element length;

and

$$Pe = \frac{u_i \cdot \Delta x_i}{D_i} \leq 2, \qquad (7)$$

where D_i is the dispersion coefficient in m^2/s.

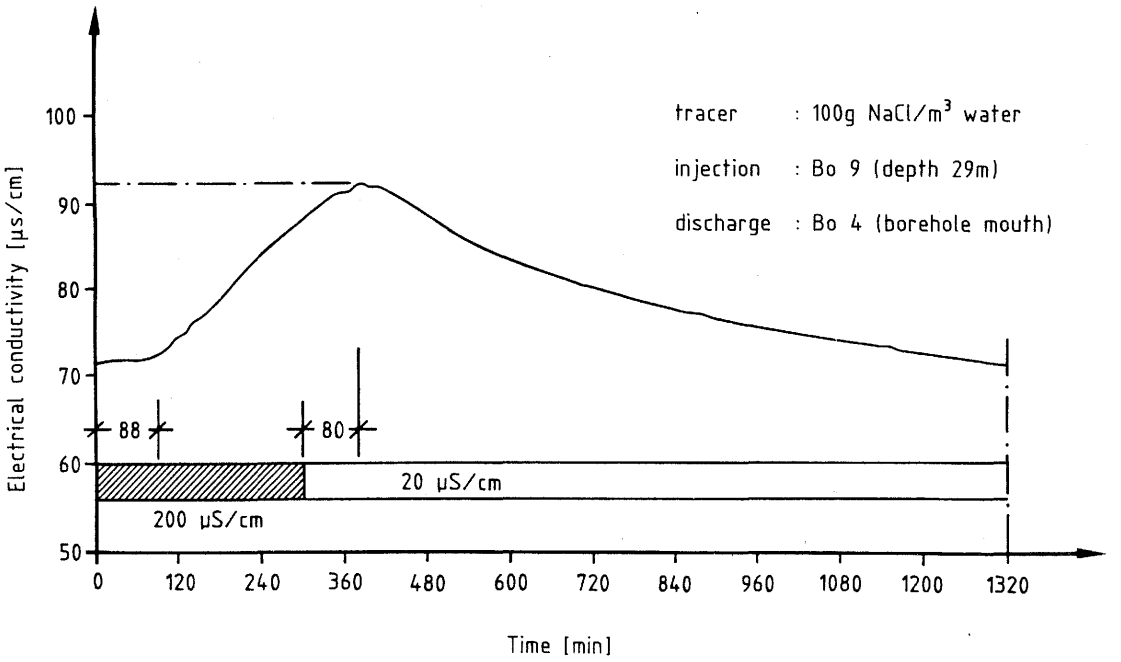

Fig. 60: Electrical conductivity as a function of time: NaCl tracer (100 g/m^3 water) injected at a depth of 29 m in borehole BK 85.009 and measured at the mouth of borehole BK 85.004

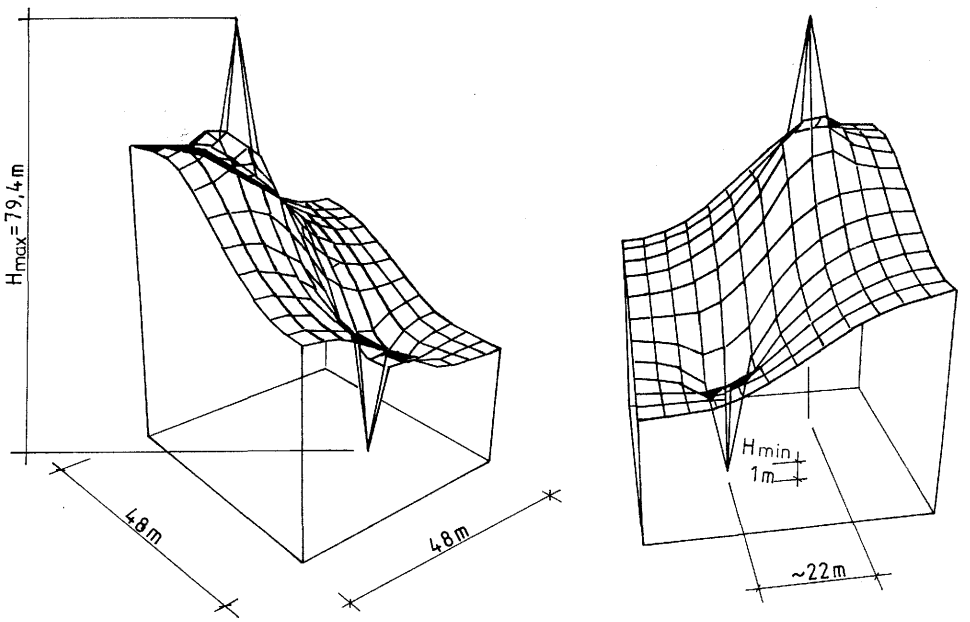

Fig. 61: Hydraulic head in a fracture system: Q = 15 l/min, k_f = 2x10^{-3} m/s, S = 10^{-8}

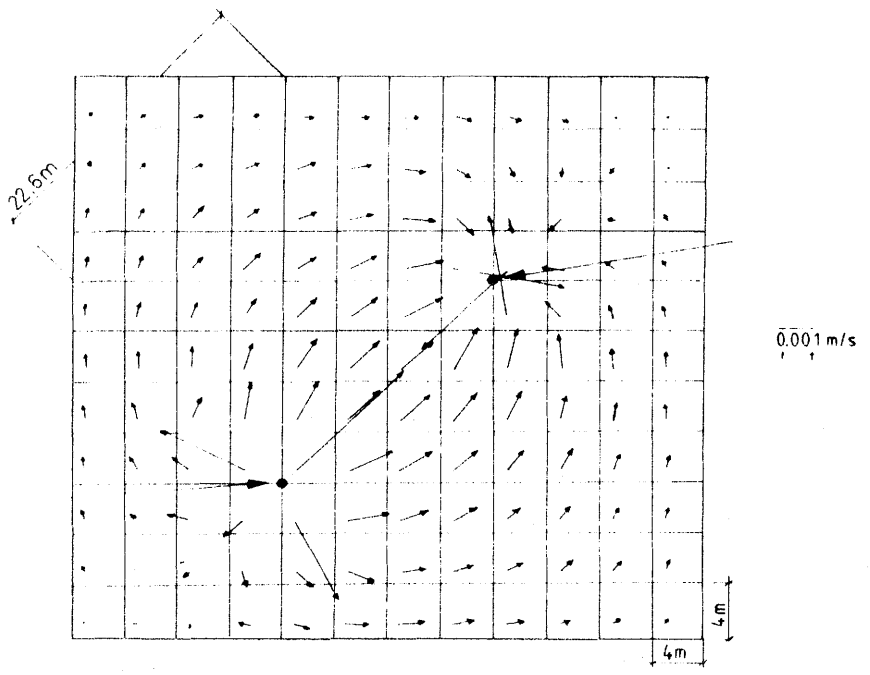

Fig. 62: Flow field, aperture = 2.2 mm, $k_f = 2x10^{-3}$ m/s

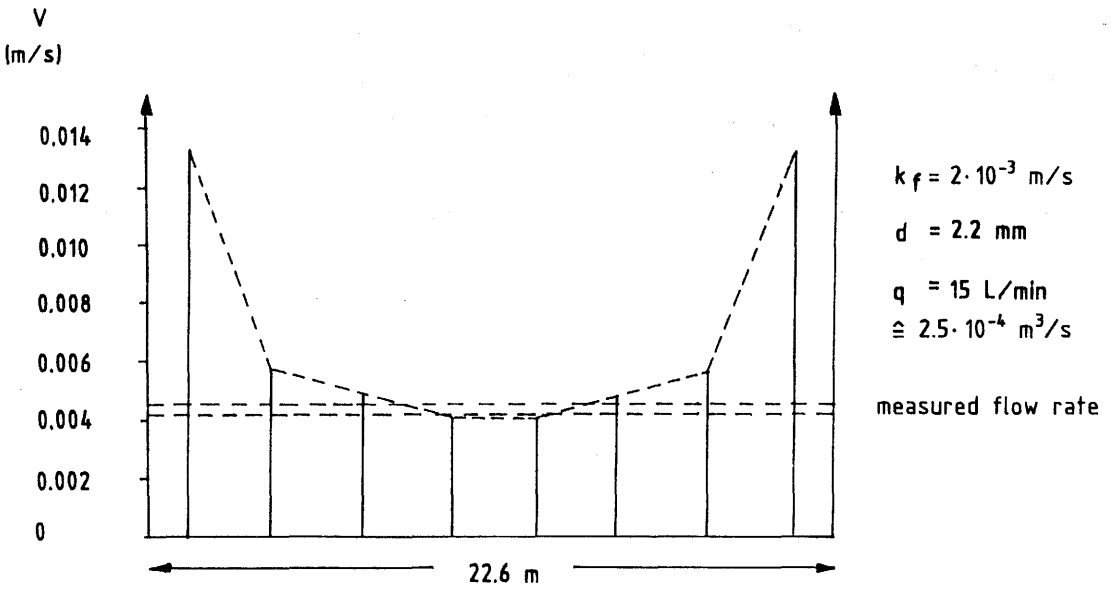

Fig. 63: Flow rate along the shortest flow path (test 300)

If these conditions are not fulfilled, then the numerical method leads to convergency problems around the source and sink in the model calculations. To avoid these oscillations, the dispersion coefficient must be made as large as possible, although one should remember to estimate its effect on the first arrival time. For this reason, the dispersion coefficient was increased in four stages from 2×10^{-5} to 2×10^{-2} m²/s. The concentration distribution in the example shown in Figure 64 is for parameter values compatible with the shortest flow path. The source and sink are each surrounded by eight elements of four nodes each. The concentration at the four nodes of the sink element is shown in Figures 65 and 67 – 70.

The first arrival time and the mean concentration at the sink is shown in Figure 66 for a dispersion coefficient of 2×10^{-4} m²/s. Oscillations do not occur for dispersion coefficients $>10^{-3}$ m²/s. The influence of the dispersion coefficient on the first arrival time and concentration as a function of time in the sink can be seen in Figure 70. Figure 71 shows the first arrival time as a function of the dispersion coefficient. Dispersion coefficients less than 10^{-4} m²/s have no importance in this particular model. The flow rate in the fracture follows a hyperbolic function when plotted versus the first arrival time. The calculated first arrival time curves for D = 0, 10^{-4}, and 10^{-3} m²/s are plotted together with the measured data (Figs. 57 – 60) in Figure 72. The calculated and measured data show good agreement for injection rates >6 l/min. The differences are greater at low water fluxes, as expected.

For an injection rate of 6 l/min and D = 0.001 m²/s the concentration distribution in the direction of flow is shown in Figure 73 at two times. The concentration distributions in the flow direction for an injection rate of 16 l/min and D = 0.01 m²/s are shown in Figure 74 for three times.

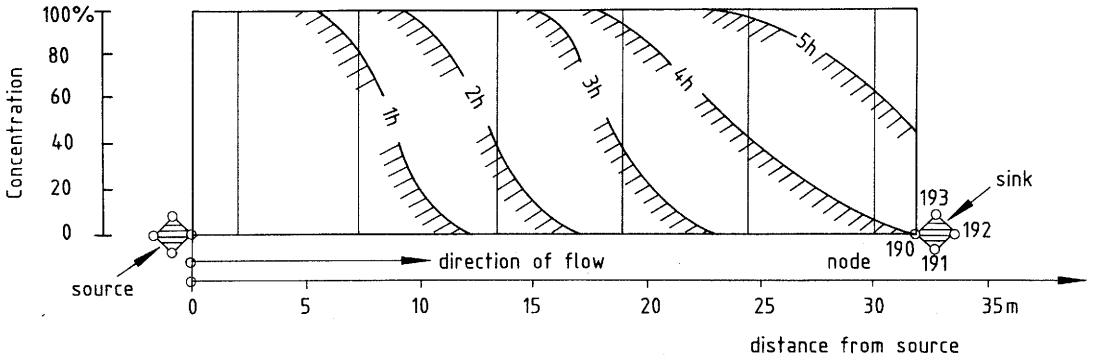

Fig. 64: Concentration distribution along the shortest flow path: D = 2×10^{-4} m^2/s, k_f = 2.3×10^{-2} m/s, S ≃ 0, Q = 6 l/min; fracture dimensions: 48x48 m, aperture: 2mm

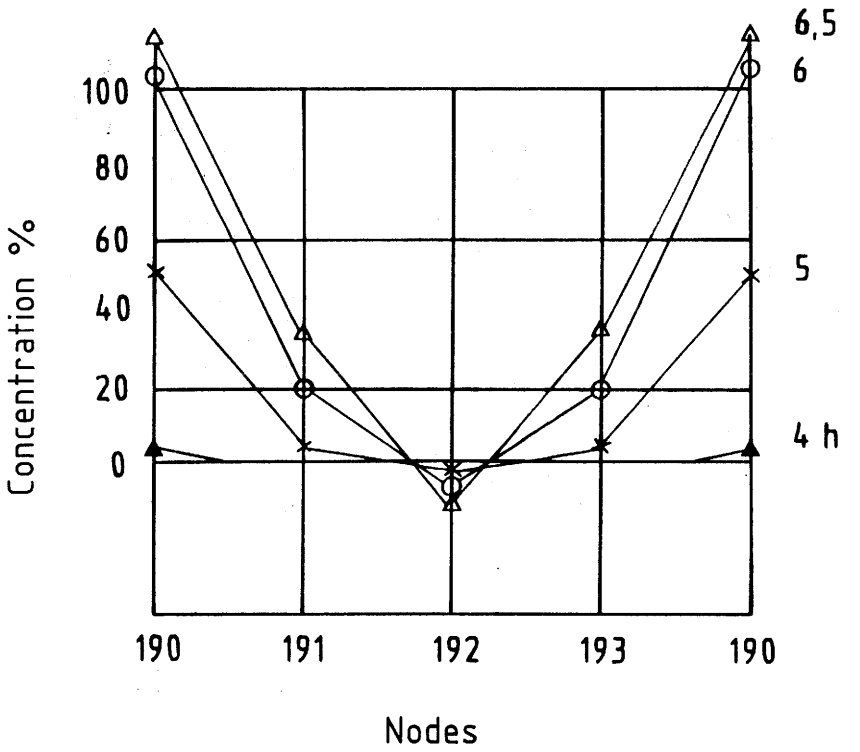

Fig. 65: Concentration at the sink as a function of time: D = 10^{-5} m/s, Q = 6 l/min

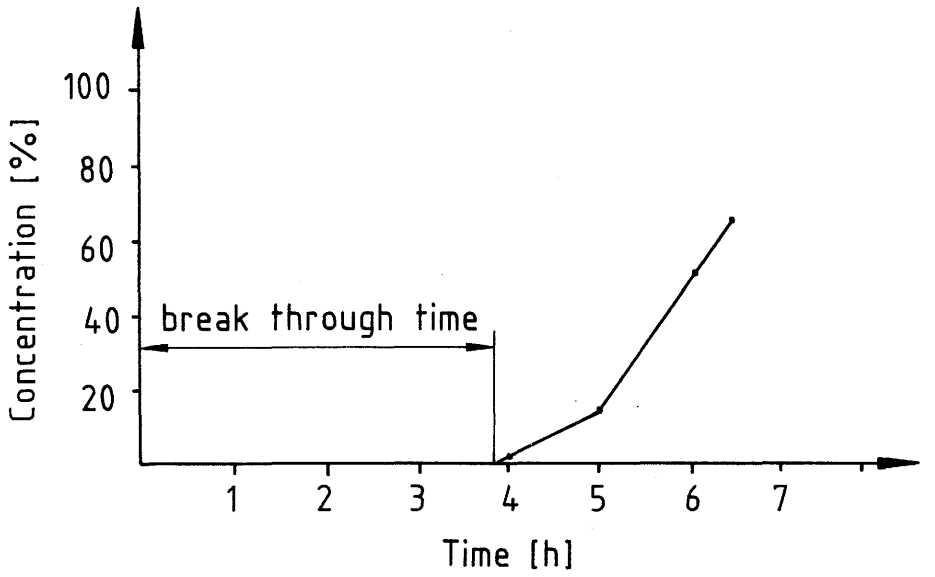

Fig. 66: Concentration at the sink as a function of time

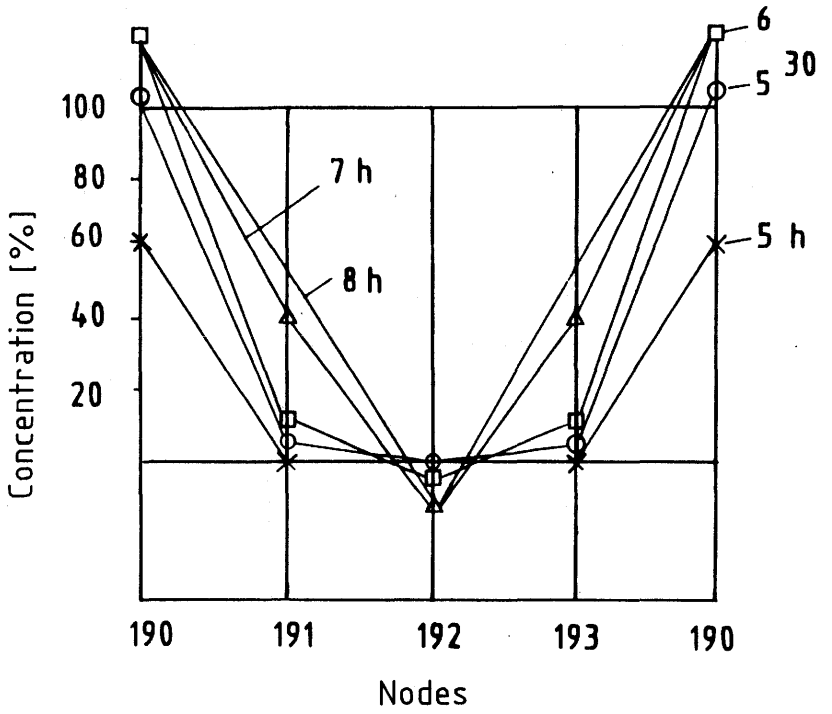

Fig. 67: Concentration distribution around the sink at different times: D = 2×10^{-5} m^2/s, Q = 6 l/min

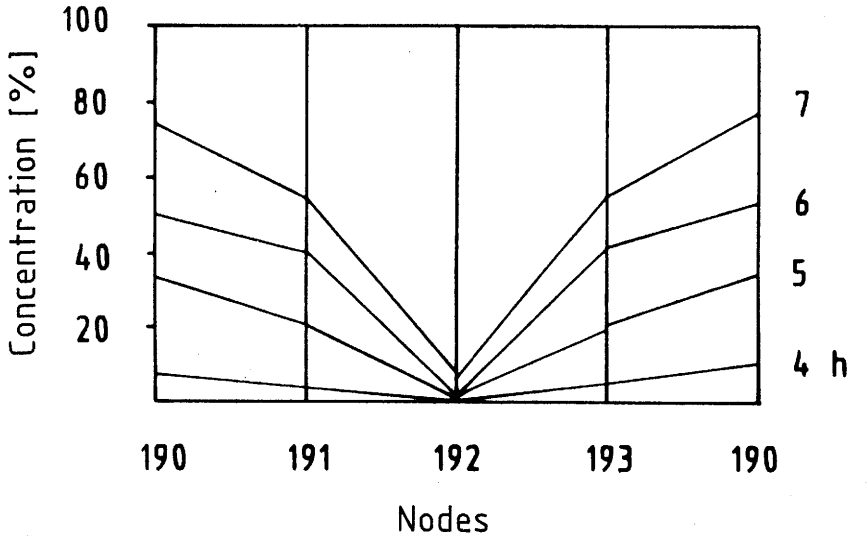

Fig. 68: Concentration distribution around the sink at different times: D = 10^{-3} m^2/s, Q = 6 l/min

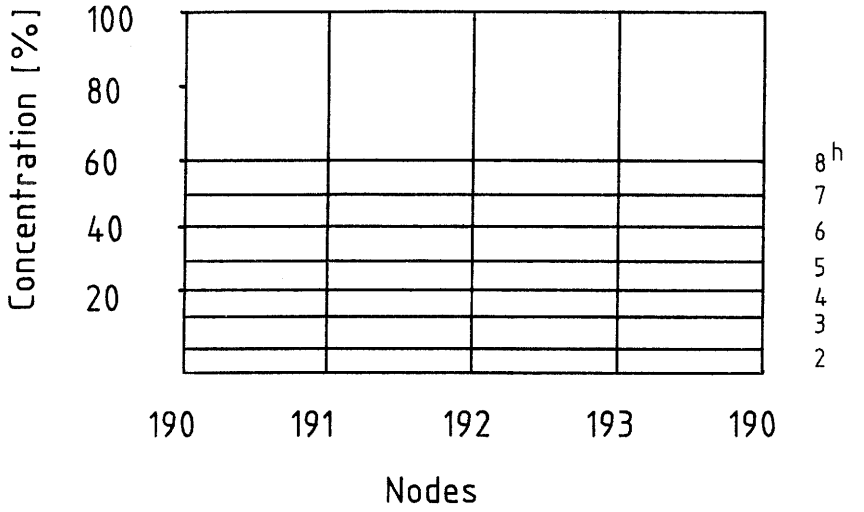

Fig. 69: Concentration distribution around the sink at different times: D = 10^{-2} m^2/s, Q = 6 l/min

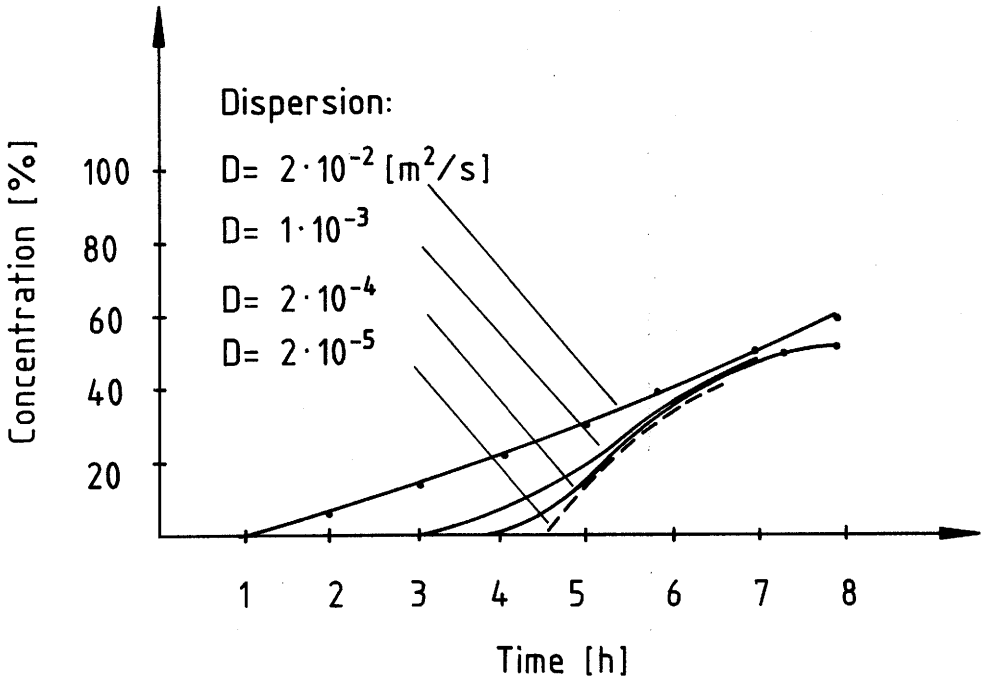

Fig. 70: Calculated concentration at the sink as a function of time using different dispersion coefficients, Q = 6 l/min, Δt = 300 s

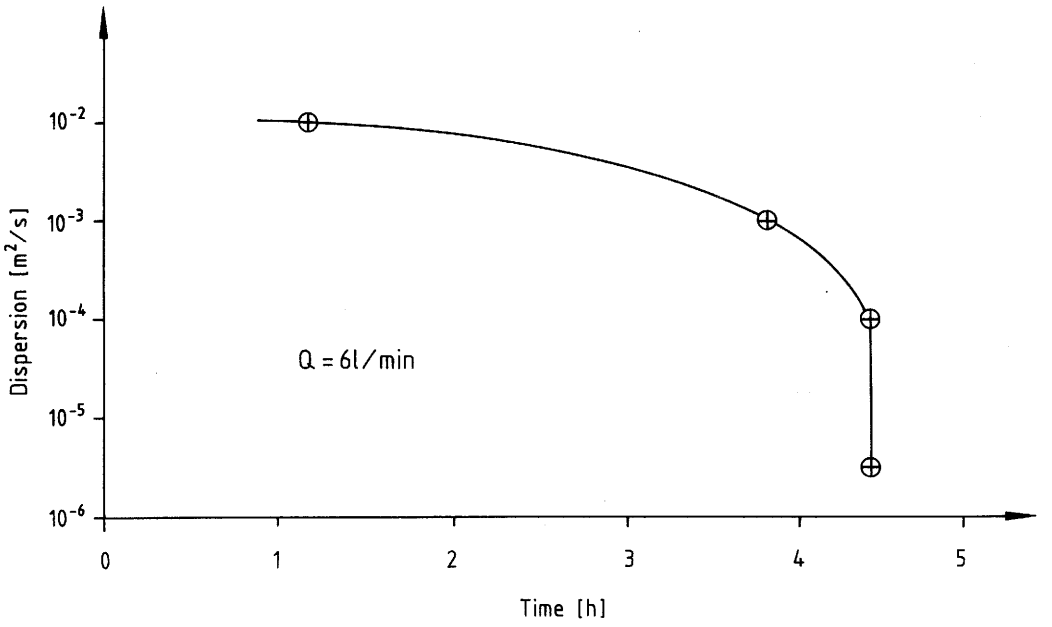

Fig. 71: First arrival times as a function of dispersion coefficient

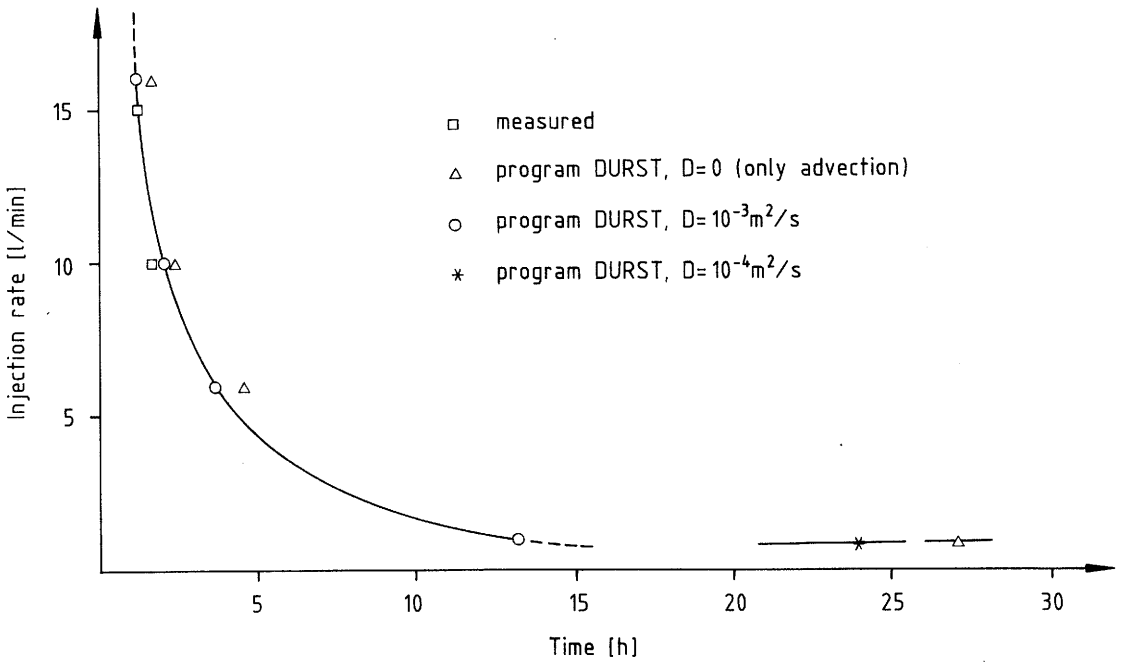

Fig. 72: First arrival times as a function of injection rate

The concentration distribution (10 % line only) is shown in Figure 75 for an injection rate of 15 l/min and $D = 0.001\ m^2/s$.

Tracer concentrations as a function of time are shown in Figures 76 – 78 at different times after injection of tracer at a constant injection rate of 10 l/min for 30 min, 1 hour, and 5 hours, respectively. These figures illustrate the relationship beteen the spreading of the tracer and injection time, as well as flow behavior that may be expected in a fracture or group of parallel fractures during flushing with freshwater.

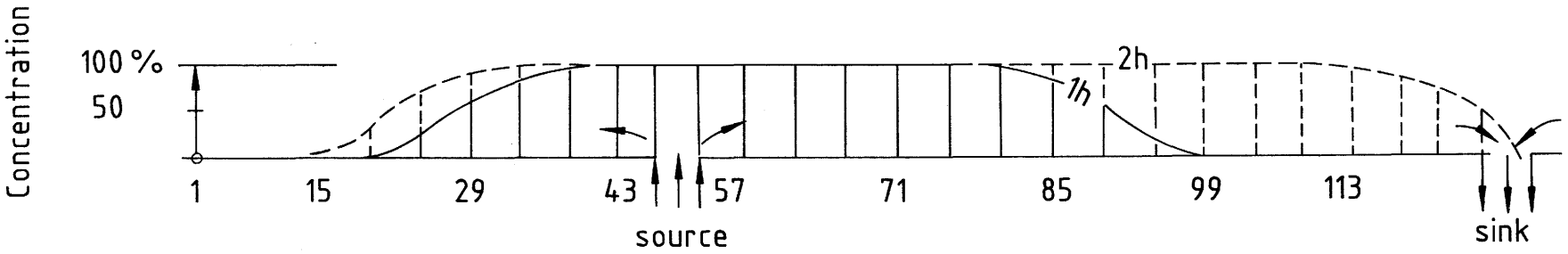

Fig. 73: Concentration distribution in the direction of flow: D = 10^{-3} m^2/s,
Q = 6 l/min, Δt = 300 s

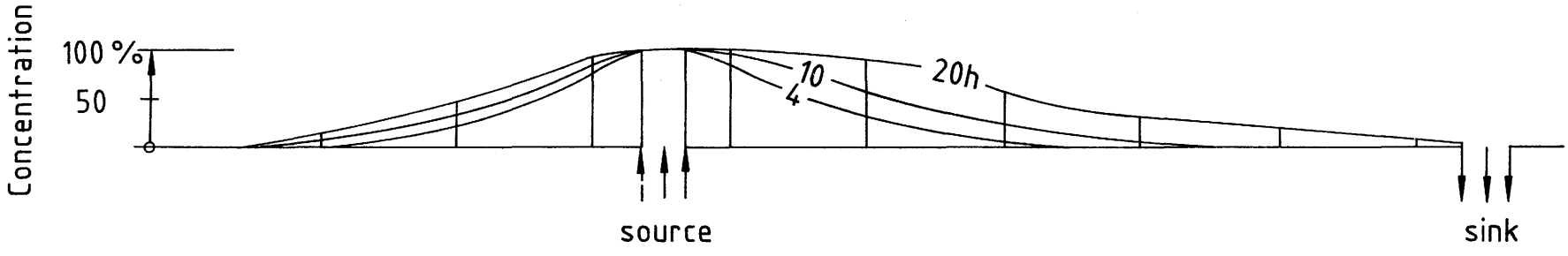

Fig. 74: Concentration distribution along the shortest flow path: D = 10^{-2} m^2/s,
Q = 16 l/min, Δt = 100 s

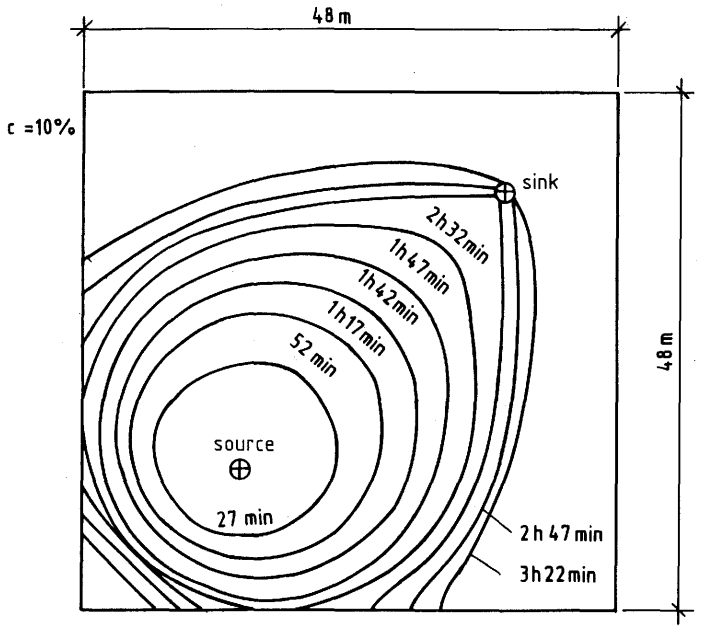

Fig. 75: Concentration distribution (isolines for c_2 = 10 %) as a function of time: Q = 15 l/s, D = 10^{-2} m^2/s

The following conclusions can be drawn from this parameter study:

- long tracer injection times require long flushing times;
- if the fracture net consists essentially of simple pipe-like channels rather than planes, then only short flushing periods are needed to restore the original conditions;
- owing to dilution effects, no conclusions can be drawn about the extent of the fracture system on the basis of short tracer tests;
- the geometric dimensions of a numerical fracture model permit further variations. To determine the geometric extent of a fracture system requires not only variation of the hydraulic and transport parameters, but also the geometric dimensions of the fracture model.

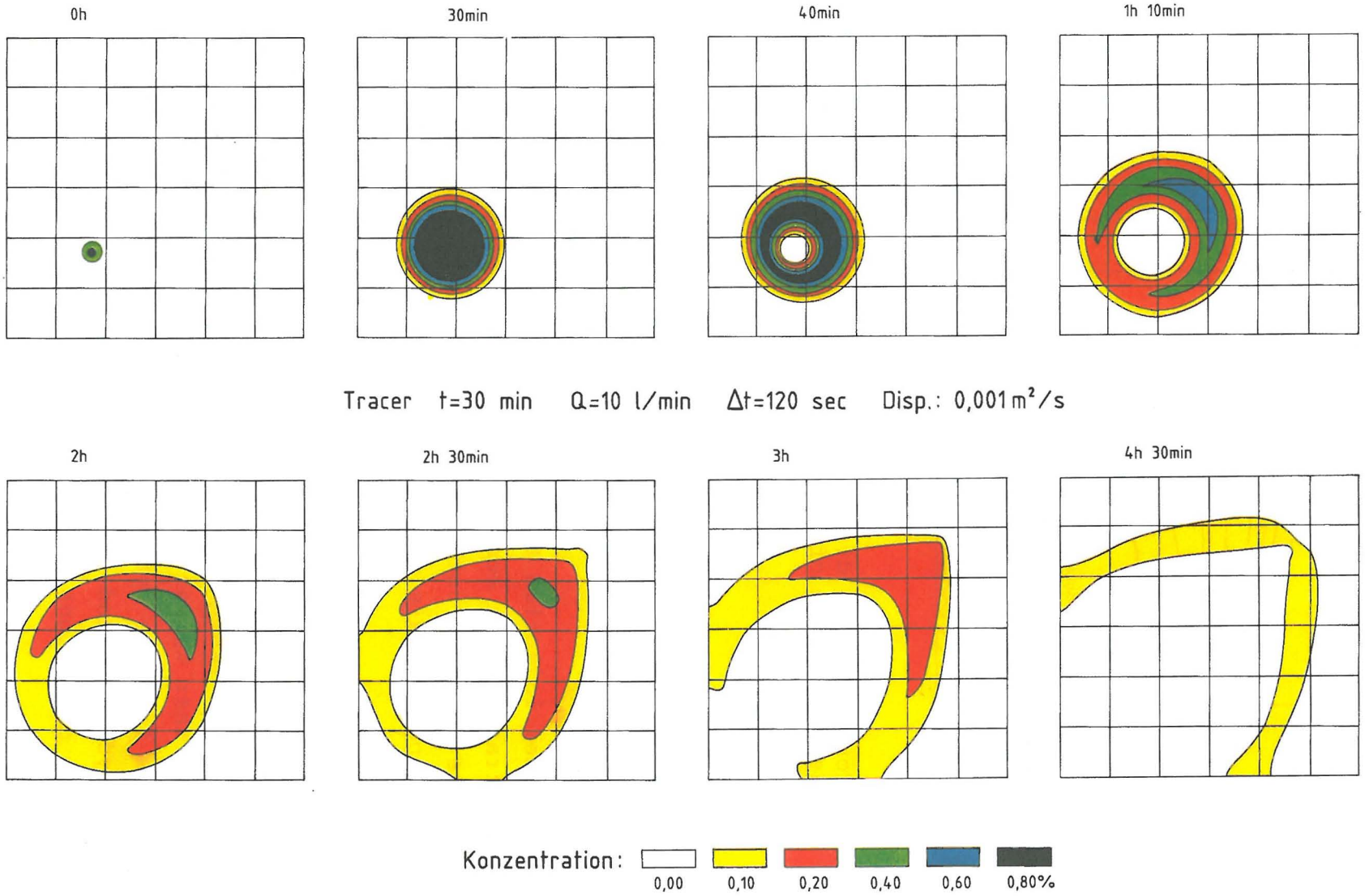

Fig. 76: Spreading of the tracer after a 30-min injection period

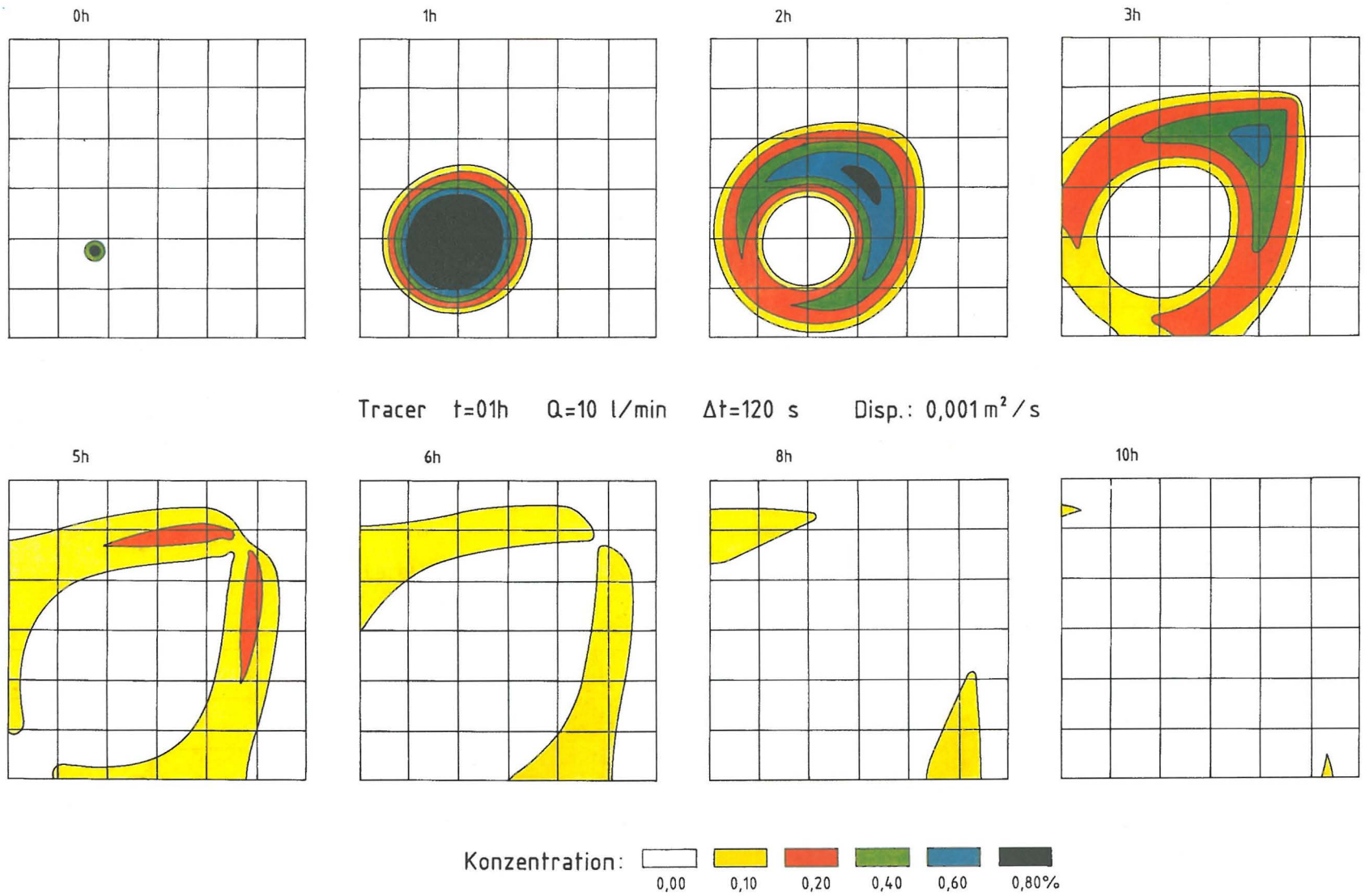

Fig. 77: Spreading of the tracer after a 1-h injection period

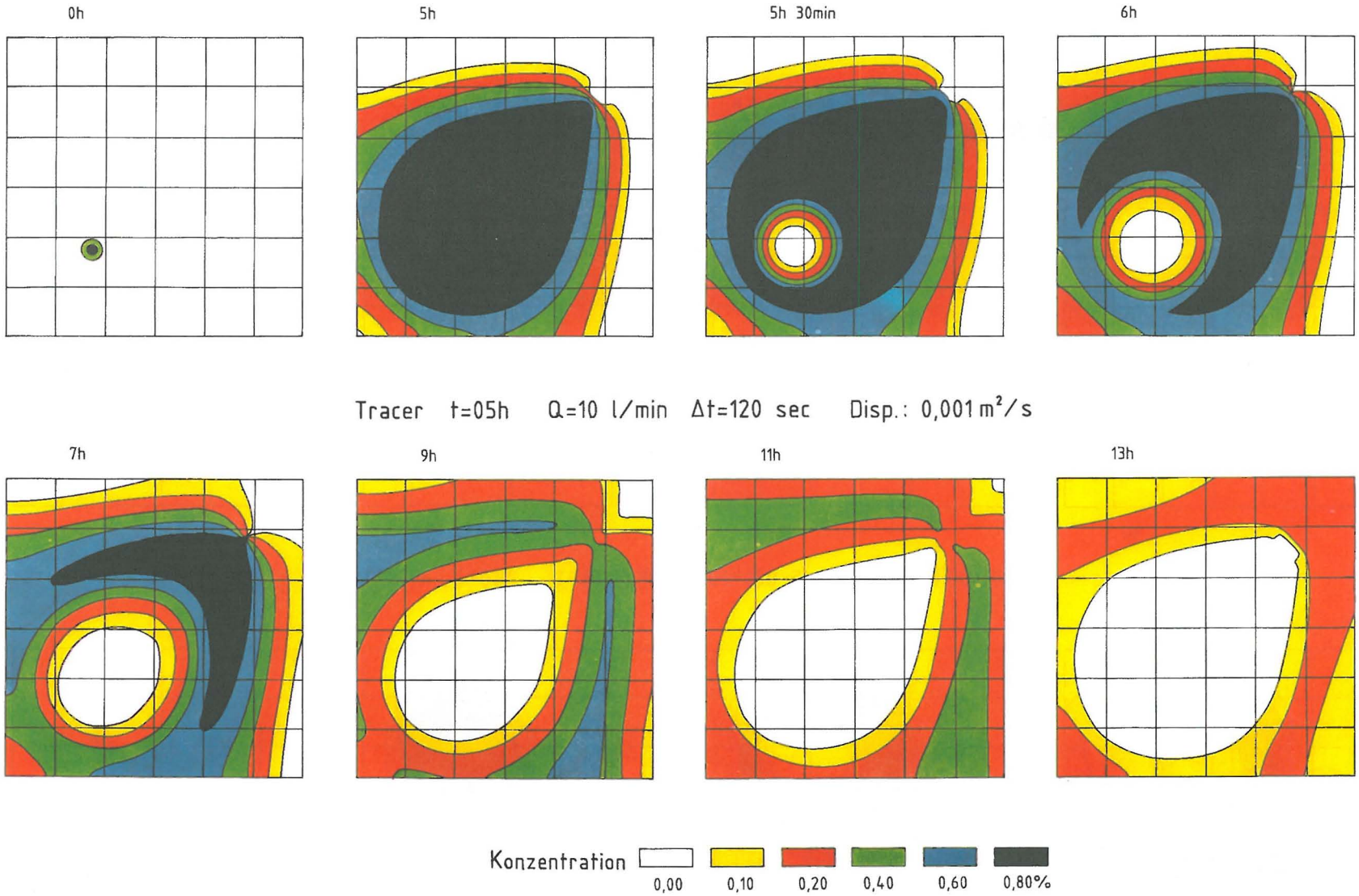

Fig. 78: Spreading of the tracer after a 5-h injection period

5.5.4 Hydraulic Plate Model of the Central Part of the Test Area

The geometry of this model is based primarily on

- geological mapping of the fractures,
- hydraulic pressure measurements during the drilling of the boreholes,
- hydraulic tracer tests, and
- conductivity measurements (fluid logging).

The elements of the model (LIEDTKE & NAUJOKS, 1990) are assumed to be pierced by twelve boreholes (Fig. 79). The points at which they penetrate the model are shown in Figure 80 as numbered circles (borehole numbers). The model consists of 33 macroelements with 56 nodes and is about 2 mm thick. It is 50x50 m wide and is connected hydraulically to the surface 400 m above it by further plate elements. These latter elements are 1 m thick and have a permeability of $k_f = 6 \times 10^{-6}$ m/s. The 2-mm-thick elements are assumed to have a permeability k_f of about 2×10^{-3} m/s. The storage capacities were determined by iteration to be $S = 10^{-5}$ beneath the floor of the drift and $S = 1$ above it. The quality of this simplified model is exemplified by the results of test VE 457:

> To prepare quasi-steady-state conditions for the simulation, the systems were "filled" with water from the surface and through borehole BK 85.004 at a rate of 4 l/min for about 300 days. The calculations were made with a constant injection rate of about 7 l/min (Fig. 81). The injection rate in the model had to be reduced slightly owing to leakage from the walls of the drift.

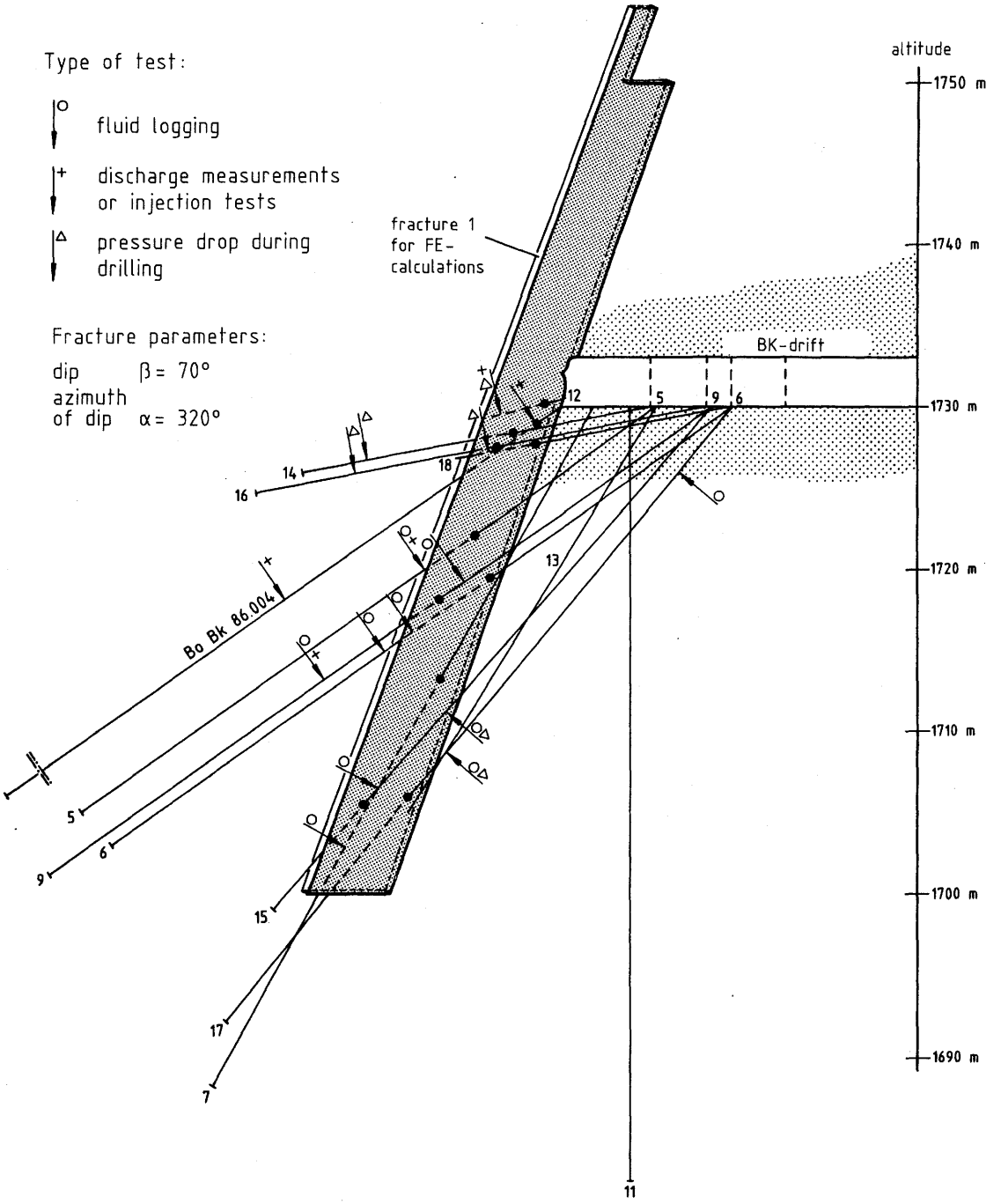

Fig. 79: Discharge of water at the Fracture System Flow Test site

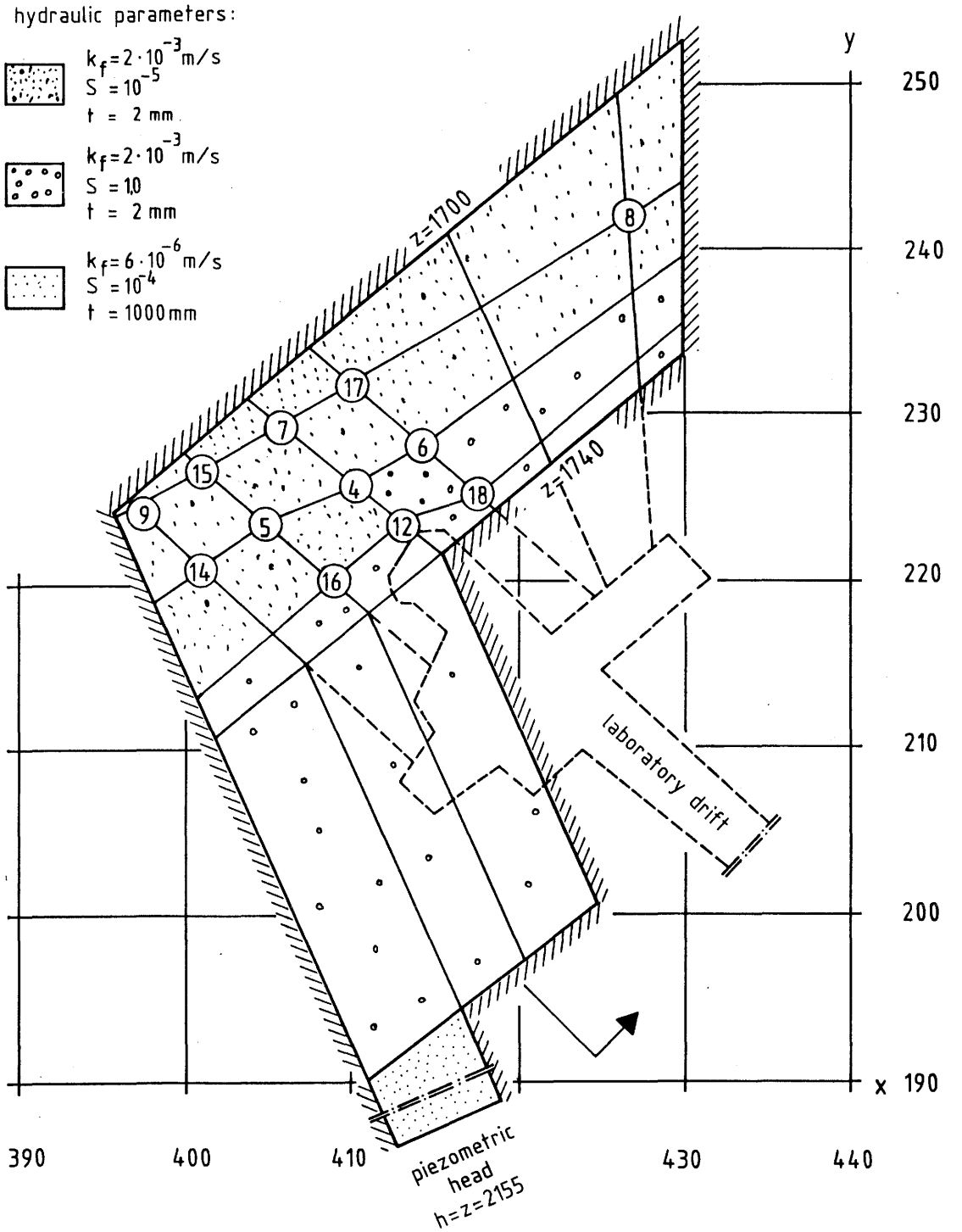

Fig. 80: Rough sketch of the finite element grid (macro-elements) used for the Fracture Flow Test computations

It can be seen by comparison of the calculated and measured results that gradual changes can be reproduced rather well with this model. Sudden changes lead to somewhat larger discrepancies as a result of the uniform permeability assumed in the model. The empirical and theoretical hydraulic heads in boreholes BK 85.004, 85.005, and 85.008 are shown in Figure 82. The velocity field at the end of the test is shown in Figure 83. Most of the injected water flows from borehole BK 85.004 chiefly into the rock mass above the floor of the drift. Later in the test, after the injection phase, the water flows with a considerably lower velocity in the opposite direction owing to the leakage mentioned above.

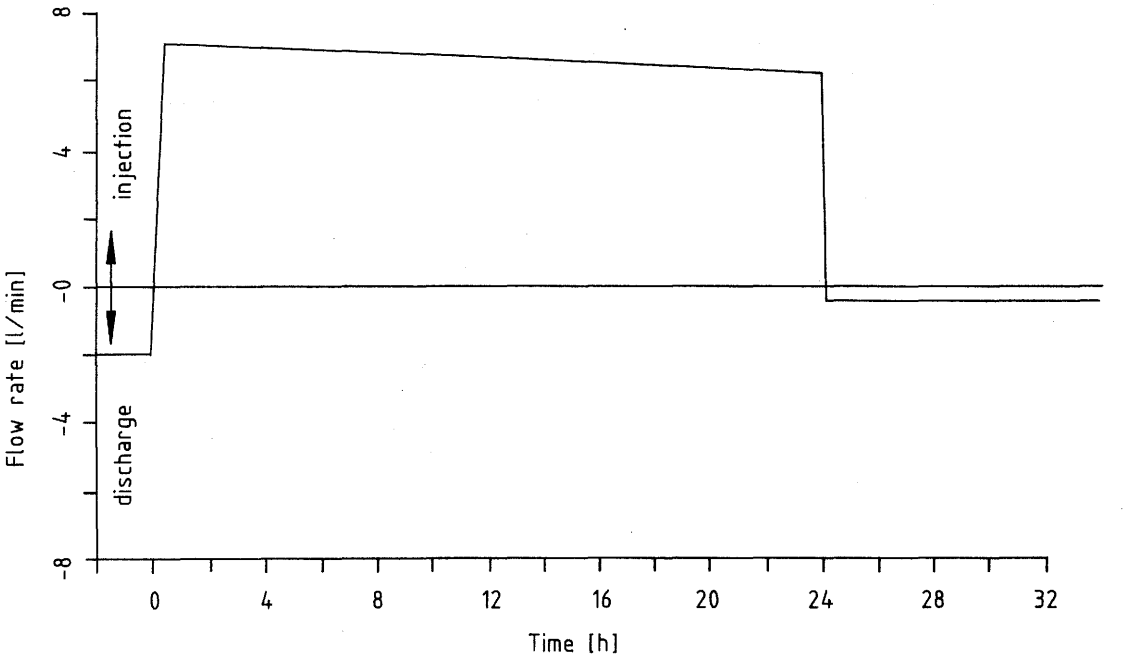

Fig. 81: Injection and discharge flow rates in borehole BK 85.004 (test 457)

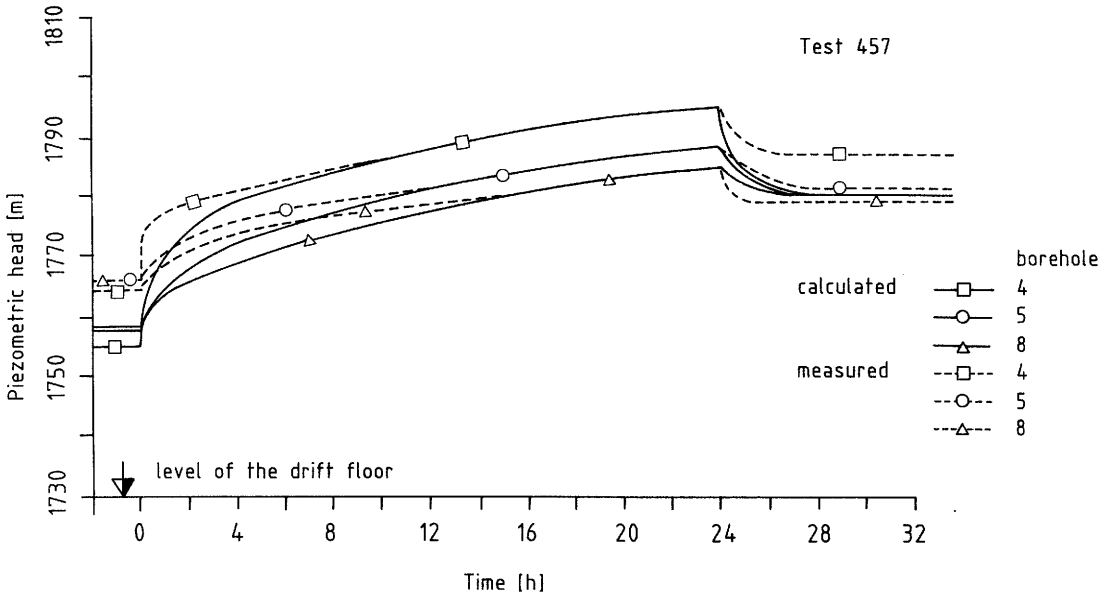

Fig. 82: Hydraulic head as a function of time in boreholes BK 85.004, BK 85.005 & BK 85.008 (test 457)

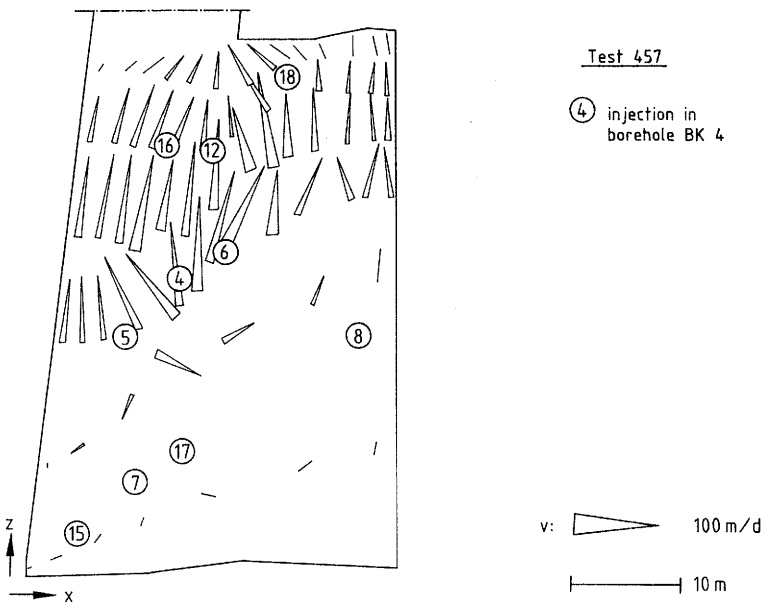

Fig. 83: Flow field in the central part of the test area 24 h after beginning of injection (test 457)

6. Summary and Conclusions

Due to the complexity of the processes involved, any satisfactory assessment of the propagation of contaminants in jointed rock has several prerequisites:

a) detailed description of the drill cores and underground geological mapping followed by statistical analysis of the fractures,
b) in-situ hydraulic tests, particularly tracer tests (possibly under non-steady-state flow conditions), and
c) numerical modeling to predict flow velocities.

The Fracture System Flow Test involved the following steps:

a) geological mapping of the fractures in the BK gallery;
b) siting the boreholes;
c) geological description of the drill cores:
   - lithology, stratigraphy, genesis,
   - hydraulic weighting factor for the fractures,
   - strike and dip of the fractures,
   - extension and apertures of the fractures,
   - mineral lining or solution phenomena on the fracture surfaces,
   - slickensides and associated lineations,
   - hydrothermal alteration of the rock in the vicinity of a fracture,
   - statistical analysis;

d) graphical fracture model assembled by interpolation of fractures between boreholes and by extrapolation beyond peripherical boreholes taking intersection of fractures into account.

e) hydraulic tests:
- discharge measurements,
- index tests (at constant pressure or flow rate),
- interference tests,
- fluid logging
- pulse tracer tests (single hole),
- dipole tracer tests.

f) hydraulic analysis:
- analytical solutions for prior estimation of hydraulic parameter values during hydraulic tests (e.g. THEIS),
- geometric fracture model using the estimated parameter values,
- numerical model computations (3-D) using the finite element method, taking individual fractures or sets of fractures into consideration,
- tracer simulations using the same model,
- comparison of the theoretical and empirical results and stepwise refinement of the assumptions,
- comparison of the tracer traveltimes under different hydraulic conditions.

The following data also proved helpful for the modeling:
- 3-D radar tomography,
- temperature borehole logs,
- conductivity borehole logs.

The work involved not only the tests themselves but also installation and testing of the equipment. Progress was made in the improvement of the instruments, particularly in the case of computer-controlled tests with active and passive packer-probe systems, automatic recording of the data and transmission to several computers, and checking of the packers and probes using mechanical connections that can be quickly coupled.

The many different possibilities for evaluating the tests, whether they are conducted under constant pressure or constant flow conditions, with computer programs using the method of finite elements made it possible to determine the required parameter values with relatively detailed models. The special feature of the DURST program system is the possibility to combine 1-, 2- and 3-dimensional elements. The calculated hydraulic or gaseous flow processes are taken as the basis for calculating fluid transport. The program system was written for a main-frame computer, but it is now possible to use it on-site with IBM-compatible PCs to do 3-D calculations for the tests so that decisions can be made on an improved theoretical basis while the tests are being conducted.

In crystalline rock that is unweathered, hydrothermally unaltered and unaffected by tectonic deformation, virtually all water percolation takes place along fractures.

The actual spatial extension, the degree of interconnection of the fractures, and their preferred orientation in space have a considerable influence on the permeability of the rock. For a study of the rock hydraulic conditions, it is essential to make a quantitative assessment of the fractures with respect to their hydraulic effectiveness. In addition, the hydraulic aspects of the rock as a whole should be assessed, since in hydrothermally altered areas dissolution and recrystallization usually lead to an increase in pore space and thus to an increase in permeability.

In the Central Aare Granite there is a whole network of hydraulically connected fractures which can often be followed for several tens of meters.

The different equilibrium hydraulic heads that have been measured at several points in the underground laboratory, particularly in the Fracture System Flow Test area, show that these hydraulic fracture networks are normally bounded by large (usually tectonic) structures. This gives rise to sub-areas which are largely independent of each other hydraulically.

The project will be continued during the next three years (Project BK III) and will involve closer cooperation with NAGRA in both the planning and the implementation of the project. BGR envisages concentrating its contributions as follows:

1. Validation of fracture-network models.
2. Tracer tests to investigate channeling, fracture dispersion and flow velocity of the transport medium in more detail.
3. Further development of multipacker-probe systems and tests to compare performance.
4. Investigation of permeability as a function of stress.
5. Further development of the DURST program system for simulating multi-phase flow.
6. Comparison of the results and methods of the Fracture System Flow Test project with those of similar projects.

Acknowledgment

The authors should like to express their gratitude to all who assisted in planning, performance and evaluation of the Fracture System Flow Test. This applies particularly to our partners at NAGRA, namely the local staff of the Grimsel Test Site, H. Abplanalp, H. P. v. Allmen, T. Baer, Dr. W. Kickmaier and P. Streich.

It also applies to the staff members of the BGR, whose engagement in situ and at the BGR during both performance and evaluation of the test enabled the succesful run of events, namely: H. Bartsch, W. Edler, Dr. J. Hanisch, F.-J. Hoppe, H. Kasten, Dr. B. Kilger, K. Kohlenberg, H. Kunz, W. Siemering and K.-H. Sprado.

Last but not least a special mention to the members of our secretariat, C. Grape, D. Hunstock, P. Mehlhorn, B. Schneider and R. Winkler, who spared no efforts as regards layout and corrections of this report.

7. References

BOSSART, P. & MARTEL, S. (1990): Hydrogeological Implications of Ductile and Brittle Deformations in the Grimsel Crystalline, Upper Aare Valley, Switzerland.- Nagra Interner Bericht; Baden.

BRÄUER, V. (1990a): Trennflächen- und Mikrorißuntersuchungen im Zentralen Aaregranit zur Interpretation von Gebirgsspannungsmessungen im Felslabor Grimsel/Schweiz.- Diss. Universität Hannover, 142 S.; Hannover.

BRÄUER, V. (1990b): Analyse des Trennflächengefüges als Grundlage für Durchströmungsversuche im Fels.- 9. Nat. Tag. "Felsmechanik", 27. - 29. März; Aachen.

BRÄUER, V., KILGER, B. & PAHL, A. (1989): Felslabor Grimsel - Ingenieurgeologische Untersuchungen zur Interpretation von Gebirgsspannungsmessungen und Durchströmungsversuchen.- Nagra Technischer Bericht, NTB 88-37: 53 S.; Baden.

BRÄUER, V., LIEDTKE, L., NAUJOKS, A. & PAHL, A. (1990): Interpretation of Fracture System Flow Tests by Fracture Analysis and Numerical Simulation.- NEA Workshop on Flow Heterogenity and Site Evaluation, 22. - 24. Oktober; Paris.

BREWITZ, W. & PAHL, A. (1986): German Participation in the Grimsel Underground Laboratory in Switzerland - Targets and Methods of In-situ Experiments in Granite for Radioactive Waste Disposal. IAEA-SM-289/24. International Symp.; Hannover.

COOPER, H. H. & JACOB, C. E. (1946): A Generalized Graphical Method for Evaluating Formation Constants and Summarizing Well Field History.- Am. Geophys. Union Trans., Vol. 27: 526 - 534.

DOE, T., OSNES, J., KENRICK, M., GEIER, J. & WARNER, S. (1987): Design of Borehole Testing Programs for Waste Disposal Sites in Crystalline Rock.- Proc. 6th International Conference on Rock Mechanics, Vol. 3; Montreal.

Empfehlung Nr. 9 des Arbeitskreises 19 der DGEG (1984): Wasserdruck-Versuch im Fels. Bautechnik 4, S. 112-117.

ERSHAGI, I. & WOODBURY, J.J. (1985): Examples of Pitfalls in Well Test Analysis.- Journal Petroleum Technology, Vol. 37: S. 335 - 341.

GÄRTNER, S. (1987): Zur diskreten Approximation kontinuumsmechanischer Bilanzgleichungen.- Bericht Nr. 24/1987 Inst. für Strömungsmechanik und Elektronisches Rechnen im Bauwesen der Universität Hannover.

HEITFELD, K.-H. & KOPPELBERG, W. (1981): Durchlässigkeitsuntersuchungen mittels WD-Versuchen. Zbl. Geol. Paläont., Teil I, H. 5/6, S. 634-661.

HILL, S. (1984): Untersuchungen über die Wechselwirkungen zwischen Porenverstopfung und Filterwiderstand mittels Tracermessungen. Mitt. des Inst. für Wasserversorgung, Abwasserbeseitigung und Raumplanung der Universität Darmstadt, Schriftenreihe WAR 18, Band XXII.

HÖLTING, B. (1989): Hydrogeologie. Enke Verlag, 3. Auflage.

KELLEY, V. A. & FRIEG, B. (Eds.) (1990): Field Investigation in the BK-Area, Grimsel Test Site, December 1989 until March 21, 1990.- Nagra Interner Bericht; Baden.

KELLEY, V. & LOEW, S. (1991): Analysis of a Pilot Crosshole Fluid Logging Test at the BK-Site, Grimsel Test Site (Part IV).- Nagra Technischer Bericht, NTB 91-09; Baden (in Vorbereitung).

KEUSEN, H. R., GANGUIN, I., SCHULER, P. & BULETTI, M. (1989): Felslabor Grimsel - Geologie.- Nagra Technischer Bericht, NTB 87-14: 120 S.; Baden.

KINZELBACH, W. (1987): Numerische Methoden zur Modellierung des Transports von Schadstoffen im Grundwasser.- R. Oldenburg Verlag München; Wien.

KOPPELBERG, W. (1986): Numerische und statistische Untersuchungen zur Durchlässigkeit geklüfteter geologischer Körper und ihrer Bestimmung durch Wasserdruckversuche.- Mitteilungen zur Ingenieurgeologie und Hydrogeologie RWTH Aachen, Heft 23; Aachen.

KRÖHN, K.-P. & ZIELKE, W. (1990): Modelling Transport in Discrete Fracture Systems with a Finite Element Scheme of Increased Consistency.- VIII International Conference on Computational Methods in Water Resources, June 11 - 15, Venice, Italy.

KRUSEMANN, G. P. & DE RIDDER, N. A. (1973): Untersuchungen und Anwendung von Pumpversuchsdaten.- Verlagsgesellschaft R. Müller.

LANGER, M., LIEDTKE, L. & PAHL, A. (1989): Felshydraulische Tests zur Beurteilung der Barrierewirkung von geklüftetem Fels.- Festschrift 65. Geburtstag Prof. Heitfeld; Aachen.

LANGGUTH, H.-R. &. VOIGT, R. (1980): Hydrogeologische Methoden.- Springer-Verlag.

LIEDTKE, L. & NAUJOKS, A. (1990): Interpretation and Numerical Simulation of Fracture System Flow Tests.- Proc. International Conference on Water Resources in Mountainous Regions; Lausanne.

LIEDTKE, L. & PAHL, A. (1984): Water Injection Test and Finite Element Calculations of Water Percolation through Fissured Granite.- Proc. CEC-NEA Workshop Design and Instrumentation of in-situ experiments in underground laboratories for radioactive waste disposal; Brüssel.

LIEDTKE, L. & PAHL, A. (1987): Transport of Dissolved Substances in Fissured Granite.- DOE/AECL '87 Conference on Geostatical, Sensitivity and Uncertainty Methods for Groundwater Flow and Radionuclide Transport Modeling; San Francisco.

LIEDTKE, L.. & PAHL, A. (1988): Calculations of Flow Along Fractures Using Structural Data.- OECD Nuclear Energy Agency and Commission of the European Communities Workshop on Sealing of Radioactive Waste Repositories, Winnipeg.

LOUIS, C. (1967): Strömungsvorgänge in klüftigen Medien und ihre Wirkung auf die Standsicherheit von Bauwerken und Böschungen im Fels.- Veröffentlichungen Institut für Bodenmechanik und Felsmechanik Universität Karlsruhe, Heft 30; Karlsruhe.

NAGRA (1981): Sondierbohrungen Juchlistock - Grimsel.- Nagra Technischer Bericht, NTB 81-07; Baden.

PAHL, A., BRÄUER, V., HEUSERMANN, St., KILGER, B. & LIEDTKE, L. (1986): Results of Engineering Geological Research in Granite. 5th Int. Congress of the IAEG; Buenos Aires.

SHEDLOVSKY, T. & SHEDLOVSKY, L. (1971): Conductometry. Techniques of Chemistry, Vol. 1: Physical Methods of Chemistry, Part IIa. Wiley & Sons; New York.

SCHNEIDER, H.-J. (1987): Durchlässigkeit von geklüftetem Fels - eine experimentelle Studie unter besonderer Berücksichtigung des Wasserabpressversuches.- Mitteilungen zur Ingenieurgeologie und Hydrogeologie, Heft 26; Aachen.

SNOW, D. T. (1965): A Parallel Plate Model of Fractured Permeable Media.- Ph. D. Thesis, University of California; Berkeley.

STALDER, H. A. (1984): Das Granitgestein des Grimsel und seine geologische Geschichte.- Nagra informiert, 4, Nr. 3/4: S. 5-10; Baden.

STOBER, I. (1985): Strömungsverhalten in Festgesteinsaquiferen mit Hilfe von Pump- und Injektionsversuchen.- Geologisches Jahrbuch, Reihe C, Heft 42; Hannover.

STRAYLE, G. (1983): Pumpversuche im Festgestein. DVGW-Schriftenreihe, S. 305-325.

WILSON, C. R., DOE, T. W., LONG, J.C.S. & WITHERSPOON, P. A. (1979): Permeability Characterization of Nearly Impermeable Rock Masses for Nuclear Waste Repository Siting.- Proc. NEY/IAEA-Workshop on Low-Flow, Low-Permeability Measurements in largely impermeable Rocks; Paris.

WOLLRATH, J. & ZIELKE, W. (1990): FE-Simulation von Strömungen im klüftigen Gestein.- Deutsche Gewässerkundliche Mitteilungen, 34, H. 1/2: S. 2 - 7.

Appendix: Test Data

The following collection of test data only covers Phase II of the Fracture Flow Test. The improvements to the instruments that had been made up to this stage permitted the tests to be run chiefly as long-term tests, which were of particular value for the problem being studied.

One hundred in-situ hydraulic tests were carried out (VE 376 – 475) in 1988-90. The summary gives an account of the type of test, duration and hydraulic boundary conditions. Most of the tests in 1988 were conducted around boreholes BK 86.003 and US 85.003 (see Fig. 1 & Section 5.3.2); most of the tests in 1989/90 were in the central part of the test area (see Fig. 1 & Section 5.3.1).

Several of the tests described could not be made use of to obtain quantitative results since these were designed primarily for development and testing of the instruments or were merely intended to be preliminary tests.

Test no.	Test design	Start of test	Test period start	Test period end	End of test	Injection borehole	Injection interval [m]	Flow rate [l/min]	Conductivity [µS/cm]	Observation borehole (open)	Discharge [l/min]	First arrival time
VE 376	Injection test	29/01/88 15:15h			01/02/88 10:00h	BK 86.003	64-65	< 1	ca. 20	US 85.003		
VE 377	Injection test	01/02/88 10:00h			02/02/88 13:50h	BK 86.003	63-64	ca. 4,9	ca. 20	US 85.003		
VE 378	Injection test	03/02/88 11:00h			04/02/88 14:45h	BK 86.003	64-65	ca. 4,9	ca. 20	US 85.003		
VE 379	Injection test	04/02/88 14:45h	04/02/88 14:45h	09/02/88 16:00h	16/03/88 09:00h	BK 86.003	64-65			US 85.003		
VE 380	Injection test	16/03/88 09:00h			18/03/88 20:00h	BK 86.003	64-65	ca. 4,9	ca. 20	US 85.003		
VE 381	Pressure reduction test	18/03/88 20:00h			21/03/88 09:00h	BK 86.003	64-65	0		US 85.003		
VE 382	Injection test	21/03/88 09:25			21/03/88 12:15h	BK 86.003	64-65	ca. 4,9	ca. 20	US 85.003		
VE 383	Injection test	21/03/88 13:15h			21/03/88 19:00h	BK 86.003	64-65	ca. 4,9	ca. 20	US 85.003		
VE 384	Injection test	22/03/88 09:15h			22/03/88 15:00h	BK 86.003	64-65	ca. 4,9	ca. 20	US 85.003		
VE 385	Injection test	23/03/88 12:00h			24/03/88 10:00h	BK 86.003	64-65	ca. 4,9	ca. 20	US 85.003		
VE 386	Tracer test	24/03/88 10:00h	24/03/88 10:00h	28/03/88 09:15h		BK 86.003	64-65	4,8 - 4,9	ca. 200	US 85.003		
			28/03/88 09:15h	31/03/88 12:00h	31/03/88 12:00h	BK 86.003	64-65	4,0 - 4,7		US 85.003		
VE 387	Tracer test	19/04/88 15:00h			21/04/88 16:00h	BK 86.003	64-65	4,5 - 4,9	ca. 200	US 85.003		
VE 388	Tracer test	22/04/88 08:00h	22/04/88 08:00h	22/04/88 12:00h	22/04/88 16:00h	BK 86.003	64-65	ca. 4,0	ca. 200	US 85.003		
VE 389	Tracer test	22/04/88 16:00h	22/04/88 16:00h	25/04/88 08:00h		BK 86.003	64-65	ca. 1,0	ca. 200	US 85.003		
			25/04/88 08:00h	29/04/88 12:00h		BK 86.003	64-65	ca. 1,0	25	US 85.003		
			29/04/88 12:00h	02/05/88 15:00h	02/05/88 15:00h	BK 86.003	64-65	ca. 1,0	ca. 200	US 85.003		
VE 390	Tracer test	02/05/88 15:00h	03/05/88 15:00h	03/05/88 15:00h		BK 86.003	64-65	4,3 - 4,9	26	US 85.003		
			03/05/88 15:00h	04/05/88 15:00h		BK 86.003	64-65	4,5 - 4,7	220	US 85.003		
			04/05/88 15:00h	05/05/88 15:00h	05/05/88 15:00h	BK 86.003	64-65	2,2 - 2,5	26	US 85.003		

Appendix 1a: Test 376 - 390

Test no.	Test design	Start of test	Test period start	Test period end	End of test	Injection borehole	Injection interval [m]	Flow rate [l/min]	Conductivity [µS/cm]	Observation borehole (open)	Discharge [l/min]	First arrival time
VE 391 to VE 416	Short term injection tests	07/06/88			06/07/88	BK 85.004						
VE 417	Tracer test	11/07/88 09:00h	11/07/88 09:00h	12/07/88 14:00h			64-65	2,2 - 3,0		US 85.003		
			12/07/88 14:00h	14/07/88 09:00h			64-65	2,7 - 3,1		US 85.003		
			14/07/88 09:00h	15/07/88 15:00h			64-65	2,5 - 2,9		US 85.003		
	Pressure reduction test		15/07/88 15:00h	22/07/88 04:00h	22/07/88 04:00h	BK 86.003	64-65	0		US 85.003		
VE 418	Tracer test	17/08/88 14/10h	17/08/88 14:10h	17/08/88 15:15h		BK 86.003	64-65	2,4 - 3,5		US 85.003		
			17/08/88 15:15h	19/08/88 04:00h		BK 86.003	64-65	2,5 - 3,0		US 85.003		
			19/08/88 04:00h	29/08/88 07:00h	29/08/88 07:00h	BK 86.003	64-65	1,7 - 2,7		US 85.003		
VE 420	Tracer test	29/08/88 09:00h	29/08/88 09:00h	31/08/88 09:00h		BK 86.003	64-65	1,6 - 2,1		US 85.003		
			31/08/88 09:00h	04/09/88 17:00h		BK 86.003	64-65	1,7 - 2,0		US 85.003		
	Pressure reduction test		04/09/88 17:00h	15/09/88 01:00h		BK 86.003	64-65	0		US 85.003		
VE 421	Interference tests during drilling phase 3	05/10/88			22/11/88							
VE 422	Pressure buildup test	09/12/88			29/01/89	GS 84.041A						
VE 423	Pressure buildup test	02/02/89			20/03/89	GS 84.041A						
VE 424 to VE 430	Pretests in the central BK area	06/02/89			14/02/89	BK 85.005						
VE 431	Pressure buildup test	20/03/89			03/07/89	GS 84.041A						

Appendix 1b: Test 391 - 431

Test no.	Test design	Start of test	Test period start	Test period end	End of test	Injection borehole	Injection interval [m]	Flow rate [l/min]	Conductivity [µS/cm]	Observation borehole (open)	Discharge [l/min]	First arrival time
VE 432	Tracer test (Single hole test with pressure and tracer pulse)	28/03/89 07:20h	28/03/89 08:30h	28/03/89 09:30h	29/03/89 08:00h	BoBK 85.005	2 - 43,5	19 (17-20)	200			
VE 433	Tracer test (Dipole test)	29/03/89 10:00h	29/03/89 10:10h	29/03/89 13:30h		BoBK 85.005	2 - 43,5	18 (17-20)	200	BoBK 85.006	2,5-3	
			30/03/89 09:00h	30/03/89 14:00h				5,0	200	BoBK 85.006	2,5	ca. 3,5 h
			31/03/89 09:00h	31/03/89 14:00h	03/04/89 09:00h			4,8 (4,6-5,0)	800	BoBK 85.006	ca. 2,75	ca. 3,5 h
VE 434	Tracer test (Dipole test)	03/04/89 09:00h	03/04/89 10:00h	03/04/89 15:00h		BoBK 85.005	2 - 43,5	2,5	800	BoBK 85.006	ca. 3,0	
			04/04/89 10:00h	04/04/89 15:00h	06/04/89 08:00h			2,5	800	BoBK 85.006	ca.2,75	
VE 435	Tracer test (Dipole test)	10/04/89	10/04/89 11:00h	10/04/89 15:15h		BoBK 85.005	2 - 43,5	ca. 7,2	800	BoBK 85.006	3,4-3,9	no result
			10/04/89 15:15h	13/04/89 09:00h	13/04/89 09:00h			5,0 - 5,5	20	BoBK 85.006		
VE 436	Pressure reduction test	13/04/89 09:00h			01/05/89	BoBK 85.005	2 - 43,5	0	-	BoBK 85.006		
VE 437	Pressure buildup tes	23/06/89 10:00h			27/06/89 13:00h	BoBK 85.005	17,5 - 18,5	0	-	BoBK 85.004 (packer in 5m)		
VE 438	Tracer test (Dipole test)	27/06/89 13:00h	28/06/89 14:00h	28/06/89 15:00h		BoBK 85.005	17,5 - 18,5	0,9	800	BoBK 85.004 (packer in 5m)	3,3	no connection
			29/06/89 09:00h	29/06/89 10:00h	29/06/89 14:00h	BoBK 85.005	17,5 - 18,5	0,9	1000	BoBK 85.004 (packer in 5m)		no connection
VE 439	Tracer test (Dipole test	29/06/89 14:00h	29/06/89 14:00h	29/06/89 15:00h		BoBK 85.005	17,5 - 18,5	0,9	1000	BoBK 85.004		1,5 h
			30/06/89 08:00h	30/06/89 08:40h	03/07/89 12:00h		17,5 - 18,5	0,9	1000	BoBK 85.004	4,4	1,5 h

Appendix 1c: Test 432 - 439

Test no.	Test design	Start of test	Test period start	Test period end	End of test	Injection borehole	Injection interval [m]	Flow rate [l/min]	Conductivity [µS/cm]	Observation borehole (open)	Discharge [l/min]	First arrival time
VE 440	Pressure buildup test BoGS 84.041A	03/07/89 14:00h				BoBK 85.005						
VE 441	Tracer test (Multi hole test)	04/07/89	04/07/89 14:45h	04/07/89 15:45h	05/07/89	BoBK 85.005	17,5 - 18,5	0,9	3000	BoBK 85.004 (packer in 5m)	1,8	no connection
										BoBK 85.006	0,6 (> 3 h)	no result
VE 442	Tracer test (Temperature test 64-74°C Multi hole test)	05/07/89 11:00h	05/07/89 11:00h	06/07/89 14:30h	07/08/89	BoBK 85.005	17,5 - 18,5	2,5	20	BoBK 85.004	ca. 4,0	
										BoBK 85.009	ca. 2,0	
VE 443	Pressure buildup test (Pretest for VE 444)	21/09/89				BoBK 85.005	18,0 - 19,0	2,5	50	BoBK 85.006		
VE 444	Tracer test (Dipole test)	25/09/89 09:30h	26/09/89 08:00h	26/09/89 13:00h	04/10/89 11:30h	BoBK 85.005	18,0 - 19,0	2,5	3000	BoBK 85.006	1,8	3,5 h
VE 445	Tracer test (Dipole test)	04/10/89 11:30h	04/10/89 11:30h	04/10/89 12:00h	13/10/89 12:00h	BoBK 85.005	18,0 - 19,0	2,5	3000	BoBK 85.006	3,0	3,0 h
VE 446	Pressure buildup test	13/10/89 12:00h			24/10/89 12:00h	BoBK 85.005	18,0 - 19,0	0	20	BoBK 85.006		
VE 447	Pressure buildup test	25/10/89 15:00h			26/10/89 05:30h	BoBK 85.005	18,0 - 19,0	1,0	20	BoBK 85.006	> 2,2	no result
VE 448	Tracer test	26/10/89 16:15h	27/10/89 09:30h	27/10/89 12:00h	03/11/89	BoBK 85.005	18,0 - 19,0	1.0	7500	BoBK 85.006	2,2	5,5
VE 449	Tracer test	03/11/89 15:15h	06/11/89 11:00h	06/11/89 16:00h	03/12/89	BoBK 85.006	18,0 - 19,0	0,5	7500	BoBK 85.006	2,0 - 2,1	7,5

Appendix 1d: Test 440 - 449

Test no.	Test design	Start of test	Test period start	Test period end	End of test	Injection borehole	Injection interval [m]	Flow rate [l/min]	Conductivity [µS/cm]	Observation borehole (open)	Discharge [l/min]	First arrival time
VE 450	Pressure buildup test	14/12/89			18/01/90	BK 85.004		0				
VE 451	Interference test (Pretest)	18/01/90	18/01/90 10:00h	18/01/90 11:15h	19/01/90	BK 85.004	16,7 - 44,7	3 - 5				
VE 452	Interference test	19/01/90	19/01/90 08:00h	19/01/90 14:00h	22/01/90	BK 85.004	16,7 - 44,7	3 - 5				
VE 453	Interference test	22/01/90	22/01/90 09:00h	22/01/90 11:00h	23/01/90	BK 85.004	2,0 - 15,0	12 - 16				
VE 454	Interference test	23/01/90	23/01/90 08:30h	23/01/90 11:30h	23/01/90	BK 85.004	7,7 - 15,7	16 - 21				
VE 455	Interference test	23/01/90	23/01/90 14:40h	23/01/90 15:40h	24/01/90	BK 85.004	2,0 - 6,0	15 - 16				
VE 456	Interference test	24/01/90	24/01/90 14:35h	24/01/90 16:05h	25/01/90	BK 85.004	16,7 - 28,7	1,1 - 1,5				
VE 457	Interference test	25/01/90	25/01/90 15:00h	26/01/90 15:00h	29/01/90	BK 85.004	6,7 - 10,7	7 - 8				
VE 458	Fluid logging	30/01/90			31/01/90	BK 85.004	6,7 - 10,7	0,5	10000	BK 85.007		
VE 459	Fluid logging	31/01/90			01/02/90	BK 85.004	6,7 - 10,7	0,5	10000	BK 85.006		
VE 460	Fluid logging	01/02/90			02/02/90	BK 85.004	6,7 - 10,7	0,5	10000	BK 88.017		
VE 461	Fluid logging	02/02/90			05/02/90	BK 85.004	6,7 - 10,7	0,5	10000	BK 85.008		
VE 462	Fluid logging	05/02/90			06/02/90	BK 85.004	6,7 - 10,7	0,5	10000	BK 85.005		
VE 463	Fluid logging	06/02/90			07/02/90	BK 85.004	6,7 - 10,7	0,5	10000	BK 88.015		
VE 464	Fluid logging	07/02/90			08/02/90	BK 85.004	6,7 - 10,7	0,5	10000	BK 85.009		

Appendix 1e: Test 450 - 464

Test no.	Test design	Start of test	Test period start	Test period end	End of test	Injection borehole	Injection interval [m]	Flow rate [l/min]	Conductivity [µS/cm]	Observation borehole (open)	Discharge [l/min]	First arrival time
VE 465	Pressure buildup test	08/02/90			07/03/90	BK 85.004						
VE 466	Pressure reduction test	07/03/90			20/03/90	BK 85.004	6,7 - 10,7					
VE 467	Pretest	20/03/90										
VE 468	Pressure buildup test	09/04/90			11/04/90	BK 86.003	4 - bottom					
VE 469	Pretest	06/90			26/06/90	BK 86.003	4 - bottom					
VE 470	Pressure buildup test	26/06/90 15:00h			02/07/90	US 85.003						
VE 471	Injection test	05/07/90 08:00h	05/07/90 10:00h	05/07/90 12:00h	05/07/90 14:00h	BK 86.003	4 - bottom	2,5 bzw. 5,0				
VE 472	Fluid logging	04/09/90			05/09/90	BK 86.003	4 - bottom			US 85.003		
VE 473	Pressure reduction test	05/09/90 16:00h			06/09/90 16:00h	BK 86.003	4 - bottom					
VE 474	Pressure buildup test	06/09/90			91							
VE 475	Withdrawal test (Pressure buildup / reduction)	10/12/90 12:00h	10/12/90 16:00h	11/12/90 08:00h		BK 86.003	4 - bottom				0,5	
			11/12/90 08:00h	11/12/90 16:00h							1	
			11/12/90 16:00h	12/12/90 08:00h							2	
			12/12/90 08:00h	12/12/90 16:00h							3	
			12/12/90 16:00h	13/12/90 00:00h							2	
			13/12/90 00:00h	13/12/90 08:00h							1	
			13/12/90 08:00h	13/12/90 16:00h	13/12/90 16:00h						4 - 5	

Appendix 1f: Test 465 - 475

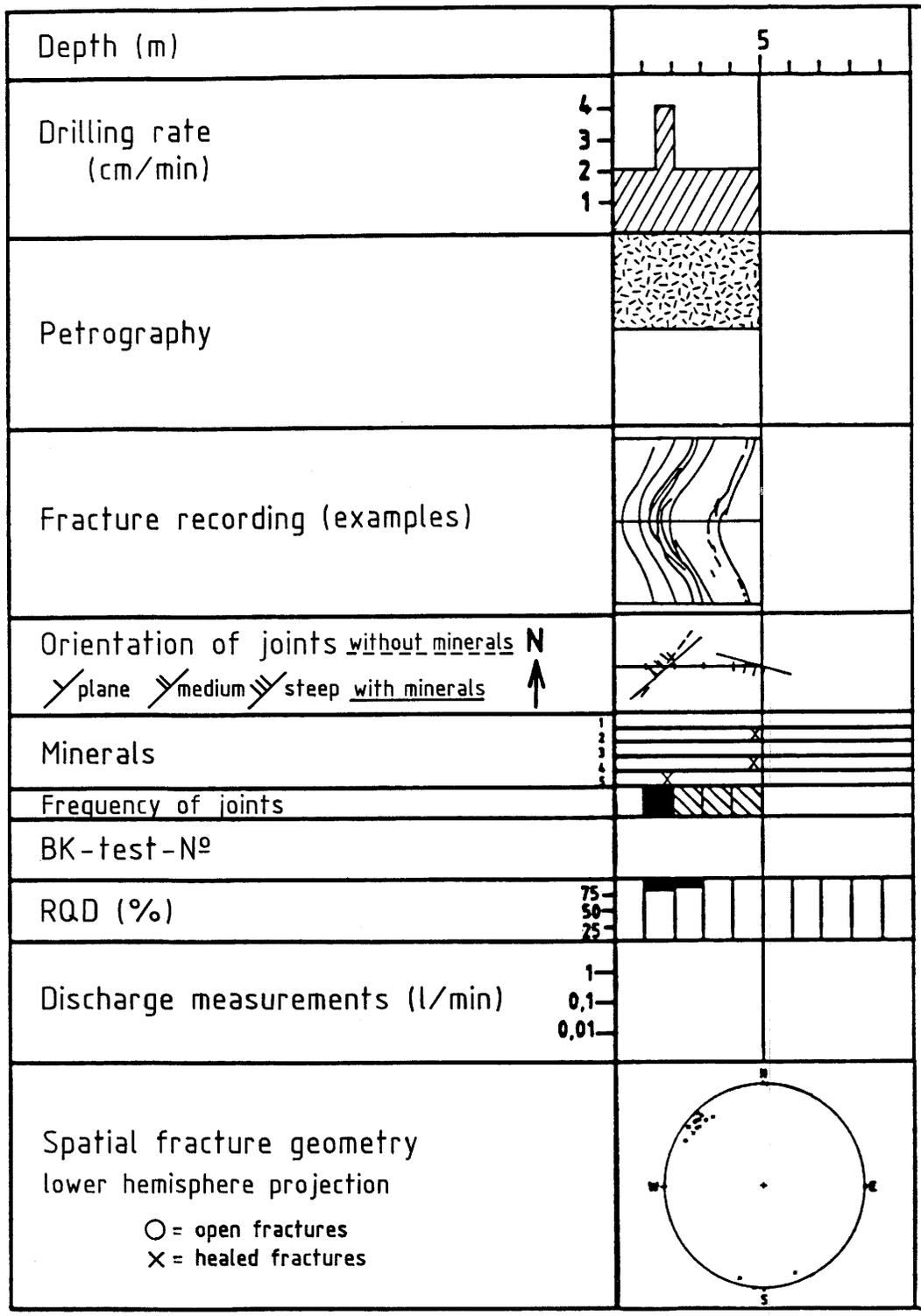

LEGEND

PETROGRAPHY: ROCKS

- CENTRAL AAREGRANITE (LIGHT)
- CENTRAL AAREGRANITE (DARK)

VEINS

- LAMPROPHYRE (KERSANTITE)
- BASIC VEINS
- APLITE

ALPINE ROCKS

- QUARTZ - VEINS
- HYDROTHERMAL ALTERATION
- MYLONITE

MINERALS:

1 = QUARTZ
2 = EPIDOTE
3 = BIOTITE
4 = CHLORITE
5 = FELDSPAR, CALCITE AND OTHERS

JOINT FREQUENCY:

- NO OPEN FRACTURES / METRE
- 1 – 2 " " "
- 3 – 4 " " "
- 5 AND MORE " " "

Federal Institute for Geosciences and Natural Resources
Report of the BGR, Ref. 2.11/Hannover

nagra **TECHNICAL REPORT NTB 91-01E**

GEOLOGY OF BOREHOLE BK 88.012

GRIMSEL TEST SITE | DAT.: | **ENCLOSURE 1**

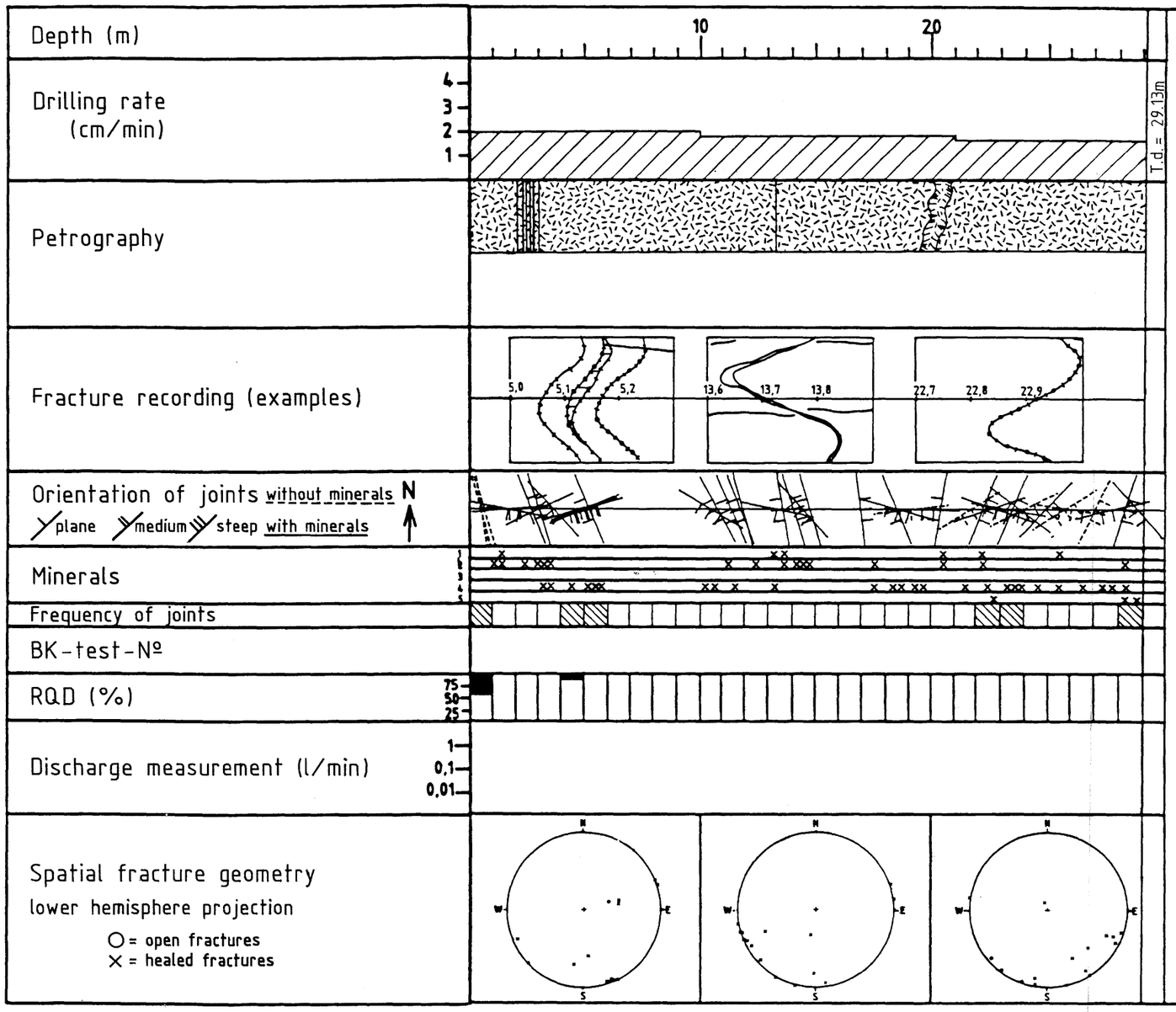

LEGEND

PETROGRAPHY: **ROCKS**

- CENTRAL AAREGRANITE (LIGHT)
- CENTRAL AAREGRANITE (DARK)

VEINS

- LAMPROPHYRE (KERSANTITE)
- BASIC VEINS
- APLITE

ALPINE ROCKS

- QUARTZ - VEINS
- HYDROTHERMAL ALTERATION
- MYLONITE

MINERALS:

1 = QUARTZ
2 = EPIDOTE
3 = BIOTITE
4 = CHLORITE
5 = FELDSPAR, CALCITE AND OTHERS

JOINT FREQUENCY:

- NO OPEN FRACTURES / METRE
- 1 - 2 " " "
- 3 - 4 " " "
- 5 AND MORE " " "

Federal Institute for Geosciences and Natural Resources
Report of the BGR, Ref. 2.11/Hannover

nagra **TECHNICAL REPORT NTB 91-01E**

GEOLOGY OF BOREHOLE BK 88.013

GRIMSEL TEST SITE | DAT.: | **ENCLOSURE 2**

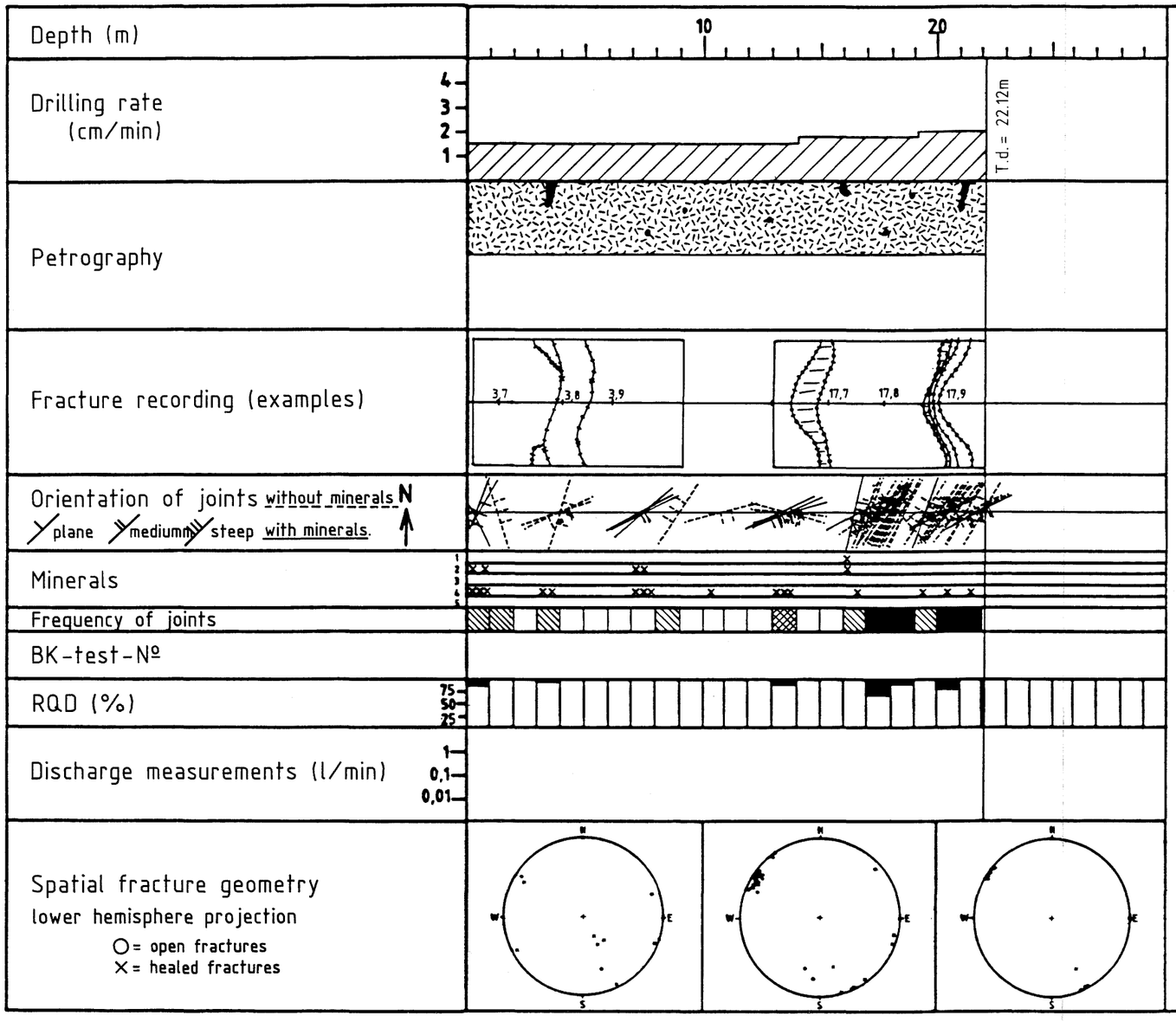

LEGEND

PETROGRAPHY: **ROCKS**

- CENTRAL AAREGRANITE (LIGHT)
- CENTRAL AAREGRANITE (DARK)

VEINS

- LAMPROPHYRE (KERSANTITE)
- BASIC VEINS
- APLITE

ALPINE ROCKS

- QUARTZ - VEINS
- HYDROTHERMAL ALTERATION
- MYLONITE

MINERALS:

1 = QUARTZ
2 = EPIDOTE
3 = BIOTITE
4 = CHLORITE
5 = FELDSPAR, CALCITE AND OTHERS

JOINT FREQUENCY:

- NO OPEN FRACTURES / METRE
- 1 - 2 " " "
- 3 - 4 " " "
- 5 AND MORE " " "

Federal Institute for Geosciences and Natural Resources
Report of the BGR, Ref. 2.11/Hannover

nagra **TECHNICAL REPORT NTB 91-01E**

GEOLOGY OF BOREHOLE BK 88.014

GRIMSEL TEST SITE | DAT.: | **ENCLOSURE 3**

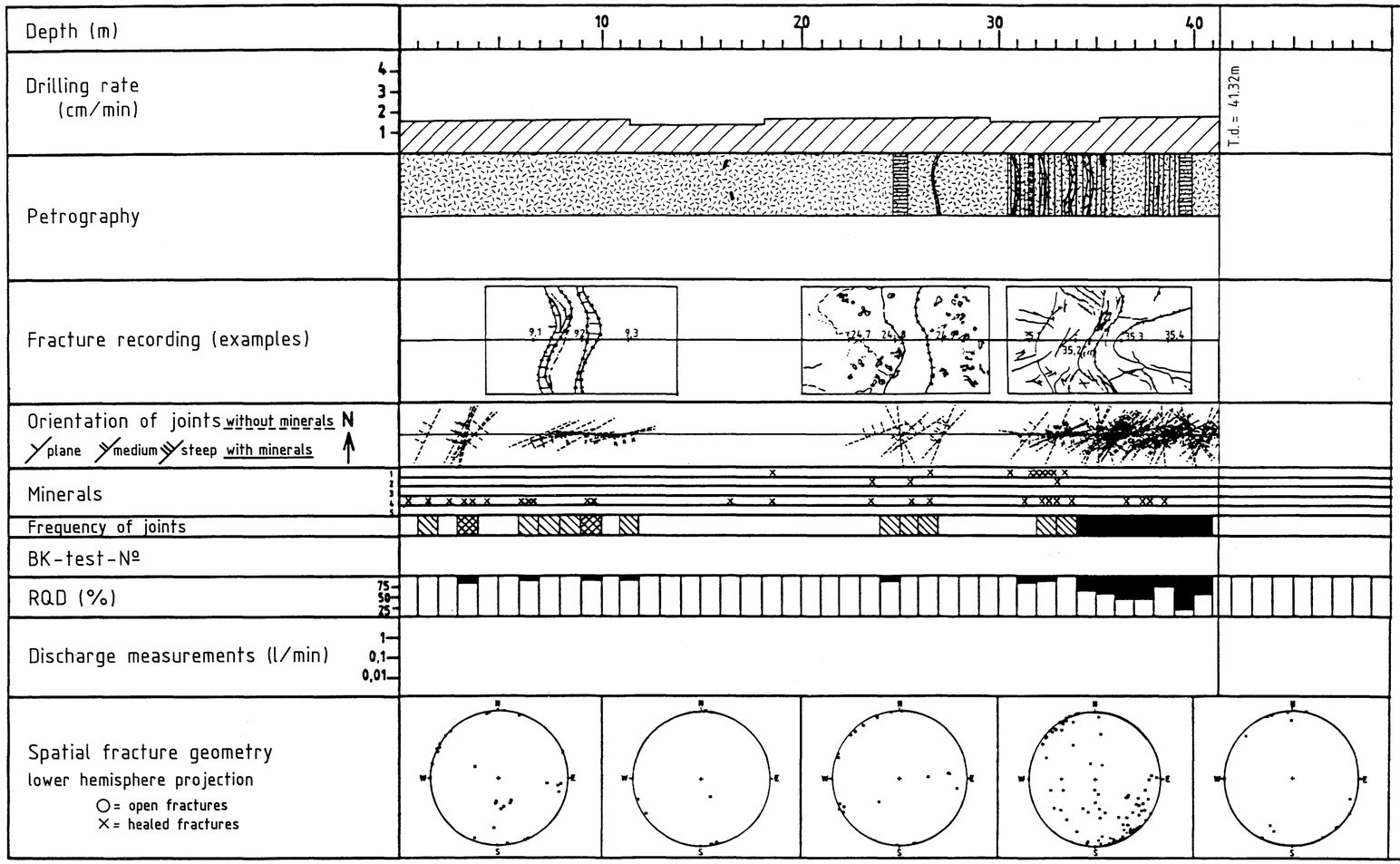

LEGEND

PETROGRAPHY: ROCKS

- CENTRAL AAREGRANITE (LIGHT)
- CENTRAL AAREGRANITE (DARK)

VEINS

- LAMPROPHYRE (KERSANTITE)
- BASIC VEINS
- APLITE

ALPINE ROCKS

- QUARTZ - VEINS
- HYDROTHERMAL ALTERATION
- MYLONITE

MINERALS:

1 = QUARTZ
2 = EPIDOTE
3 = BIOTITE
4 = CHLORITE
5 = FELDSPAR, CALCITE AND OTHERS

JOINT FREQUENCY:

- NO OPEN FRACTURES / METRE
- 1 - 2 " " "
- 3 - 4 " " "
- 5 AND MORE " " "

Federal Institute for Geosciences and Natural Resources
Report of the BGR, Ref. 2.11/Hannover

nagra **TECHNICAL REPORT NTB 91-01E**

GEOLOGY OF BOREHOLE BK 88.015

GRIMSEL TEST SITE | DAT.: | **ENCLOSURE 4**

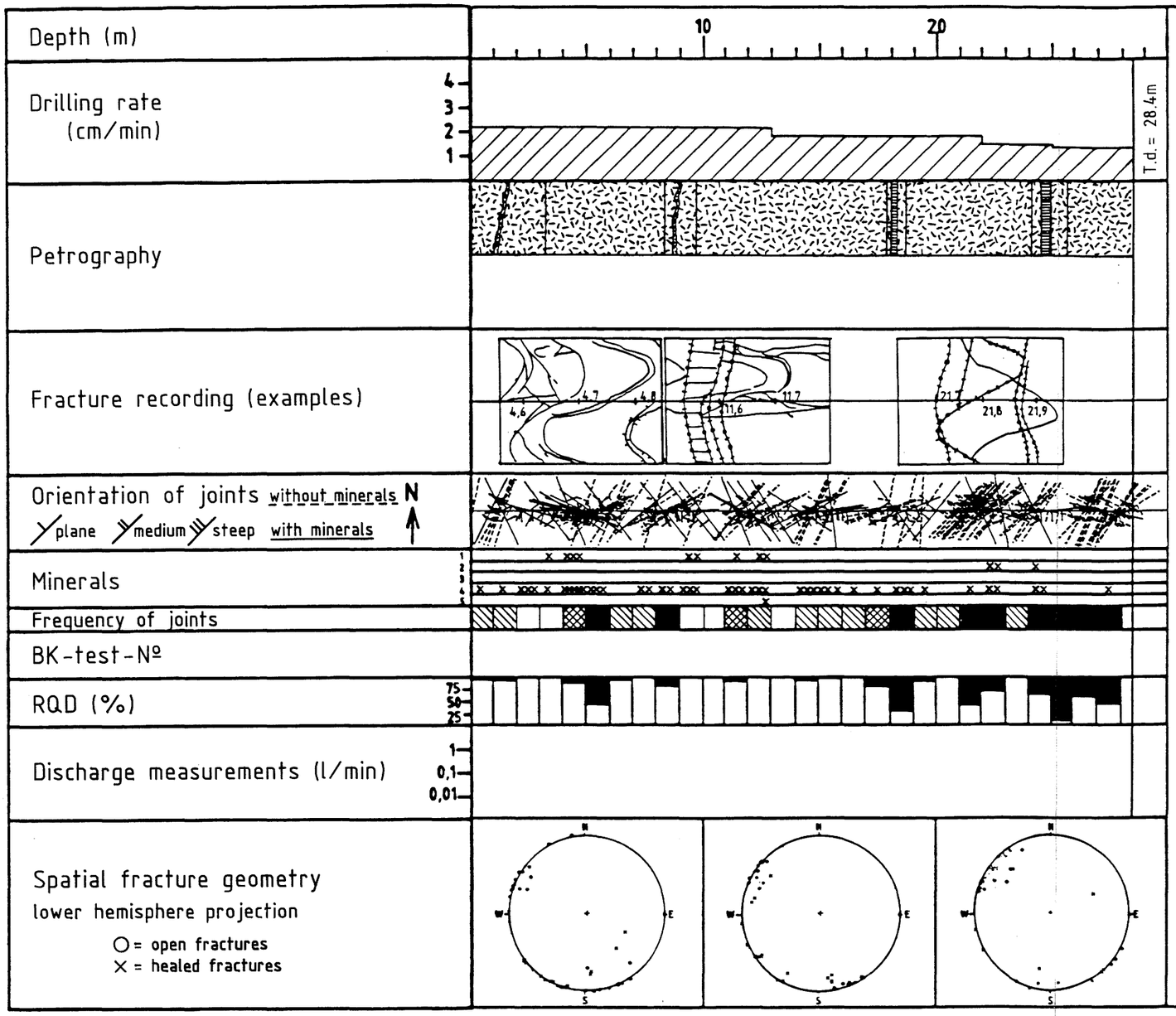

LEGEND

PETROGRAPHY : ROCKS

- CENTRAL AAREGRANITE (LIGHT)
- CENTRAL AAREGRANITE (DARK)

VEINS

- LAMPROPHYRE (KERSANTITE)
- BASIC VEINS
- APLITE

ALPINE ROCKS

- QUARTZ - VEINS
- HYDROTHERMAL ALTERATION
- MYLONITE

MINERALS :

1 = QUARTZ
2 = EPIDOTE
3 = BIOTITE
4 = CHLORITE
5 = FELDSPAR, CALCITE AND OTHERS

JOINT FREQUENCY :

- NO OPEN FRACTURES / METRE
- 1 - 2 " " "
- 3 - 4 " " "
- 5 AND MORE " " "

Federal Institute for Geosciences and Natural Resources
Report of the BGR, Ref. 2.11/Hannover

nagra **TECHNICAL REPORT NTB 91-01E**

GEOLOGY OF BOREHOLE BK 88.016

GRIMSEL TEST SITE | DAT.: | **ENCLOSURE 5**

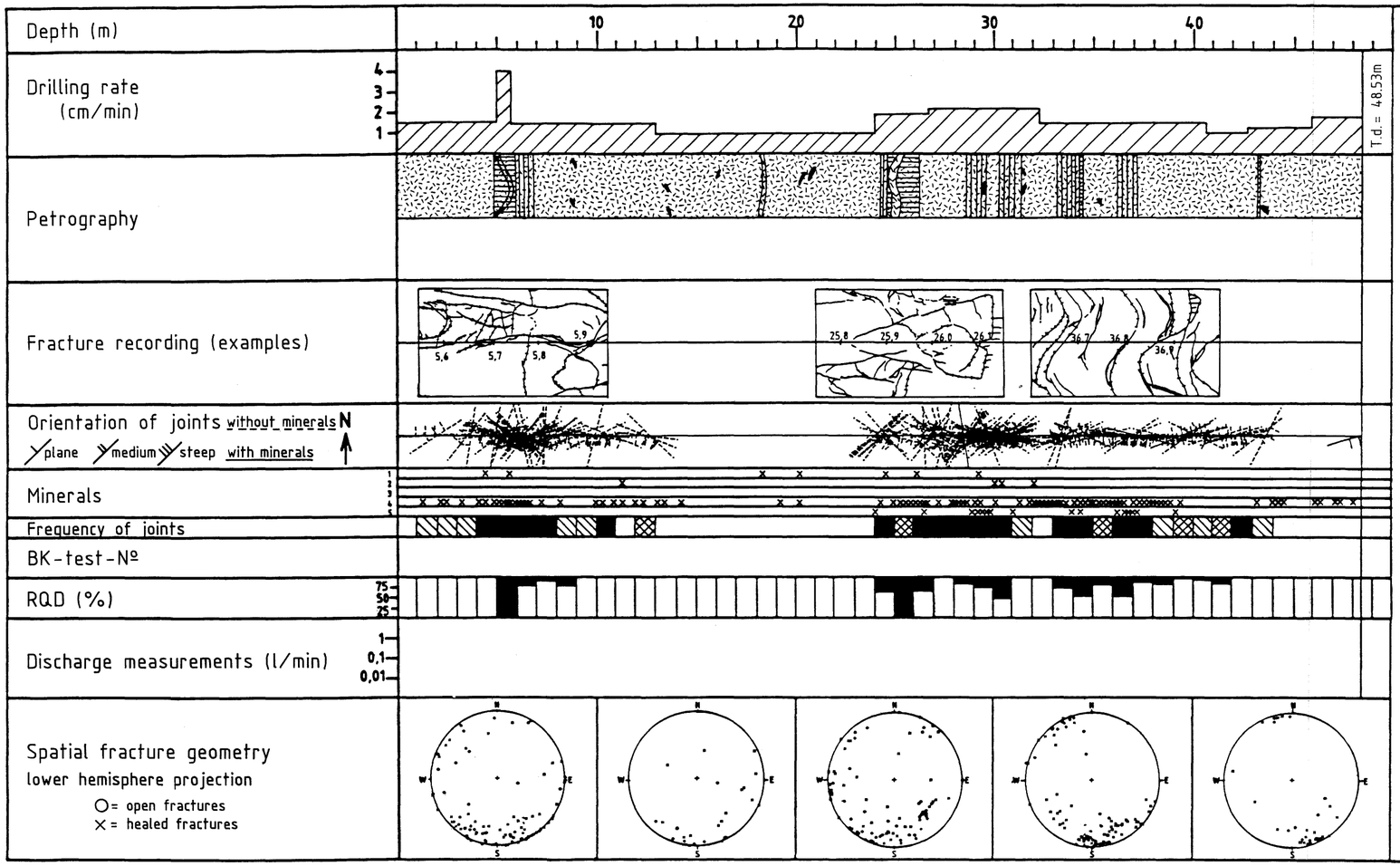

LEGEND

PETROGRAPHY: ROCKS

- CENTRAL AAREGRANITE (LIGHT)
- CENTRAL AAREGRANITE (DARK)

VEINS

- LAMPROPHYRE (KERSANTITE)
- BASIC VEINS
- APLITE

ALPINE ROCKS

- QUARTZ - VEINS
- HYDROTHERMAL ALTERATION
- MYLONITE

MINERALS:

1 = QUARTZ
2 = EPIDOTE
3 = BIOTITE
4 = CHLORITE
5 = FELDSPAR, CALCITE AND OTHERS

JOINT FREQUENCY:

- NO OPEN FRACTURES / METRE
- 1 - 2 " " "
- 3 - 4 " " "
- 5 AND MORE " " "

Federal Institute for Geosciences and Natural Resources
Report of the BGR, Ref. 2.11/Hannover

nagra TECHNICAL REPORT NTB 91-01E

GEOLOGY OF BOREHOLE BK 88.017

GRIMSEL TEST SITE | DAT.: | **ENCLOSURE 6**

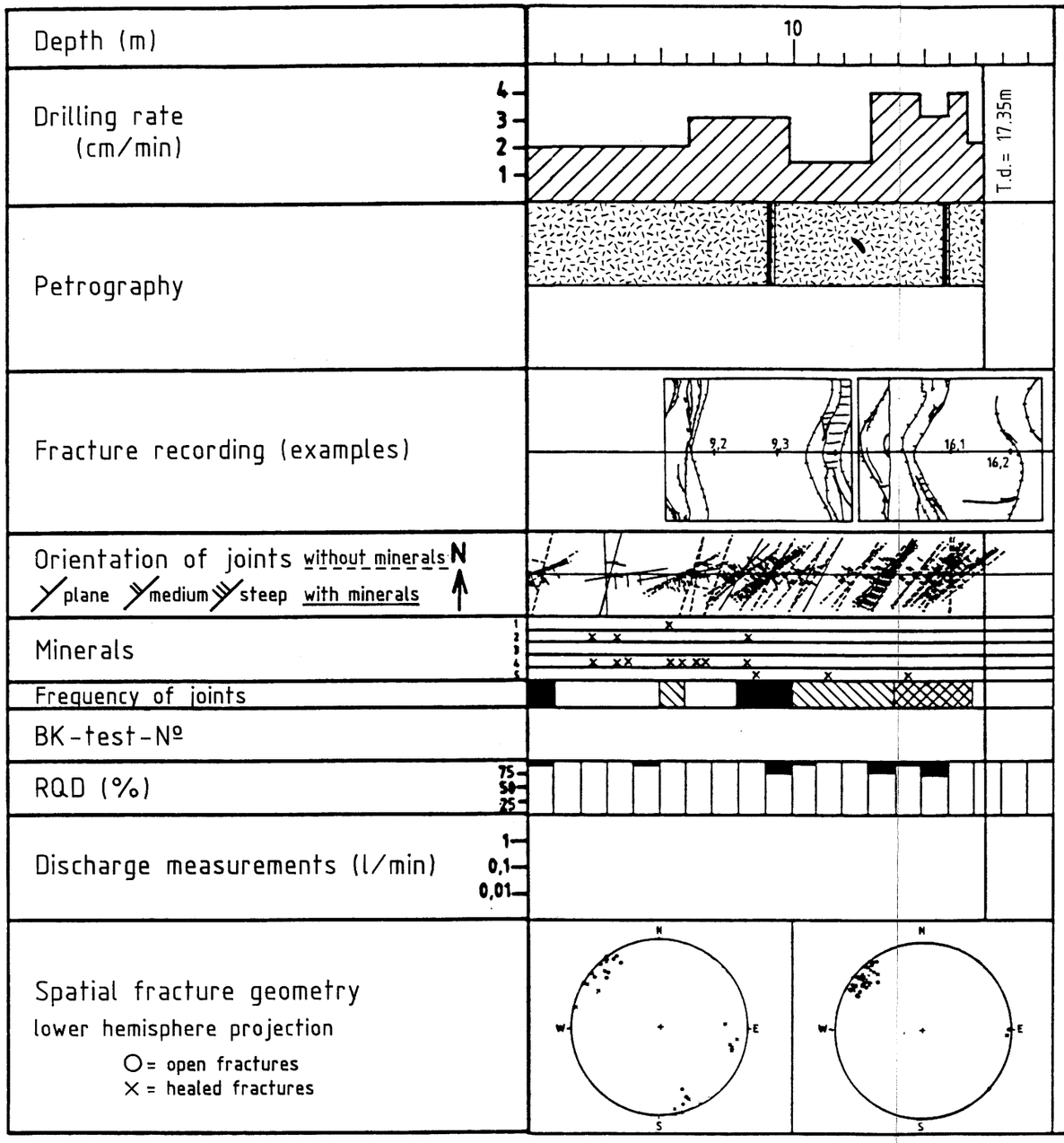

LEGEND

PETROGRAPHY : **ROCKS**

- CENTRAL AAREGRANITE (LIGHT)
- CENTRAL AAREGRANITE (DARK)

VEINS

- LAMPROPHYRE (KERSANTITE)
- BASIC VEINS
- APLITE

ALPINE ROCKS

- QUARTZ - VEINS
- HYDROTHERMAL ALTERATION
- MYLONITE

MINERALS :

1 = QUARTZ
2 = EPIDOTE
3 = BIOTITE
4 = CHLORITE
5 = FELDSPAR, CALCITE AND OTHERS

JOINT FREQUENCY :

- NO OPEN FRACTURES / METRE
- 1 - 2 " " "
- 3 - 4 " " "
- 5 AND MORE " " "

Federal Institute for Geosciences and Natural Resources
Report of the BGR, Ref. 2.11/Hannover

nagra **TECHNICAL REPORT NTB 91-01E**

GEOLOGY OF BOREHOLE BK 88.018

GRIMSEL TEST SITE | DAT.: | **ENCLOSURE 7**